Probabilistic Accident Consequence Uncertainty Analysis

Dispersion and Deposition Uncertainty Assessment

Volume 3 Appendices C, D, E, F and G

A Joint Report Prepared by U.S. Nuclear Regulatory Commission and Commission of European Communities

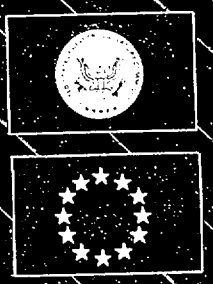

A13

NUREG/CR–6244
EUR 15855EN
SAND94–1453
Vol. 3

Probabilistic Accident Consequence Uncertainty Analysis

Dispersion and Deposition Uncertainty Assessment

Appendices C, D, E, F, and G

Manuscript Completed: November 1994
Date Published: January 1995

Prepared by
F. T. Harper
Sandia National Laboratories, USA

S. C. Hora
University of Hawaii at Hilo, USA

M. L. Young
Sandia National Laboratories, USA

L. A. Miller
Sandia National Laboratories, USA

C. H. Lui
U.S. Nuclear Regulatory Commission, USA

M. D. McKay
Los Alamos National Laboratory, USA

J. C. Helton
Arizona State University, USA

L. H. J. Goossens
Delft University of Technology
The Netherlands

R. M. Cooke
Delft University of Technology
The Netherlands

J. Pasler-Sauer
Research Center, Karlsruhe
Germany

B. Kraan
Delft University of Technology
The Netherlands

J. A. Jones
National Radiological Protection Board
United Kingdom

Prepared for

Division of Systems Technology
Office of Nuclear Regulatory Research
U.S. Nuclear Regulatory Commission
Washington, DC 20555–0001
NRC Job Code L2294

Commission of the European Communities
DG XII and XI
200, rue de la Loi
B–1049 Brussels
CEC Contract Numbers F13P–Ct92–0023 and 93–ET–001

Publication no. EUR 15855 EN of the
Commission of the European Communities,
Dissemination of Scientific and Technical Knowledge Unit,
Directorate-General Telecommunications, Information Market and
Exploitation of Research
Luxembourg

LEGAL NOTICE

Abstract

The development of two new probabilistic accident consequence codes, MACCS and COSYMA, was completed in 1990. These codes estimate the risks presented by nuclear installations based on postulated frequencies and magnitudes of potential accidents. In 1991, the US Nuclear Regulatory Commission (NRC) and the Commission of the European Communities (CEC) began a joint uncertainty analysis of the two codes. The ultimate objective of the joint effort was to develop credible and traceable uncertainty distributions for the input variables of the codes. As a first step, a feasibility study was conducted to determine the efficacy of evaluating a limited phenomenological area of consequence calculations (atmospheric dispersion and deposition parameters) and to determine whether the technology exists to develop credible uncertainty distributions on the input variables for the codes. Expert elicitation was identified as the best technology available for developing a library of uncertainty distributions for the selected consequence parameters.

The study was formulated jointly and was limited to the current code models and to physical quantities that could be measured in experiments. The elicitation procedure was devised from previous US and EC studies with refinements based on recent experience. Elicitation questions were developed, tested, and clarified. Sixteen internationally recognized experts from nine countries were selected using a common set of selection criteria. Probability training exercises were conducted to establish ground rules and set the initial boundary conditions. Experts developed their distributions independently. Results were processed with an equal weighting aggregation method, and the aggregated distributions were processed into code input variables. To validate the distributions generated for the wet deposition input variables, samples were taken from these distributions and propagated through the wet deposition code model. Resulting distributions closely replicated the aggregated elicited wet deposition distributions. To validate the distributions generated for the dispersion code input variables, samples were taken from the distributions and propagated through the Gaussian plume model (GPM) implemented in the MACCS and COSYMA codes. Resulting distributions were found to well replicate aggregated elicited dispersion distributions consistent with the GPM assumptions.

Valuable information was obtained from the elicitation exercise. Project teams from the NRC and CEC cooperated successfully to develop and implement a unified process for the elaboration of uncertainty distributions on consequence code input parameters. Formal expert judgment elicitation proved valuable for synthesizing the best available information. Distributions on measurable atmospheric dispersion and deposition parameters were successfully elicited from experts involved in the many phenomenological areas of consequence analysis.

Contents

Preface

This volume is the third of a three-volume document that summarizes a joint project conducted by the US Nuclear Regulatory Commission and the Commission of European Communities to assess uncertainties in the MACCS and COSYMA probabilistic accident consequence codes. These codes were developed primarily for making estimates of the risks presented by nuclear reactors based on postulated frequencies and magnitudes of potential accidents. This three-volume document reports on an ongoing project intended to assess uncertainty in the MACCS and COSYMA offsite radiological consequence calculations for hypothetical nuclear power plant accidents. A panel of 16 experts was formed to compile credible and traceable uncertainty distributions for the dispersion and deposition code input variables that affect offsite radiological consequence calculations. The expert judgment elicitation procedure and its outcomes are described in these volumes.

Volume III contains six appendices that describe the specific methods used by the atmospheric dispersion and deposition panels. This volume includes descriptions of the probability assessment principles, the expert identification and selection process, the weighting methods used for combining the expert judgments, and the inverse modeling methods. It also contains the case structures, a non-Gaussian information survey, and summaries of the MACCS and COSYMA consequence codes.

Volume I of this document includes a complete description of the joint consequence uncertainty study. Volume II contains two appendices that include (1) the rationales for the dispersion and deposition data provided by the 16 experts who participated in the elicitation process (2) the tabulated elicited information, and (3) short biographies of the 16 experts.

Acknowledgments

The authors would like to acknowledge all the participants in the expert judgment elicitation process, in particular the dispersion and deposition expert panels. While we wrote and edited the report, organized the process, and processed the results, the experts provided the technical content that is the foundation of this report. Dr. Detlof von Winterfeldt is acknowledged for his contribution as elicitor in several expert sessions.

The authors would also like to express their thanks for the support and fruitful remarks from Dr. G. N. Kelly (CEC/DG XII), Dr. R. Serro (CEC/DG XI), and Dr. J. Glynn (USNRC).

We would also like to acknowledge several institutes that facilitated the collection of unpublished experimental information used in the probabilistic training and evaluation of the dispersion and deposition experts. The authors want to thank Dr. T. Mikkelsen and coworkers at Riso and the Danish Center for Atmospheric Research, Denmark; Dr. R. Brown at British Gas, UK; Dr. B. Jolliffe at NPL Teddington, UK; Dr. G. Deville-Cavelin at IPSN/Cadarache, France; Dr. P. Berne at IPSN/Grenoble, France; Dr. Y. Belot at IPSN/Fontenay-aux-Roses, France; Dr. J. Duyzer at TNO/Delft, The Netherlands; and Dr. J. Slanina at ECN/Petten, The Netherlands.

The authors also greatly appreciate the technical assistance of Ms. Ina Bos of Delft University of Technology, The Netherlands; the support of Ms. Darla Tyree and Ms. Judy Jones of Sandia National Laboratories, USA.; and the extensive assistance and guidance provided by Tim Peterson of Tech Reps, Inc., in the preparation of this report.

This report is written under the following contracts:

Contract No. L2294, United States Nuclear Regulatory Commission, Office of Nuclear Regulatory Research, Division of Safety Issue Resolution.

Contract No. F13P-Ct92-0023, Commission of European Communities, Directorate-General for Science, Research and Development, XII Radiation Research.

Contract No. 93-ET-001, Commission of European Communities, Directorate-General of Environment, Nuclear Safety and Civil Protection, XI-A-1 Radiation Protection.

APPENDIX C

Principles for Probability Assessment

Expert Identification and Selection

C. Principles for Probability Assessment, Expert Identification and Selection

C.1 Principles for Probability Assessment

The key element of the joint CEC/NRC project is the use of experts to establish probability distributions for uncertain parameters. As a foundation for the development of a common CEC/NRC elicitation protocol, eleven principles were distilled from the views presented by the EC and US team members responsible for probability assessments. In this appendix, these jointly developed principles of probability assessments are discussed. Additional discussions of these principles can be found in the references to this appendix.[1,2] For the most part, these principles are the same as those that guided the NUREG-1150 process. Any deviations from the principles defined for the NUREG-1150 process are explained in the 11 probability assessment principles listed below.

1. The issues analyzed using expert opinion should have the potential to make a significant impact on the estimates of consequences and uncertainty in consequences.

2. The assessments should be limited to issues where alternative sources of information—such as experimental or observational data or validated computer models—are not available, or where multiple sources of information provide conflicting or incomplete evidence.

3. Experts should be required to respond only to questions about physically measurable quantities, but undertaken in the context of the presuppositions being used. If the elicitation variables differ from the code input variables, processing of elicitation variable distributions may be required to obtain distributions for code input variables. This principle was not explicitly stated for NUREG-1150, but it was followed. Elicitation variable processing is necessary to a larger extent in this study than in the NUREG-1150 study because this uncertainty study is designed for fixed codes. The models in NUREG-1150 had the flexibility to be modified to fit the elicitation responses if necessary.

4. The issues should be presented to the experts in an unambiguous manner without the potential for preconditioning or biasing the responses.

5. Discussion of issues and alternative opinions should take place in structured and controlled meetings where the exploration of alternative beliefs is encouraged while the pressure to conform is inhibited.

6. The selection of experts should be made to ensure that a wide diversity of expertise is admitted, thus encouraging the inclusion of alternative points of view. The selection of experts should preclude direct stakeholders in the findings from participating as members of the expert panel.

7. Experts should be trained in the practice of expressing knowledge and beliefs as probability distributions.

8. Elicitation of expert opinion should be accomplished using techniques and instruments that reflect the state of the art in subjective probability assessment.

9. The method for combining/evaluating expert judgment should encourage experts to state their true opinions.

10. The experts should be identified with their probabilities and the rationales for those probabilities. (In NUREG-1150 experts were allowed to remain anonymous if they desired.) This principle requires that all probability assessments and rationales behind them must be accessible for a full peer review, if warranted, by CEC and/or NRC officials. For that purpose only, the assessments and rationales are associated with the experts' names and affiliations. For all other purposes, all experts' names and affiliations will not be associated with the probability assessments and rationales.

11. It should be possible for scientific peers to review and, if necessary, reproduce all calculations. This principle requires that the calculation models be fully specified beforehand and all ingredient data be assessable.

C.2 Agenda of First Expert Meeting

The preparation for elicitation took place in a meeting with the experts conducted approximately four weeks prior to the probability elicitation. Preparation for elicitation

requires that the experts be introduced to the purposes of the study, including how their judgments are to be used. The experts should also be introduced to background material about the subject area and to the science of probability elicitation. This required the project staff to prepare and distribute materials explaining the general subject area, the relation of the questions posed to the parameters in the model, and the specific initial conditions and assumptions to be used in answering the elicitation questions. Training was conducted to introduce the experts to the psychological biases in judgment formation and to give them feedback on their performance in assessing probability distributions. This training was accomplished using questions that emulate the assessment task but which have known answers.

The experts were given presentations on the elicitation issues and participated in a seminar on expert judgment methods. The agenda for the first meeting with the experts is presented in Tables C.1 and C.2.

Table C.1 Agenda of First Expert Meeting Wednesday, April 14, 1993

Topic:	Presented By:
Introduction	Louis Goossens (TUD)
Overview of project	Fred Harper (SNL)
Probabilistic training	Steve Hora (UHH)
Overview of MACCS and COSYMA consequence codes	Jürgen Päsler-Sauer (KfK) LeAnn Miller (SNL)
Introduction to dispersion elicitation variables and case structure	Jürgen Päsler-Sauer
Introduction to deposition elicitation variables and case structure	LeAnn Miller
Continuation of probabilistic training: training exercise	Steve Hora
Discussion	All

Table C.2 Agenda of First Expert Meeting Thursday, April 15, 1993

Topic:	Presented By:
Assessment of training exercise	Steve Hora
Discussion of aggregation by simple averaging	Steve Hora
Discussion of aggregation using performance based weighting	Roger Cooke
Expert feedback on elicitation variable definition	Experts
Brief description of chemical and physical properties of source term from a nuclear power plant accident	J. Brockmann (SNL)
Clarification of issues: lists of all uncertainty issues to be considered in uncertainty distributions, issues addressed as part of case structure, and issues that are outside the scope of the project were discussed collectively.	All

C.3 Expert Identification and Selection

The purpose of the expert selection process was to select experts in the dispersion and deposition fields from the pool of American and European experts. The following procedure was employed to select the experts:

1. A list of experts was compiled by searching through the literature and requesting nominations from organizations familiar with the areas.

2. The experts were contacted and Curriculum Vitae (CV) were requested (suggestions for additions to the list of experts were also requested from each expert contacted).

3. Objective selection boards studied the CVs and selected eight dispersion experts and eight deposition experts according to selection criteria agreed on before initiating the process. Two selection boards were involved in the selection process: a board from the EC selected the European experts and a board from the US selected the American experts. In the US, the selection board was made up of technical personnel from the University of New Mexico, the Inhalation Toxicology Research Institute, and Sandia National Laboratories. The EC selection board was composed of knowledgeable faculty members from the Delft University of Technology and the University of Utrecht.

The selection criteria were as follows:

- reputation in the field of dispersion or deposition;
- experimental experience in the field of dispersion or deposition;
- number and quality of publications in the field of interest;
- familiarity with uncertainty concepts;
- diversity in background;
- awards;
- balance of views; and
- interest in the project.

4. The experts were judged by the CVs received. The experts were ranked according to the above criteria. Subjectivity in the selection process was minimized as much as possible by scoring each expert according to each criterion and summing the scores.

C.4 Justification for Panel Size

Much has been written regarding the optimal number of experts in an assessment of this type. Meyer and Booker recommend that the number of experts should fall between five and 10;[3] Armstrong recommends from six to 12.[4] It was decided by the NRC/CEC staff that panel size would be set at eight (four supplied by the US and four supplied by the EC). Some of the objectives to be considered when establishing the size of a panel are presented below:

The first and most important reason for larger panels is to include adequate diversity on the panel.[3,4] If there are many points of view, many experts should be included.

If enough experts with different perspectives are present, the information exchange provides a better basis for the assessments.

As in a statistical sample, the non-systematic biases disappear as the number of experts increases.

Among the purposes for limiting the size of panels are:

The practical reasons of cost and schedule feasibility.

The efficiency of meetings, which decreases if the number of participants becomes too large.

The statistical limitations: If experts are correlated (similarity in background), there is a statistical upper limit above which additional experts provide no more benefit.[5]

C.5 References

1. Cooke, R., Delft University of Technology, "Expert Judgment Study on Atmospheric Dispersion and Deposition," Reports of the Faculty of Technical Mathematics and Informatics no. 91-81, Delft, The Netherlands, 1991.

2. Hora, S.C., and R.L. Iman, "Expert Opinion and Risk Analysis: The NUREG 1150 Methodology," *Nuclear Science and Engineering*, 102: 323-331, 1989.

3. Meyer, M., and J. Booker, *Eliciting and Analyzing Expert Judgment: A Practical Guide*, Academic Press, Orlando, FL, 1991.

4. Armstrong, J. S., *Long-Range Forecasting; from Crystal Ball to Computer*, Wiley, New York, NY, 1985.

5. Chhibber, S., and G. Apostolakis, "Some Approximations Useful to the Use of Dependent Information Sources," Reliability Engineering and System Safety, 42: 67-86, 1993.

APPENDIX D

Equal and Performance Based Weighting Methods for Combining Expert Judgments

D. Equal and Performance Based Weighting Methods for Combining Expert Judgments

D.1 Introduction

This appendix reviews the alternative aggregation schemes applied to the data elicited in this study. The dispersion and deposition experts provided 5th, 50th, and 95th percentile values for the cumulative distribution of each elicitation variable for each case (i.e., set of initial and boundary conditions for a question). The project staff was responsible for aggregating the individual expert distributions (5th, 50th, and 95th percentile values) into a single probability distribution for each elicitation variable and case. Although the equal weighting form of aggregation was chosen for the development of distributions over the consequence code input parameters,* performance based weighting schemes were also applied to the elicited results so that these results would be available for exploring the robustness of alternative weighting schemes in the context of consequence measures.** A more extensive discussion of performance based weighting may be found in the draft document entitled "Methods for CEC\USNRC Accident Consequence Uncertainty Analysis of Dispersion and Deposition," published by the Delft University of Technology in the Netherlands.[1] Much of the information contained in this appendix is derived from that document.

D.2 Overview of EXCALIBR

The EXCALIBR computer program[2] was used in this study to aggregate the individual expert distributions. The EXCALIBR software system, developed under CEC sponsorship, is designed to develop both equal and performance based weighted aggregated distributions from individual elicited distributions. The inputs for EXCALIBR are the individual percentile assessments of the experts on both the elicitation variables and the seed variables. The seed variables are the variables used to evaluate (score) the experts' assessments. The true values of the seed variables are known to members of the elicitation team but not to the experts. EXCALIBR uses the elicited distributions over the seed variables to score the experts' assessments with respect to calibration (statistical likelihood). EXCALIBR also evaluates the distributions provided by the experts in terms of the informativeness of the distributions.*** EXCALIBR then computes various combinations and generates the aggregated distribution based on the weighting scheme chosen by the user. In the equal weighting scheme, the calibration and informativeness scores are not used; the distributions of the individual experts are assigned equal weight.

D.3 Measuring Performance

Performance based weighting is an available option after the project analysts have decided what is meant by good performance, how good performance is measured, and how performance measures can be translated into weights in a combination algorithm.[3] The basic prerequisite is the establishment of metrics by which to measure an expert's ability to accurately assess the cumulative probability distribution for an uncertain variable. The EXCALIBR system of performance based aggregation is based on the evaluation of experts' assessments with respect to calibration and informativeness. This section reviews the concepts of calibration and informativeness.

D.3.1 Calibration

Calibration measures the statistical likelihood that actual experimental results correspond, in a statistical sense, with

* As discussed in Section 3 5 1, Volume I of this document, investigating different weighting schemes was not the objective of this joint project A programmatic decision was therefore made to assign all experts equal weight

** A peer review panel of the NUREG-1150 study questioned the use of the equal weighting scheme without consideration of other methods. Sufficient information was subsequently elicited in the present study to allow the application of alternative weighting schemes to the elicited data.

*** To a large degree, the informativeness of a distribution is determined by the width of the uncertainty band, that is, a distribution with a narrow range between the 5th and 95th percentile parameter values will typically provide more information about the parameter than a distribution with a broader range between these percentile values However, informativeness is also influenced by the placement of the median between the 5th and 95th percentiles; that is, the placement of the median halfway between (with regard to the background measure) these percentiles is less informative than a placement near either the 5th or 95th percentile.

the expert's assessments. Each expert receives a calibration score, which is determined by his percentile assessments for items whose true values are known post hoc, and by the true values themselves.

Call p = (0.05, 0.45, 0.45, 0.05) the "theoretical" distribution for the experimental results falling

- below the 5th percentile,
- between the 5th and 50th percentiles,
- between the 50th and 95th percentiles, and
- above the 95th percentile,

respectively. Calibration measures how well this theoretical distribution is supported by the actual experimental results. For a given expert, let $s = (s_1, s_2, s_3, s_4)$ be the sample distribution generated by the expert's assessments and the experimental results, where

s_1 = proportion of experimental results falling below the 5th percentile,
s_2 = proportion of experimental results falling between the 5th and 50th percentiles,
s_3 = proportion of experimental results falling between the 50th and 95th percentiles, and
s_4 = proportion of experimental results falling above the 95th percentile.

The sample distribution, s, varies from expert to expert because the experts choose their percentiles differently. To determine for each expert how well the sample distribution, s, supports the theoretical distribution p, we ask "How likely is it that we should see such a difference between s and p, if s were really generated by random samples from p?" More precisely, we first compute the relative information $I(s,p)$ of s with respect to p:

$$I(s,p) = \sum_{i=1}^{4} s_i \ln(s_i/p_i)$$

$I(s,p)$ is always non-negative, and the closer s is to p, the smaller is $I(s,p)$. Calibration is now measured as the probability that a random sample of appropriate size drawn from p would produce a discrepancy at least as great as $I(s,p)$. This probability is a number between zero and one, with larger values corresponding to "s closer to p" and hence to better calibration.

In scoring calibration, each expert is regarded as a statistical hypothesis, namely:

For each experimental result, there is a 5% chance that it lies below the 5th percentile, a 45% chance that it lies between the 5th and 45th percentile, a 45% chance that it lies between the 50th and 95th percentile, and a 5% chance that it lies above the 95th percentile; moreover, for different experiments these chances are independent.

The decision maker algorithm in the performance-based weighting method (see Section D.4) wants experts for whom the corresponding statistical hypothesis is well supported by the data obtained from the seed variables; that is, if an expert gives 90 percent probability bands for a large number of variables, then we might expect that 10 percent of all variables will actually fall outside his bands. If the expert has assessed 20 variables for which the realizations are known, then three or four of the 20 variables falling outside these bands would be no cause for alarm, as this can be interpreted as sampling fluctuation. The above hypothesis would still be reasonably supported by the data. If 10 of the 20 variables fell outside the bands, we should be worried, as it is difficult to believe that so many outliers should result from fluctuations. Statistical likelihood measures the degree to which data support the corresponding statistical hypothesis.

The proper interpretation of a calibration score requires knowledge of the number of realizations on which it is based, and scores based on different numbers of realizations cannot be directly compared.

D.3.2 Informativeness

To measure informativeness, a background measure is assigned to each query variable.**** The background measures are either uniform or loguniform. Simply put, if one uses a log scale, the background measure is logarithmic, whereas if one uses the natural scale of the variable, the background measure is linear. The choice of background measure usually has a small effect, but in certain cases a modest effect has been found. On the basis of experience, the following default rule has been chosen: If the smallest interval that includes all expert percentiles exceeds three orders of magnitude, use a loguniform background; otherwise use a uniform background. In the data sets analyzed in this study, the choice of background measure had little effect.

EXCALIBR associates probability densities with the assessments of each expert for each query variable in such

**** Query variables are called "elicitation variables" in the main report.

a way that (1) the densities agree with the expert's percentile assessments, and (2) the densities are minimally informative with respect to the background measure, given the percentile constraints. Informativeness is scored per variable per expert by computing the relative information of the expert's density for that variable with respect to the background measure. Overall informativeness per expert is the average of the information scores over all variables. This average is proportional to the relative information in the expert's joint distribution over all variables under the assumption that the variables are independent. Information scores are always positive, and—other things being equal—experts with high information scores are preferred.

To find these minimally informative distributions the background measure must be restricted to a finite range outside of which the expert densities must be zero. This intrinsic range is taken, per variable, by finding the smallest interval that includes all expert percentiles and the realization (if present) and extends this by 10 percent above and below. The 10 percent overshoot rule is used only in the measurement of information and is not output with the decision maker. Changing this range by a large amount has a negligible effect on the decision maker.

The information score is a positive number, with increasing values indicating greater information relative to the background measure. Since the intrinsic range depends on the expert assessments, this range can change as experts are added or deleted, and this can exert a small influence on the information scores of the remaining experts. Information is a slow function; that is, large changes in the percentile assessments produce only modest changes in the information score. On a data set with 20 realizations, calibration scores typically vary over four orders of magnitude, but information scores seldom vary by more than a factor of 3. The performance based weights are proportional to a product of calibration and information scores. The calibration score is the more important measure. The information score serves to modulate between more or less equally well calibrated experts. This prevents the eventuality that very informative distributions (very narrow confidence bands) should compensate for very poor calibration.

D.4 Combining Expert Assessments

The performance based weighting schemes implemented in EXCALIBR emphasize calibration and give little emphasis to informativeness. Thus experts who are skilled at expressing uncertainty but not knowledgeable in the subject field of study will receive more weight than those who are poor in probability assessment but very knowledgeable in the substantive field of study.

All the EXCALIBR combination schemes are examples of linear pooling; that is, the combined distributions are weighted sums of the individual experts' distributions, with non-negative weights adding to one. Different combination schemes are distinguished by the method according to which the weights are assigned to densities. These schemes are designated "decision makers." The three decision makers (combination schemes) implemented in EXCALIBR are the equal weight, global weight, and item weight decision makers. These three combination schemes are described briefly in this section.

D.4.1 Equal Weight Combination Scheme

The equal weight combination scheme assigns equal weight to each density. If N experts have assessed a given set of variables, the weights for each density are $1/N$. For variable i in this set the decision maker's density is given by:

$$f_{ewdm,i} = (1/N)\sum_{j=1}^{N} f_{j,i}$$

where $f_{j,i}$ is the density associated with expert j's assessment for variable i.

D.4.2 Global Performance Weight Combination Scheme

Global weights are determined, per expert, by the expert's calibration score and overall information score. The calibration score is determined per expert by his assessments of the seed variables (see Section D.10). The overall information score is the (relative) information in the expert's joint distribution over the seed variables.***** For expert j, the same weight is used for all variables assessed. Hence for variable i the global performance weight density is:

***** Because experts are queried only about marginal distributions, the decision maker regards the variables as independent (otherwise joint distributions should have been assessed). In this case the information in the joint distribution is the sum of the information of the marginal distributions.

$$f_{gwdm,i} = \sum_{j=1}^{N} w_j f_{j,i}$$

where w_j is the global weight. These weights satisfy a "proper scoring rule" constraint. That is, under suitable assumptions an expert achieves his maximal expected weight in the long run by, and only by, stating percentiles that correspond to his true beliefs.

D.4.3 Item Performance Weight Combination Scheme

As with global weights, item weights are performance based weights that satisfy a proper scoring rule constraint; they are based on calibration and informativeness. Whereas global weights use an overall measure of informativeness, item weights are determined per expert *and* per variable in a way that is sensitive to the expert's informativeness for each variable. This approach enables an expert to up- or down-weight himself for each variable by choosing a more or less informative distribution for that variable. Roughly speaking, more informative distributions are obtained by choosing percentiles that are closer together, whereas less informative distributions result when the percentiles are farther apart. Item weights depend on the expert and on the item. Hence the item weight density for variable i is:

$$f_{iwdm,i} = \sum_{j=1}^{N} w_{j,i} f_{j,i}$$

where $w_{j,i}$ is the item weight.

D.5 Advantages of Equal Weighting Scheme

An important advantage of equal weights is the simplicity and ease of application of the method. In this regard, equal weighting is often justified on the basis of Ockham's razor: when selecting among equal theories, take the least complicated. Another advantage of equal weighting is that the weights are fixed and subsequently not subject to tampering. Equal weights can tend to reduce the impact of extreme observations (i.e. a large weight combined with an outlier). With equal weights, the extremes of the resulting distributions are equal to the extremes of the assessed distributions, which insures that the width of the aggregated distribution will not be dominated by the overconfidence of any one expert. However, with performance based weighting the impact of an outlier can be completely eliminated (because of low performance scores) with a low or zero weight assigned to the distribution with which it is associated. Performance based weighting makes the assumption that the experts' performance on the variables of interest will be similar to their performance on the seed variables. This assumption is not required to implement the equal weighting scheme.

Many past formal expert elicitation studies (e.g., NUREG-1150,[4] WIPP,[5] Yucca Mountain,[6] etc.) have aggregated the results from the different experts by weighting each of the experts equally. Von Winterfeldt and Edwards[7] suggest that going beyond equal weighting is of little practical value. In addition, the evaluation of performance may not always be defensible.

D.6 Advantages of Performance Based Weighting Scheme

The primary potential advantages of performance measurement and performance based weighting are:

- calibration and information scores are provided to experts, thereby sensitizing them to possible biases;
- the weight allotted to individual expert distributions is determined by performance on seed variables;
- they provide techniques for evaluating of the use of expert subjective distributions in the assessment of uncertainty in decision-support modeling.

Performance based weighting schemes also have the potential to be less dependent on expert selection than the equal weighting scheme. The main burden in performance measurement is the measurement of expert calibration. The seed variables must resemble the variables of interest as closely as possible. The objectives of performance measurement are served only if performance on seed variables plausibly correlates with performance on variables of interest. The generation of seed variables therefore places demands on the uncertainty analyst: He must find actual experiments that resemble these hypothetical measurements as closely as possible and that can be conditionalized in the required manner. In addition, performance weights can be subject to high variance as a result of the dependence of the method on the seed variables. Changing the seed questions could potentially greatly impact the weights. The stability of weights, however, can be evaluated by considering subsets of the

seed questions. Performance assessment techniques, even if the information is not applied to the development of weights, have the potential of providing some indication of the robustness of the results of expert elicitation exercises.

D.7 Scoring and Weighting of Joint NRC/CEC Results

This section reviews the scores and weights calculated by EXCALIBR for the dispersion and deposition assessments. The tables below present the equal and performance based scores and weights for the assessments.****** The aggregated distribution is labeled DM (decision maker) in these tables. The "Number realiz" columns in the tables refer to the number of seed variables used to score the assessments. The remaining column headings are defined below:

Mean rel. inform, total:

Average information score calculated relative to the background measure over all items (i.e., both seed and elicitation variables).

Mean rel. infor, realiz:

Average information score calculated relative to background measure over only the seed variables.

UnNorm weight:

Product of calibration score and mean rel.infor realiz. if calibration score is not below significance level.

Normalized weight, no DM:

Weights used in computing decision maker; for item weights no values are shown, since these weights are assigned per item per expert.

Normalized weight, with DM:

Weights which would be used if DM were added as new "virtual expert"; indicates performance of DM relative to experts.

Tables D.1 through D.6 show that, in the performance based weighting schemes, some of the experts have been assigned zero weight. For global and item weighting, an expert is assigned zero weight if his calibration score is below the "significance level." The significance level is determined using optimization techniques.

Performance based weights were not calculated for wet deposition. It was originally intended that the same experts would assess wet and dry deposition variables. However, during the elicitation it appeared that very few experts considered themselves able to assess both sets of variables and it was necessary to split the deposition into wet and dry deposition groups. As a result, there were not enough seed variables to enable the performance based combinations of assessments for wet deposition.

The weights listed for dry deposition in Table D.5 show that item based aggregated dry deposition distribution is based solely on the Expert 2 distribution. Cooke[1] provides the following explanation for this performance based weighting result:

> It is well known that, within the deposition literature, large differences exist between theoretical predictions and empirical measurements of deposition velocity. Most experts apparently answered the elicitation questions in the following way: they used a theoretical model to derive their median assessment, and accounted for the possibility of large measured values by choosing a high 95% upper bound. This caused most realizations to fall above their median assessments. Since roughly half of the realizations should lie below the median assessments, this feature drives their calibration score down. Only Expert 2 accounted for the possibility of high measured values by raising his median assessment above the "theoretical values". Expert 2, subsequently, was very well calibrated and received all of the weight in both the item and global decision makers (for this reason these two decision makers coincide and only the item weight decision maker is shown).

The above explanation assumes that the seed variables used to calibrate the experts are sufficiently representative of dry deposition variables as a whole. There is no independent evidence for this assumption. It is also possible, therefore, that the seed variable data are unusual.

For dispersion, the total mean relative information scores are higher than the mean relative information scores over the seed variables. This is because the seed variables correspond to actual measurements, which are generally obtained close to the source, where the uncertainty is smaller. This effect is not observed on the deposition variables, which is reasonable because the uncertainty in atmospheric dispersion predictions increases with the distance from the source, whereas the uncertainty in deposition velocities is not likely to vary with distance from the source.

****** The experts are numbered 1 through 8 in these tables This numerical system does not correspond in any way to the alphabetic notation for experts used in Volume II of this document.

Table D.1 Dispersion: scores and weights, equal weights

Results of scoring experts.

Significance level: — Weight: equal Calibration power: 1.0

Expert name	Calibr.	Mean rel. infor.		Number	UnNorm	Normalized weight	
		total	realiz	realiz	weight	no DM	with DM
Expert 1	0.00010	2.078	1.281	23	0.00013	0.12500	0.00033
Expert 2	0.00010	1.594	1.431	23	0.00014	0.12500	0.00037
Expert 3	0.00100	1.504	1.285	23	0.00129	0.12500	0.00330
Expert 4	0.13000	1.286	1.242	23	0.16142	0.12500	0.41390
Expert 5	0.03000	1.092	1.622	23	0.04867	0.12500	0.12480
Expert 6	0.00500	1.590	1.540	23	0.00770	0.12500	0.01974
Expert 7	0.01000	1.508	1.506	23	0.01506	0.12500	0.03861
Expert 8	0.02000	1.840	1.312	23	0.02625	0.12500	0.06730
DM	0.15000	0.811	0.862	23	0.12935		0.33166

Table D.2 Dispersion: scores and weights, item weights

Results of scoring experts.

Significance level: 0.020 Weight: item Calibration power: 1.0

Expert name	Calibr.	Mean rel. infor.		Number	UnNorm	Normalized weight	
		total	realiz	realiz	weight	no DM	with DM
Expert 1	0.00010	2.078	1.281	23	0		0
Expert 2	0.00010	1.594	1.431	23	0		0
Expert 3	0.00100	1.504	1.285	23	0		0
Expert 4	0.13000	1.286	1.242	23	0.16142		0.13288
Expert 5	0.03000	1.092	1.622	23	0.04867		0.04006
Expert 6	0.00500	1.590	1.540	23	0		0
Expert 7	0.01000	1.508	1.506	23	0		0
Expert 8	0.02000	1.840	1.312	23	0.02625		0.02160
DM	0.90000	1.024	1.087	23	0.97849		0.80545

Table D.3 Dispersion: scores and weights, global weights

Results of scoring experts.

Significance level: 0.030 Weight: global Calibration power: 1.0

Expert name	Calibr.	Mean rel. infor.		Number	UnNorm	Normalized weight	
		total	realiz	realiz	weight	no DM	with DM
Expert 1	0.00010	2.078	1.281	23	0	0	0
Expert 2	0.00010	1.594	1.431	23	0	0	0
Expert 3	0.00100	1.504	1.285	23	0	0	0
Expert 4	0.13000	1.286	1.242	23	0.16142	0.76834	0.25142
Expert 5	0.03000	1.092	1.622	23	0.04867	0.23166	0.07581
Expert 6	0.00500	1.590	1.540	23	0	0	0
Expert 7	0.01000	1.508	1.506	23	0	0	0
Expert 8	0.02000	1.840	1.312	23	0	0	0
DM	0.36000	0.857	1.200	23	0.43196		0.671278

Table D.4 Dry Deposition: scores and weights, equal weights

Results of scoring experts.

Significance level: — Weight: equal Calibration power: 1.0

Expert name	Calibr.	Mean rel. infor.		Number	UnNorm	Normalized weight	
		total	realiz	realiz	weight	no DM	with DM
Expert 1	0.00010	1.953	1.799	14	0.00018	0.12500	0.00025
Expert 2	0.52000	1.434	1.339	14	0.69651	0.12500	0.98587
Expert 3	0.00100	1.702	1.503	14	0.00150	0.12500	0.00213
Expert 4	0.00100	1.734	1.820	14	0.00182	0.12500	0.00258
Expert 5	0.00010	1.792	1.792	14	0.00018	0.12500	0.00025
Expert 6	0.00100	2.234	2.457	14	0.00246	0.12500	0.00348
Expert 7	0.00100	1.695	1.869	14	0.00187	0.12500	0.00265
Expert 8	0.00050	1.985	1.581	14	0.00079	0.12500	0.00112
DM	0.00100	1.103	1.184	14	0.00118		0.00168

Table D.5 Dry Deposition: scores and weights, item weights

Results of scoring experts.

Significance level: 0.520 Weight: item Calibration power: 1.0

Expert name	Calibr.	Mean rel. infor.		Number	UnNorm	Normalized weight	
		total	realiz	realiz	weight	no DM	with DM
Expert 1	0.00010	1.953	1.799	14	0		0
Expert 2	0.52000	1 434	1.339	14	0.69651		0.50000
Expert 3	0.00100	1.702	1.503	14	0		0
Expert 4	0.00100	1.734	1.820	14	0		0
Expert 5	0.00010	1.792	1.792	14	0		0
Expert 6	0.00100	2.234	2.457	14	0		0
Expert 7	0.00100	1.695	1.869	14	0		0
Expert 8	0.00050	1.985	1.581	14	0		0
DM	0.52000	1.434	1.339	14	0.69651		0.50000

Table D.6 Wet Deposition: scores and weights, equal weights

Results of scoring experts.

Significance level: — Weight: equal Calibration power: 1.0

Expert name	Calibr.	Mean rel. infor.		Number	UnNorm	Normalized weight	
		total	realiz	realiz	weight	no DM	with DM
Expert 1	0.00010	2.139	2.066	5	0.00021	0.14286	0.00004
Expert 3	0.73000	1.823	1.773	5	1 29402	0.14286	0.24369
Expert 4	0.73000	1.163	0.791	5	0.57728	0.14286	0.10872
Expert 5	0.73000	1.992	1.882	5	1.37419	0.14286	0.25879
Expert 6	0.60000	1.846	2.128	5	1.27707	0.14286	0.24050
Expert 7	0.06000	1.979	1.974	5	0.11845	0.14286	0.02231
Expert 8	0.01000	2.740	3.108	5	0.03108	0.14286	0.00585
DM	0.73000	1.060	0.874	5	0.63771		0.12010

D.8 Discrepancy and Robustness Analysis

Discrepancy and robustness analysis are two additional evaluation tools available in EXCALIBR that allow further analysis of the individual and aggregated distributions. The EXCALIBR software package allows these analyses to be performed for both items and experts. Discrepancy analysis can be used to indicate how much the decision maker distribution differs from the distributions of the individual experts or to identify those items for which there is the greatest disagreement among the experts. Robustness analysis can indicate the impact of an individual seed variable on the performance aggregated decision maker or show how the decision maker distribution would be affected if an expert had not participated in the panel.

D.8.1 Discrepancy Analysis

In performing discrepancy analysis on experts, the average relative information of each expert's distributions is computed relative to the decision maker's distributions. This indicates how much the decision maker differs from the individual experts. Tables D.7 through D.10 present the results of a discrepancy analysis performed for the experts for the equal and item based decision makers. The lower the Rel.Inf. to DM score, the greater the agreement between the aggregated distribution and the individual expert distribution. Perfect agreement is indicated by zero. Tables D.7 and D.8 indicate that, for dispersion, the distribution provided by Expert 4 most resembles the aggregated distribution for both the equal and item based distributions. However, the Rel.Inf. to DM Expert 4 score is much lower for item weights than for equal weights, as would be expected because Expert 4 was assigned the greatest weight in the development of the item based aggregated dispersion distributions. Table D.10 indicates that the item based dry deposition distribution was simply the distribution provided by Expert 2. In the equal weight dry deposition discrepancy analysis results listed in Table D.9, the distribution provided by Expert 2 does not receive the lowest Rel.Inf. to DM score.

Tables D.8 and D.10 indicate that the degree to which an expert's distributions resemble those of the performance based decision maker do not strictly coincide with the expert's weights. Comparing Tables D.2 and D.8, we see that Experts 7 and 8 more closely resemble the decision maker for seed variables than Expert 5, even though Expert 5 has more weight. This is a natural effect of the optimization routine; an expert may receive zero weight not because his performance is low, but because his distributions do not differ much from distributions of better calibrated experts. Including such experts does not improve the score of the decision maker. Tables D.7 and D.9 show that the relative information of an expert proportionate to the equal weight decision maker tends to be about 0.5 for seed items. This observation may be taken as an indication of how well the experts' distributions agree with each other. For the item weight decision makers, the variation across experts is greater because the experts do not exert equal influence on the decision maker.

D.8.2 Robustness Analysis

For robustness analysis on experts, the experts are removed from the data set one at a time, and the decision maker is recalculated. Tables D.11 through D.14 list the result of the robustness analysis on experts for both equal and item weights. For dispersion, the effect of removing one expert for the equal weight DM is seen in Table D.11. Compared with the individual discrepancies between the experts and the equal weight DM (Table D.7), the effect of removing one expert is small. For the item weight DM the same is true (Tables D.8 and D.12), although the effect of removing one expert is more variable. Tables D.11 and D.12 show that the greatest difference between the original aggregated distribution and the aggregated distribution developed by eliminating one of the expert-distribution results from the exclusion of the Expert 2 and Expert 4 distributions for equal and item weights respectively. The dry deposition results in Table D.14 again show the dependence of the aggregated item based dry deposition results on a single distribution, that of Expert 2.

For robustness analysis on items, the seed variables are removed one at a time and the decision maker is recalculated. Because the equal weight decision maker is not affected by this operation, robustness on items is not performed for the equal weight decision maker. Tables D.15 and D.16 show the results for the item weight decision makers for dispersion and dry deposition respectively. For the dispersion item results listed in Table D.15, there did not appear to be a large difference between the impact of any one seed variable. The deposition results listed in Table D.16 however indicate that the item based aggregated results were dominated by two seed variables.

Table D.7 Dispersion: discrepancy analysis for experts, equal weights

Results of scoring experts and Experts Relative Information to DM.
Weights: equal

Expert name	Calibr.	Mean rel. infor.		Rel. Inf. to DM	
		total	realiz	total	realiz.
Expert 1	0.00010	2.078	1.281	1.094	0.398
Expert 2	0.00010	1.594	1.431	0.943	0.672
Expert 3	0.00100	1.504	1.285	0.769	0.445
Expert 4	0 13000	1.286	1.242	0 486	0.397
Expert 5	0 03000	1 092	1.622	0.588	0.596
Expert 6	0.00500	1.590	1.540	0.686	0.693
Expert 7	0.01000	1.508	1.506	0.609	0.595
Expert 8	0.02000	1.840	1.312	0.879	0.526
DM	0.15000	0.811	0.862	0	0

Table D.8 Dispersion: discrepancy analysis for experts, item weights

Results of scoring experts and Experts Relative Information to DM.
Weights: item

Expert name	Calibr.	Mean rel. infor.		Rel. Inf. to DM	
		total	realiz	total	realiz.
Expert 1	0.00010	2.078	1.281	1.074	0.789
Expert 2	0.00010	1.594	1.431	0.951	0.828
Expert 3	0.00100	1.504	1.285	0.746	0.626
Expert 4	0.13000	1.286	1.242	0.301	0.160
Expert 5	0.03000	1.092	1.622	0.642	0.514
Expert 6	0.00500	1.540	1.540	0.660	0.658
Expert 7	0.01000	1.506	1.506	0.582	0.510
Expert 8	0.02000	1.840	1.312	0.744	0.485
DM	0.15000	1.024	1.087	0	0

Table D.9 Dry Deposition: discrepancy analysis for experts, equal weights

Results of scoring experts and Experts Relative Information to DM.
Weights: equal

Expert name	Calibr.	Mean rel. infor.		Rel. Inf. to DM	
		total	realiz	total	realiz.
Expert 1	0.00010	1.953	1.799	0.852	0.554
Expert 2	0.52000	1.434	1.339	0.419	0.363
Expert 3	0.00100	1.702	1.503	0.555	0.288
Expert 4	0.00100	1.734	1.820	0.610	0.577
Expert 5	0.00010	1.792	1.792	0.651	0.578
Expert 6	0.00100	2.234	2.457	1.137	1.199
Expert 7	0.00100	1.695	1.869	0.618	0.649
Expert 8	0.00050	1.985	1.581	0.860	0.466
DM	0.00100	1.103	1.184	0	0

Table D.10 Dry Deposition: discrepancy analysis for experts, item weights

Results of scoring experts and Experts Relative Information to DM.
Weights: item

Expert name	Calibr.	Mean rel. infor.		Rel. Inf. to DM	
		total	realiz	total	realiz.
Expert 1	0.00010	1.953	1.799	1.551	0.915
Expert 2	0.52000	1.434	1.339	0	0
Expert 3	0.00100	1.702	1.503	0.910	0.495
Expert 4	0.00100	1.734	1.820	1.269	1.003
Expert 5	0.00010	1.792	1.792	1.263	1.051
Expert 6	0.00100	2.234	2.457	1.748	1.269
Expert 7	0.00100	1.695	1.869	1.357	1.084
Expert 8	0.00050	1.985	1.581	1.382	1.287
DM	0.52000	1.434	1.339	0	0

Table D.11 Dispersion: robustness on experts, equal weights

Robustness analysis on Experts.
Significance level: — Weight: equal Calibration power: 1.0

Excluded Expert name	Rel. inf. to background		Calibration	Rel. Inf. to original DM	
	total	realiz		total	realiz.
None	0.862	0.811	0.150	0	0
Expert 1	0.795	0.894	0.25000	0.072	0.059
Expert 2	0.816	0.860	0.15000	0.042	0.060
Expert 3	0.812	0.866	0.25000	0.039	0.028
Expert 4	0.822	0.897	0.06000	0.038	0.050
Expert 5	0.674	0.842	0.25000	0.181	0.021
Expert 6	0.796	0.851	0.25000	0.041	0.034
Expert 7	0.775	0.855	0.25000	0.070	0.024
Expert 8	0.794	0.840	0.15000	0.073	0.056

Table D.12 Dispersion: robustness on experts, item weights

Robustness analysis on Experts.
Significance level: 0.020 Weight: item Calibration power: 1.0

Excluded Expert name	Rel. inf. to background		Calibration	Rel. Inf. to original DM	
	total	realiz		total	realiz.
None	1.087	1.024	0.900	0	0
Expert 1	1.023	1.087	0.90000	0.000	0.000
Expert 2	1.015	1.049	0.90000	0.001	0.004
Expert 3	1.024	1.087	0.90000	0.001	0.002
Expert 4	1.193	1.227	0.44000	0.450	0.241
Expert 5	0.875	1.069	0.85000	0.191	0.035
Expert 6	1.021	1.076	0.51000	0.002	0.007
Expert 7	0.980	1.087	0.90000	0.004	0.000
Expert 8	0.981	1.108	0.51000	0.133	0.086

Table D.13 Dry Deposition: robustness on experts, equal weights

Robustness analysis on Experts.

Significance level: — Weight: equal Calibration power: 1.0

Excluded Expert name	Rel. inf. to background total	realiz	Calibration	Rel. Inf. to original DM total	realiz.
None	1.184	1.103	0.001	0	0
Expert 1	1.107	1.172	0.00100	0.023	0.014
Expert 2	1.169	1.334	0.00100	0.058	0.116
Expert 3	1.096	1.178	0.00100	0.013	0.013
Expert 4	1.107	1.171	0.00100	0.022	0.016
Expert 5	1.111	1.173	0.00100	0.026	0.015
Expert 6	1.131	1.175	0.00100	0.047	0.030
Expert 7	1.154	1.173	0.00100	0.063	0.014
Expert 8	1.124	1.284	0.00100	0.041	0.110

Table D.14 Dry Deposition: robustness on experts, item weights

Robustness analysis on Experts.

Significance level: 0.520 Weight: item Calibration power: 1.0

Excluded Expert name	Rel. inf. to background total	realiz	Calibration	Rel. Inf. to original DM total	realiz.
None	1.339	1.434	0.520	0	0
Expert 1	1.434	1.339	0.52000	0	0
Expert 2	1.262	1.529	0.05000	0.905	0.554
Expert 3	1.434	1.339	0.52000	0	0
Expert 4	1.434	1.339	0.52000	0	0
Expert 5	1.434	1.339	0.52000	0	0
Expert 6	1.444	1.339	0.52000	0	0
Expert 7	1.430	1.339	0.52000	0	0
Expert 8	1.434	1.339	0.52000	0	0

Table D.15 Dispersion: robustness on items, item weights

Robustness analysis on Items.
Significance level: 0.020 Weight: item Calibration power: 1.0

Excluded Item name	Rel. inf. to background total	Rel. inf. to background realiz	Calibration	Rel. Inf. to original DM total	Rel. Inf. to original DM realiz.
B-1-220 chi/Q	1.031	1.806	0.47000	0.043	0.016
B-1-315 chi/Q	1.021	1.074	0.47000	0.059	0.022
B-2-220 chi/Q	1.030	1.079	0.47000	0.043	0.016
B-2-315 chi/Q	1.066	1.032	0.86000	0.072	0 055
B-3-300 chi/Q	0.907	1 172	0.43000	0.245	0.160
B-3-600 chi/Q	0.962	1.153	0 86000	0.167	0.090
B-4-300 chi/Q	0.991	1.071	0.86000	0.059	0.011
B-4-600 chi/Q	1.022	1.081	0.47000	0.059	0.022
B-5-600 chi (y)	1.030	1.093	0.43000	0.062	0.017
B-5-600 chi (z)	1.051	1.250	0.47000	0.142	0.133
B-5-600 sig-y	1.050	1.101	0.86000	0.025	0.013
B-5-600 sig-z	1.054	1 120	0.86000	0.025	0.015
C-60-1 chi/Q	0.985	1.224	0.43000	0.132	0.109
C-60-2 chi/Q	1.045	1.080	0.86000	0.025	0.015
C-60-3 chi/Q	1.040	1.072	0 86000	0.024	0.018
C-120-1 chi/Q	1.012	1.103	0.97000	0.048	0.014
C-120-2 chi/Q	1 045	1.081	0.86000	0.025	0.015
C-120-3 chi/Q	1.040	1.071	0.86000	0.024	0.018
C-240-1 chi/Q	1.012	1.103	0.97000	0.048	0.014
C-240-2 chi/Q	1.045	1.081	0.86000	0.025	0.015
C-240-3 chi/Q	1.195	1.040	0.76000	0.211	0.073
D-60 sig-z	1.127	1.085	0.86000	0.103	0.035
D-60 sig-y	1.084	1.078	0.40000	0.264	0.063

Table D.16 Dry Deposition: robustness on items, item weights

Robustness analysis on Items.
Significance level: 0.520 Weight: item Calibration power: 1.0

Excluded Item name	Rel. inf. to background total	Rel. inf. to background realiz	Calibration	Rel. Inf. to original DM total	Rel. Inf. to original DM realiz.
None	1 339	1.434	0.52000	0	0
DD-E-1 0.55 mu	1.436	1.345	0.38000	0	0
DD-E-1 0.7 mu	1.436	1.346	0.38000	0	0
DD-E-1 0.9 mu	1 436	1.346	0.38000	0	0
DD-E-1 1.2 mu	1.436	1.342	0.58000	0	0
DD-E-1 1.6 mu	1.435	1.340	0.58000	0	0
DD-E-2 0.55 mu	1.436	1.345	0.38000	0	0
DD-E-2 0.7 mu	1.436	1.346	0.58000	0	0
DD-E-2 0.9 mu	1.436	1.346	0.58000	0	0
DD-E-2 1.2 mu	1.436	1.342	0.58000	0	0
DD-E-2 1.6 mu	1.435	1.340	0.58000	0	0
DD-E-2 2.3 mu	1.344	1.290	0.38000	0.180	0.016
DD-E-2 3.2 mu	1.434	1.335	0.58000	0	0
DD-E-2 4.2 mu	1.322	1.264	0.66000	0.255	0.164
DD-F 0.5-2.0	1.436	1.345	0.38000	0	0

D.9 Analyses of Equal and Performance Based Aggregated Elicited Dispersion and Deposition Distributions

This section analyzes the aggregated equal and item based distributions. The figures discussed in this section are presented after Tables D.17 through D.20, which contain the information used in the MACCS calculations.

D.9.1 Equal Weighted and Item Based Weighting: Dispersion Distributions

Figures representing the central measure and the uncertainty measure of the elicitation variables for the eight dispersion experts, along with the equal and item weight based aggregated results, are presented in Figures D.1 through D.10. As the figures show, very little difference is observed between the median assessments produced using the two aggregation methods. Figures D.7 and D.8 indicate that the item weight performance scheme can have the effect of significantly narrowing the aggregated uncertainty band that would be produced by equal weighting. Figures D.9 and D.10 show that the item weighting scheme has typically served to increase the value of the 5th percentile and decrease the value of the 95th percentile, although the difference between the 5th and 95th percentile values resulting from the two weighting schemes is much less than an order of magnitude.

D.9.2 Equal Weighted and Item Based Weighting: Dry Deposition Velocity Distributions

Figures representing the central measure and the uncertainty measure of the dry deposition velocities are presented for both aerosols and elemental iodine for the eight deposition experts in Figures D.11 to D.14, along with the equal and item based aggregated results. The difference between the equal and item based weighting results plotted in Figure D.13 for the 50th percentile values of the dry deposition velocity of elemental iodine are negligible. The differences between the item and equal weighted results for the 95th/5th percentile ratios, though not negligible, are nevertheless not great. The differences between the values obtained with the two weighting methodologies for the median aggregates for the dry deposition velocity of aerosols as plotted in Figure D.11, however, are substantial. As discussed in Section D.6, the item based aggregated results for dry deposition are established on the assessments of only one expert. The impact of the difference between the dry deposition equal and performance based weighted distributions on a consequence analysis is discussed in the next section.

D.9.2.1 Impact of Differences Between Equal and Item Based Aggregation of Dry Deposition Data on Consequence Calculations

MACCS calculations were performed to evaluate the potential impact of the difference between equal and item based aggregated distributions. Two cases were analyzed. All parameters in the code were held constant with the exception of the dry deposition velocity. Samples of 20 dry deposition velocities were randomly selected from the equal and item based aggregated distributions, and the code was run 20 times for each case. The distributions used for these cases were those for which the greatest difference was observed between the equal and item based weighting methods. The wind speed, constant weather, and stability class were defined consistent with the initial and boundary conditions defined for the distributions. No evacuation was assumed. The results are discussed below.

Case 1

The first case is for deposition to an urban area for a particle size of 3 μm. Table D.17 contains the different percentile values of the distributions from EXCALIBR. Table D.18 shows the resulting consequence measures.

Case 2

For the second comparison, the distributions for forest and particle size of 3 μm were used. The information on these calculations is presented in Tables D.19 and D.20. The difference between the mean value for the doses is likely the result of the equal weighting distributions producing samples with higher deposition velocities than the performance based distributions. Therefore, more material is being removed from the plume early in its transport (i.e., before the plume reaches farmland and population). Because of this condition, the population dose is lower for

the equal weighting than for the performance based weighting. Note that the difference in minimum doses exhibited in the following tables is related to the difference in maximum deposition velocity.

Table D.17 Dry deposition velocity distributions for an urban area and a particle size of 3 μm; EXCALIBR percentiles

	Dry Deposition Velocity (cm/s)		
	5%	50%	95%
Equal Weighting			
EXCALIBR	.035	.46	19
Performance Based Weighting			
EXCALIBR	.08	4.0	30

Table D.18 Population dose for an urban area and a particle size of 3 μm for both EARLY and CHRONC data

	Population Dose (person-Sv)		
	min.	mean	max.
EARLY			
Equal Weighting	2880	36500	65600
Performance Based Weighting	1510	30100	61900
CHRONC			
Equal Weighting	19600	486000	1060000
Performance Based Weighting	9580	441000	1040000

Table D.19 Dry deposition velocity distributions for forest and a particle size of 3 μm

	Dry Deposition Velocity (cm/s)		
	5%	50%	95%
Equal Weighting			
EXCALIBR	.115	1.85	208
Performance Based Weighting			
EXCALIBR	.08	4.0	30

Table D.20 Population dose for forest and a particle size of 3 μm

	Population Dose (person-Sv)		
	min.	mean	max.
EARLY			
Equal Weighting	178	17400	33700
Performance Based Weighting	2760	23900	33400
CHRONC			
Equal Weighting	634	347000	972000
Performance Based Weighting	14500	462000	984000

The indication from the above cases is that the different aggregation schemes did not make much difference in the median and upper percentile results for both early and chronic results, but observable differences were found in the lower percentiles. Because the middle and upper percentiles tend to dominate the results of interest to the risk and regulatory communities, this difference is not likely to be of much concern. It is not surprising that little difference was demonstrated because the overall placement of the central mass of the uncertainty distributions is similar in the equal weighted scheme and the performance based weighting scheme. However, a calculation based on the median values would probably result in a visible difference in consequence measures.

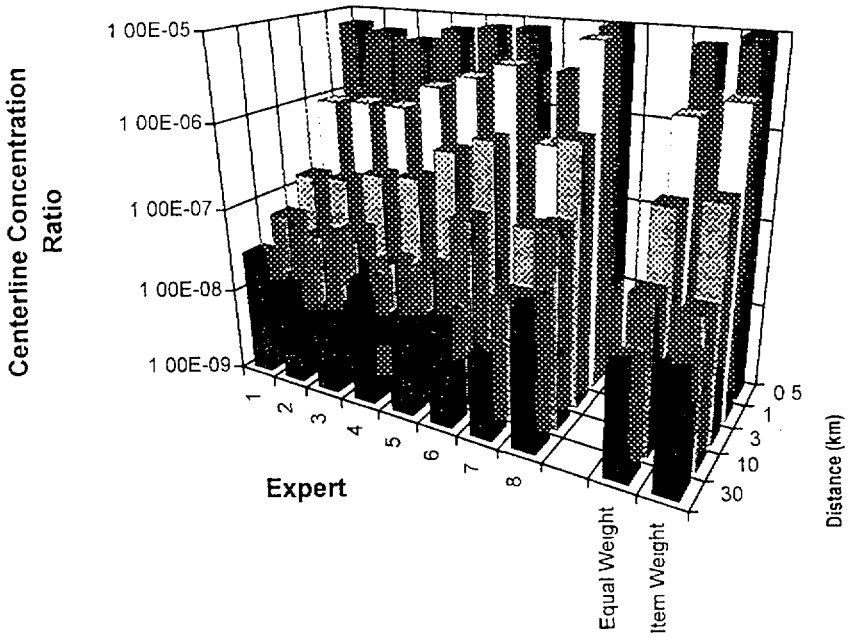

Figure D.1 Elicited values for 50th percentile χ_c/Q, stability class A

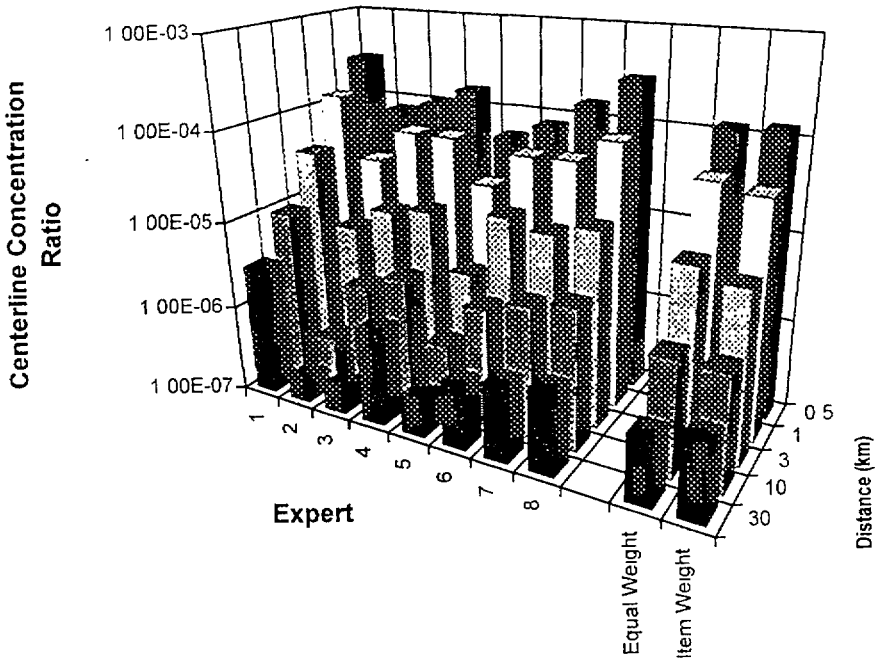

Figure D.2 Elicited values for 50th percentile χ_c/Q, stability class E/F

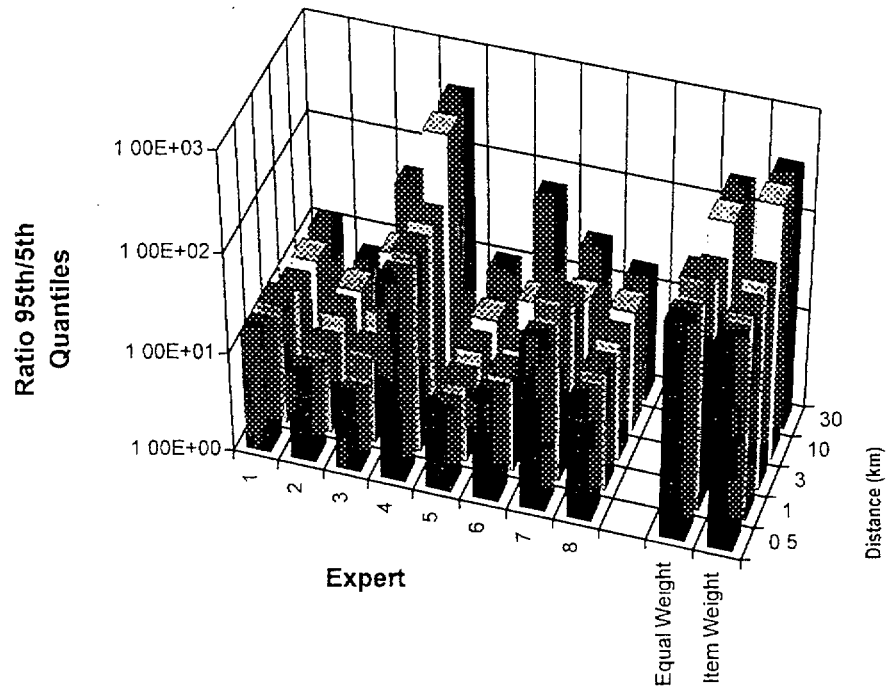

Figure D.3 Ratio of 95th/5th percentile elicited χ_c/Q, stability class A

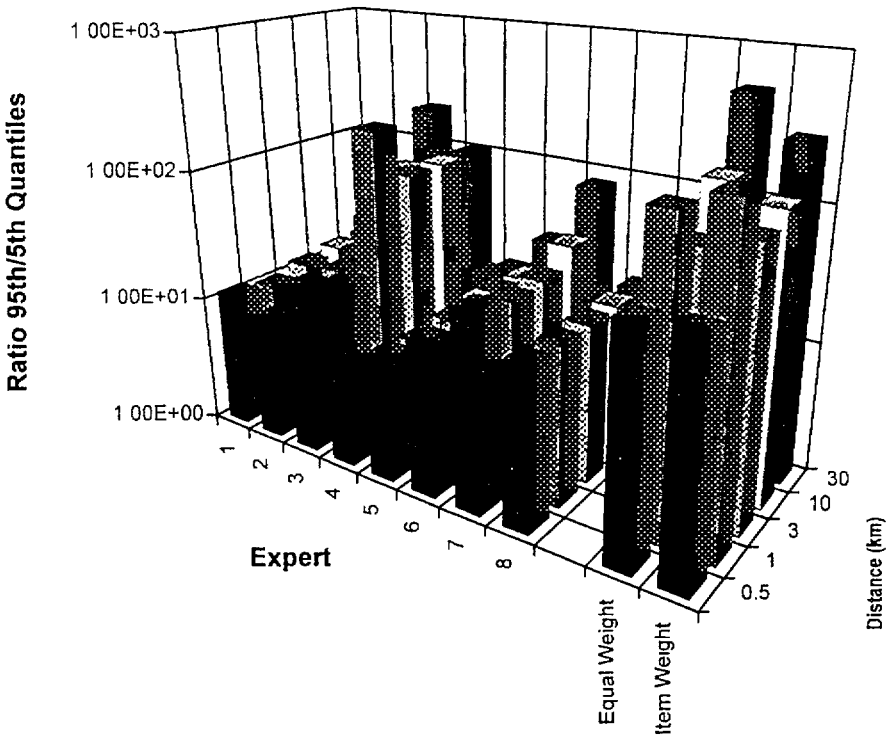

Figure D.4 Ratio of 95th/5th percentile elicited χ_c/Q, stability class E/F

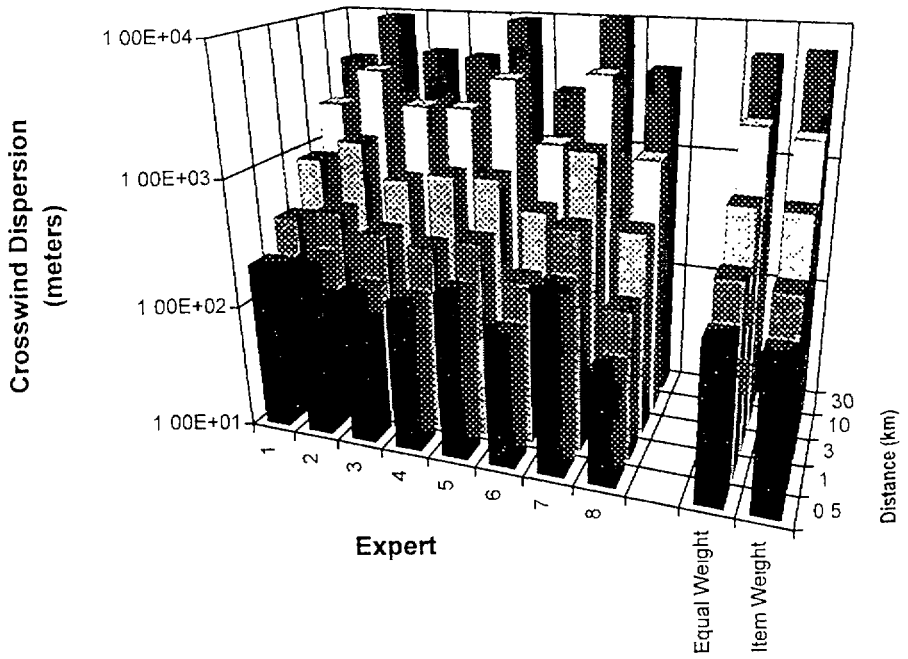

Figure D.5 50th percentile elicited s_y (crosswind dispersion) values, stability class A

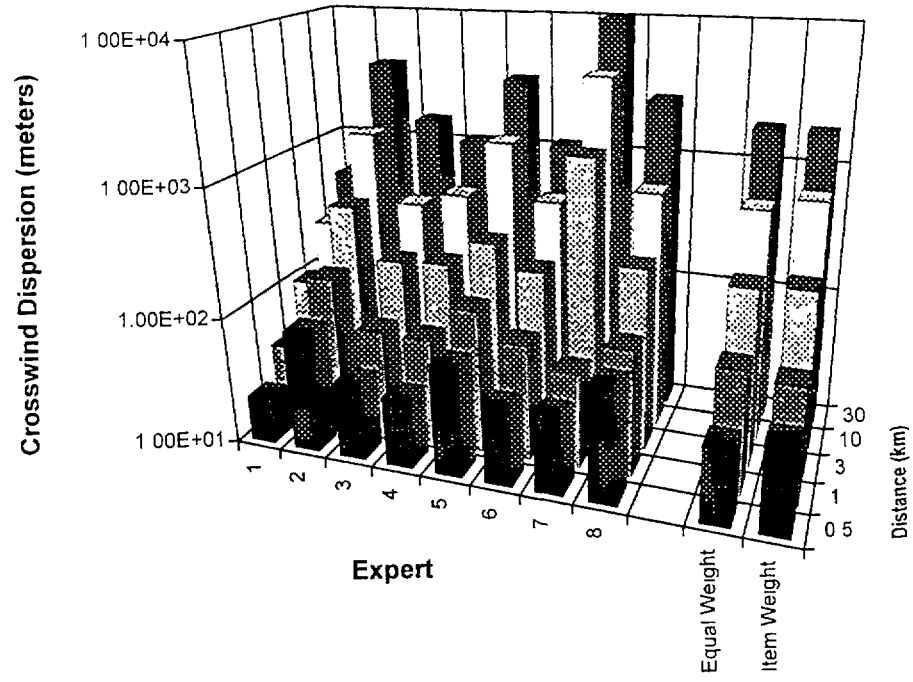

Figure D.6 50th percentile elicited s_y (crosswind dispersion) values, stability class E/F

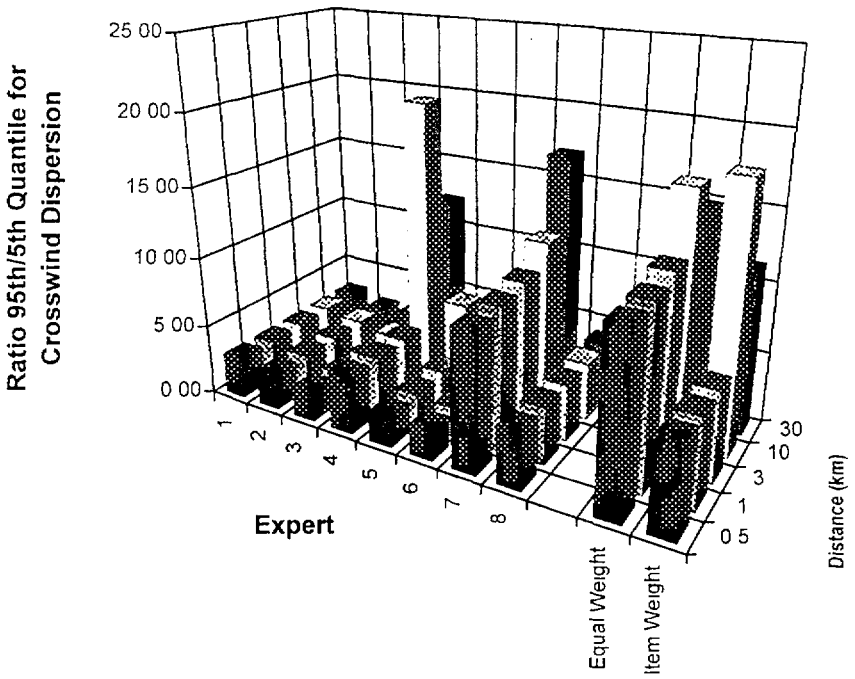

Figure D.7 Ratio of elicited 95th/5th percentiles for the elicited s_y (crosswind dispersion), stability class A

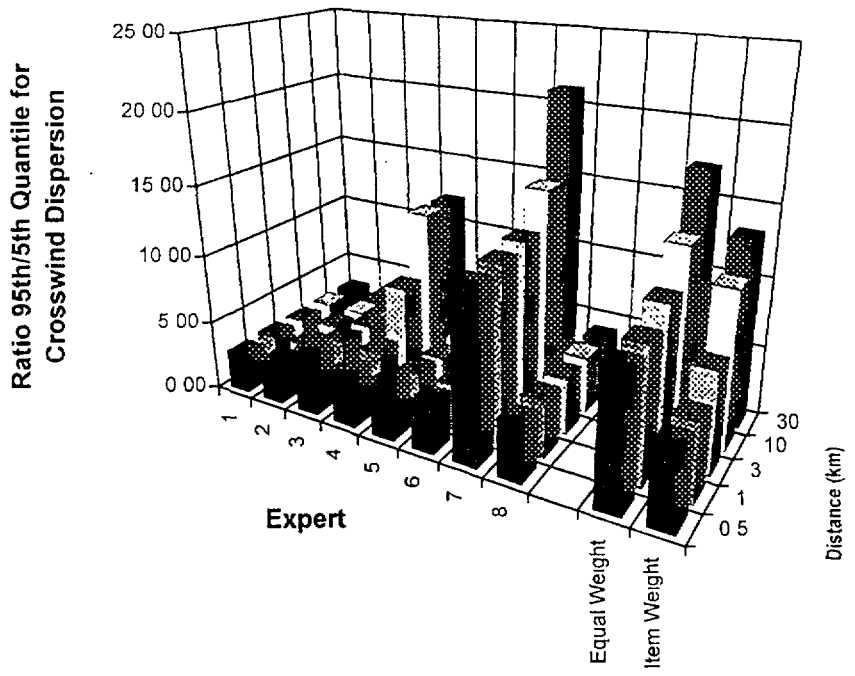

Figure D.8 Ratio of elicited 95th/5th percentiles for s_y (crosswind dispersion). stability class E/F

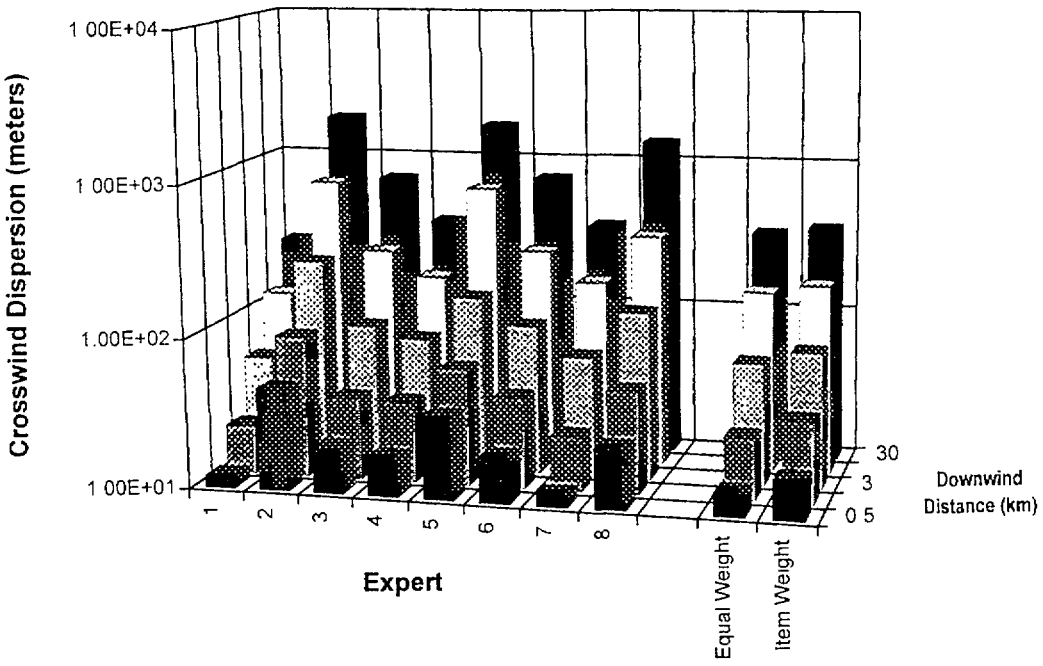

Figure D.9 Elicited and aggregated 5th percentile data for s_y (crosswind dispersion), stability class E/F

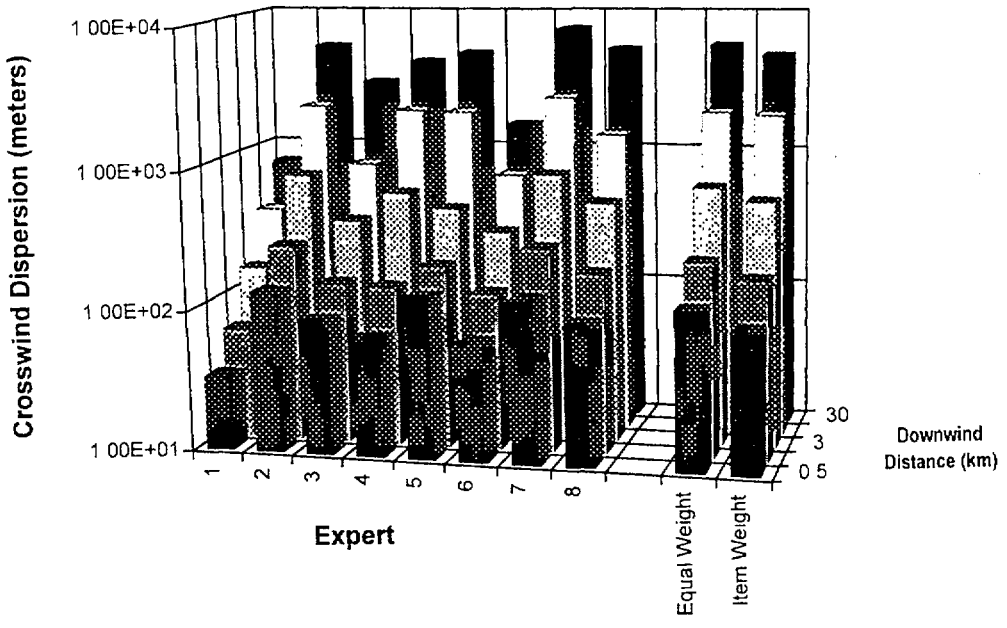

Figure D.10 Elicited and aggregated 95th percentile data for s_y (crosswind dispersion), stability class E/F

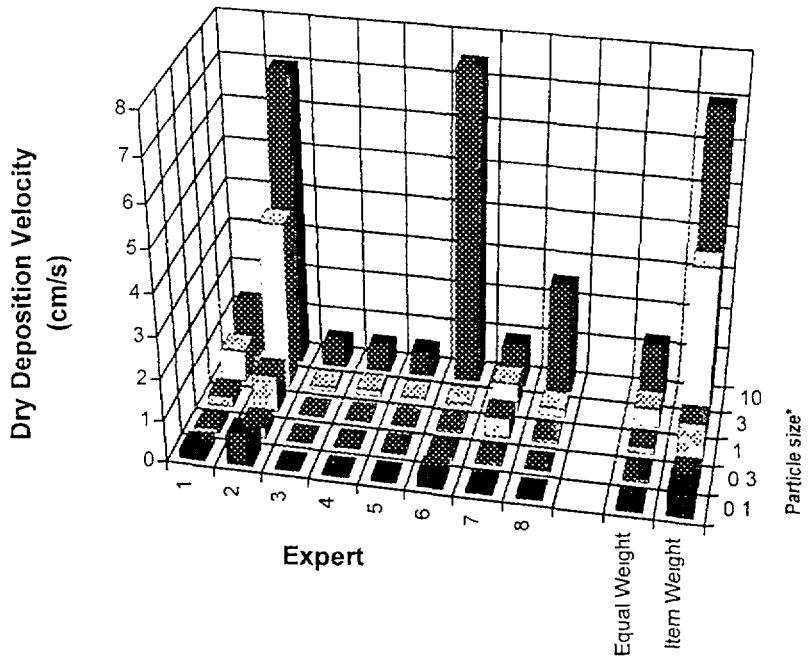

Figure D.11 50th percentile elicited dry deposition velocity of aerosols onto urban surface, wind speed 2 m/s

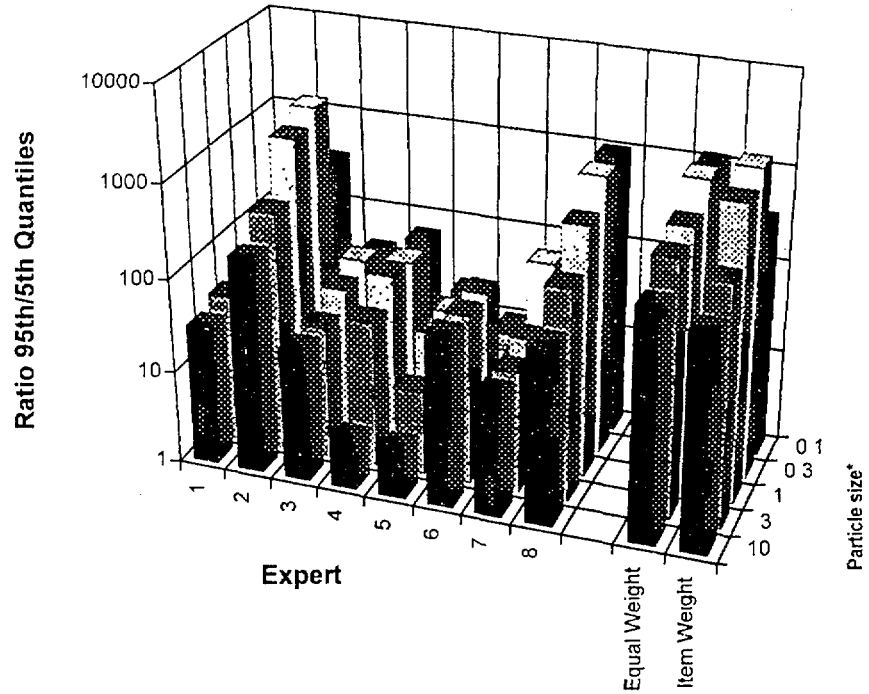

Figure D.12 Ratio of 95th/5th percentile elicited aerosol dry deposition velocity; urban surface, wind speed 2 m/s

* The order of the particle size parameters (expressed in μm) differs between Figures D 11 and D.12 so the data can be viewed more clearly

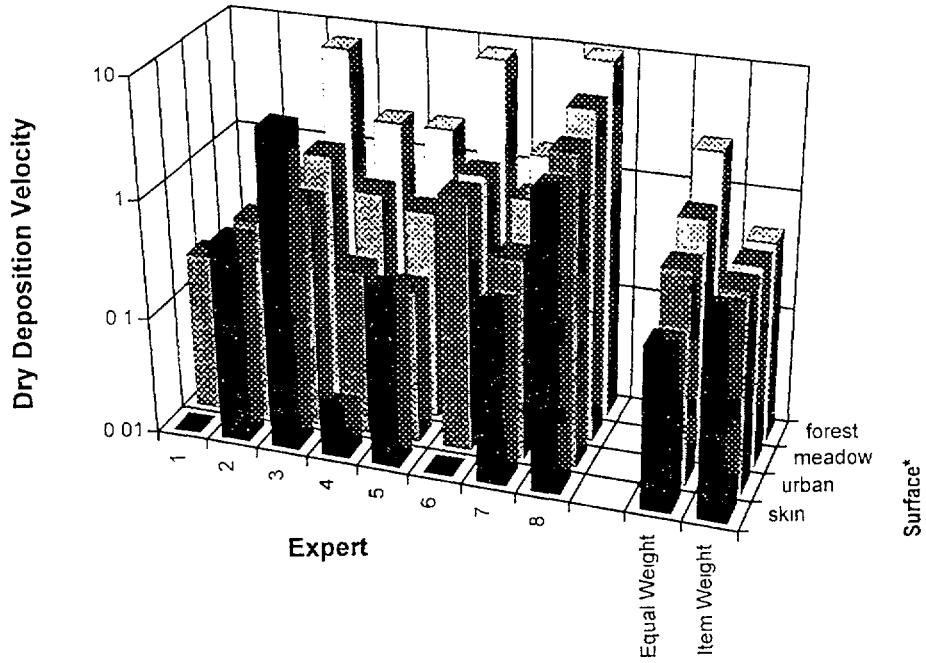

Figure D.13 Elicited 50th percentile dry deposition velocities of elemental iodine; wind velocity 2 m/s

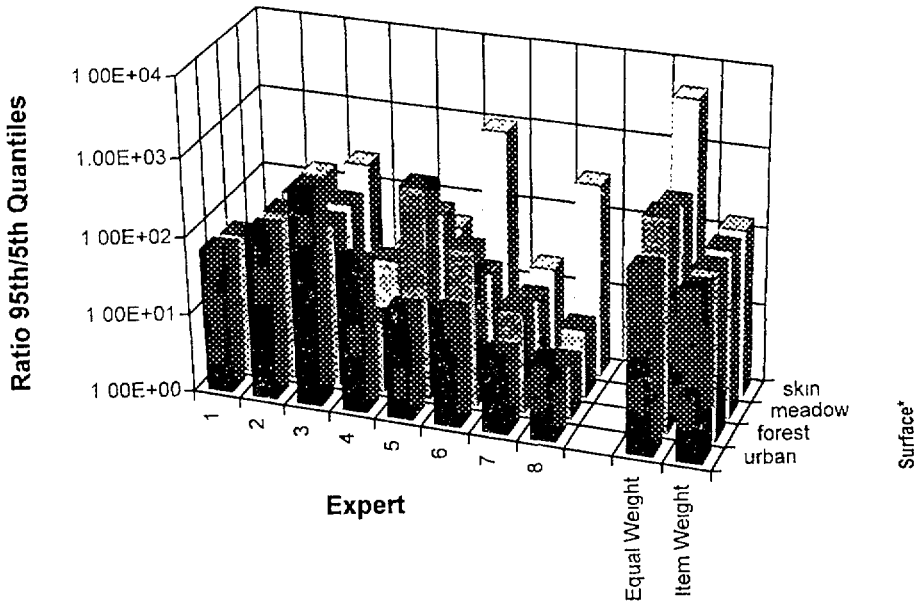

Figure D.14 Ratio 95th/5th elicited percentile values for the dry deposition elemental velocity of iodine, wind velocity 2 m/s

* The order of the surface parameters differs between Figures D 13 and D 14 so the data can be viewed more clearly

D.10 Dispersion and Deposition Seed Variables

The seed variables listed in this section were used in the determination of weights for the performance based weighting aggregation schemes implemented in this project. Cooke[8] has provided the following description of seed variables:

> It will often arise that the decision maker needs assessments for events, none of which will be observed within a required time frame. This typically occurs in risk analysis, where probabilities for unlikely and nonrepetitive events must be assessed. In this case the model must be "seeded" with other events, whose outcome are known, or become known within a short time. These seed variables must be drawn from the experts' area of expertise, but need not pertain to the problem at hand. Weights are then determined on the basis of seed variables and used to define the decision maker's distributions for the variables of interest. The choice of meaningful seed variables is difficult, and critical.

The seed variables used in this project were derived from experiments in the same field as the elicitation variable. Finding seed variables for dispersion and deposition required finding actual tracer experiments performed under circumstances that were amenable to the case structure of the variables of interest. Three sets of tracer experiments were found suitable for dispersion, two sets of aerosol experiments were found suitable for dry deposition, and one iodine experiment was found suitable for wet deposition.

At the time of the elicitation, the experimentally determined value of the seed variable in question was known by the normative expert, but not by the substantive assistant. Most of the seed variables listed are from recent experiments which had not been published at the time of the elicitation.

D.10.1 Dispersion Seed Variables

Twenty-three seed variables were defined for the dispersion panel. The B, C and D cases in the dispersion case structure, as presented in Appendix F, are seed variables derived from the following experiments:

1. The B-cases are based on Danish tracer experiments called BOREX '92, "Concentration fluctuations measured during the BOREX '92 elevated plume experiment" conducted by Erik Lyck, Per Loefstroem, Hans E. Joergenson and Torben Mikkelsen of the Danish Center for Atmospheric Research, P.O. Box 358, DK-4000 Roskilde.

2. The C- cases are based on French tracer experiments at the Cadarache Nuclear Research Center conducted by B. Crabol and G. Deville-Cavelin, "Assessment of dispersion of fission products in the atmosphere following a reactor accident under meteorological conditions of low wind speeds with or without high temporal and spatial variability in wind speeds and direction," November, 1984, experiment 12.

3. The D-cases are based on British experiments performed by British Gas, Midlands Research Station (Dr. R. Brown), Solihull, UK and the National Physical Laboratory (Dr. B. Jolliffe), Teddington, UK, experiment 73 on October 20, 1992.

Danish Experiments

These experiments come from the so-called BOREX '92 tracer experiments, cited as "Concentration fluctuations measured during the BOREX '92 elevated plume experiment."

Two experiments were used for seed variable questions. The first experiment concerned a tracer experiment, and the second experiment concerned an experiment in which measurements were carried out using a Light Detecting and Ranging (LIDAR) system. In conducting a tracer experiment, collectors are positioned along the travel direction of the plume. These collectors measure ground level concentrations. The release of both experiments consisted of sulfur hexafluoride (SF_6), which was used because it does not easily disintegrate and can therefore be measured at relatively large distances from the source.

A LIDAR system can be viewed as a detection instrument. The system consists of a pulsed laser, a photodetector and preamplifiers, a transient recorder, a PC-controlled data storage system, and a monitoring facility. The principle of the LIDAR can be explained as follows: Pulsed laser radiation of very short duration is transmitted horizontally through the aerosol plume, where a small fraction

proportional to the number of aerosols in the measurement volume is backscattered into the telescope. The time between transmission and reception of a light pulse indicates the range between the particles and the LIDAR. At the same time, the intensity of the signal reflects the particle concentration in the small volume occupied by the traveling light pulse. The data processing of measured backscatter profiles has been performed in order to correct the LIDAR measurements for range dependence and extinction.

For most of the stability classes, either tracer or LIDAR experiments were available. The meteorological data were rather complete and were determined at a 10 minute average; it contained either the temperature lapse rate or Monin-Obukhov length, windspeed, σ_θ (the standard deviation of wind direction fluctuation in horizontal direction), surface roughness, and release height. The downwind distances varied from 220 to 600 m.

Because most of the experiments concerned measurements of ground level concentration and standard deviations of the plume, the experts were queried about these variables.

French Experiments

The French experiments involved assessments of the dispersion of fission products in the atmosphere following a reactor accident under meteorological conditions of low windspeeds with or without high temporal spatial variability in windspeed and direction.

The determination of meteorological conditions was performed using four weather stations, which were located on the experimental site at Cadarache, France. The meteorological data consisted of wind speed and wind direction (at different heights), the sampling time, and the vertical temperature lapse rate.

The release of 40 kg of SF_6 was made at a constant rate during one hour. Along the travel direction of the plume, collectors were positioned to measure ground level concentrations. The data acquired in this experiment therefore consisted of ground level concentrations at various distances for various sampling times. Hence the experts were queried about the ground level concentration at various downwind distances for various sampling times ranging from one to four hours after the start of the release.

British Experiments

The British experiments were performed by Dr. R. Brown from the British Gas Midlands Research Station, Solihull, and Dr. B. Joliffe from the National Physics Laboratory, Teddington. The experiment, known as Experiment 23, was performed on October 20, 1992.

These experiments were also carried out using a LIDAR system. The material released contained 90% nitrogen and 10% methane and was released from a 1-m-diameter source. With the LIDAR system, concentrations of gas at various downwind distances were measured. At each downwind distance, detailed meteorological data on the wind speed and wind direction were acquired. Additional measurements were carried out at the source in order to determine the vertical wind profiles and turbulence length scales.

The data acquired was used to look for fluctuations or relative effects in the concentration close to the source, and hence the experts were queried about the standard deviation of the vertical as well as the crosswind concentration at 60 m from the source at one minute sampling time.

D.10.2 Deposition Seed Variables

Nineteen deposition seed variables were defined (14 on dry deposition and 5 on wet deposition). The B-cases in the dry deposition case structure, as presented in Appendix F, are seed variables derived from the following experiments:

1. One seed variable is based on experiments in the Netherlands on dry deposition velocities performed by ECN (Energy Centre of the Netherlands, Petten, the Netherlands), personal communication with Dr. J. Slanina.

2. The other seed variable is based on experiments performed by TNO (Netherlands Research Organization for Applied Scientific Research, Delft, the Netherlands), J. H. Duyzer and F. C. Bosveld, "Measurements of dry deposition fluxes of O_3 NO_x, SO_2 and particles over grass/heathland vegetation and the influence of surface in homogeneity," KNMI-TNO/MT report R 88/111, 1988.

Dutch Experiments I

The Dutch experiments come from KNMI/TNO/The Netherlands, aerosol measurements at two locations in the Netherlands (Duyzer, Bosveld, 1988). Aerosols of specified particle sizes were released and collected, from which dry deposition velocities were measured. Several experiments took place.

One experiment was over moorland and peatland with vegetation consisting of 40-cm-high tussocks and old dry grass partly filling the spaces between the tussocks and underlain by a wet peat layer. Wind speeds were an average of 5 m/s measured at a 5-m height. The surface roughness length was reported to be 5 cm, ± 1 cm. Particle sizes between 0.55μm and 1.6μm were used.

One experiment was over heather and green grass where vegetation only partly covered the soil. Wind speeds were an average of 5 m/s measured at a 5-m height. The surface roughness length was reported to be 4.5 cm, ± 1.5 cm. Particle sizes between 0.55μm and 4.2μm were used.

Dutch Experiments II

These experiments come from ECN/The Netherlands, aerosol measurements at one location in the Netherlands. Aerosols of specified particle sizes (ranging from 0.5μm to 2.0μm) were released and collected, from which dry deposition velocities were measured. Several experiments took place.

French Experiments

The B-cases in the wet deposition case structure as presented in Appendix F are seed variables based on French experiments conducted by C. Caput, H. Camus, D. Guthier, and Y. Beot, "Etude experimental du lavage de L'iode par la pluie", *Radioprotection*, 1993, Vol. 1. These elemental iodine washout experiments were carried out at two locations in France and at various wind speeds and rain intensities.

D.11 References

1. Cooke, R.M., L.H.J. Goossens, and B.C.P. Kraan, Delft University of Technology, "Methods for CEC/USNRC Accident Consequence Uncertainty Analysis of Dispersion and Deposition – Performance Based Aggregating of Expert Judgments and PARFUM Method for Capturing Modeling Uncertainty," EUR-15856-EN, Luxembourg, June 1994.

2. Cooke, R., and D. Solomatine, Delft University of Technology and SoLogic Delft, "EXCALIBR, Integrated System for Processing Expert Judgments, Version 3.0: User's Manual," Delft, The Netherlands, 1992.

3. Cooke, R. M., *Experts in Uncertainty: Opinion and Subjective Probability in Science*, Oxford University Press, New York, NY, 1991.

4. NRC (U.S. Nuclear Regulatory Commission), "Severe Accident Risks: An Assessment for Five U.S. Nuclear Power Plants," NUREG-1150, Washington, DC, December 1990.

5. Trauth, K.M., R.P. Rechard, and S.C. Hora, Sandia National Laboratories, "Expert Judgment as Input to Waste Isolation Pilot Plant Performance-Assessment Calculations: Probability Distributions of Significant System Parameters," SAND91-0625, Albuquerque, NM, February 1993.

6. Bonano, E.J., et al., Sandia National Laboratories, "Elicitation and Use of Expert Judgment in Performance Assessment for High-Level Radioactive Waste Repositories," NUREG/CR-5411, SAND89-1891, Albuquerque, NM, May 1990.

7. Von Winterfeldt, D., and W. Edwards, *Decision Analysis and Behavioral Research*, Cambridge University Press, London, UK, 1986

8. Cooke, R., Delft University of Technology, "Expert Judgment Study on Atmospheric Dispersion and Deposition," Reports of the Faculty of Technical Mathematics and Informatics no. 91-81, Delft, The Netherlands, 1991.

APPENDIX E

Inverse Modeling Methods

E. Inverse Modeling Methods

E.1 Introduction

The development of uncertainty distributions over the most important code input variables (in terms of impact on code output) is a necessary prerequisite to the performance of code uncertainty analyses. The distributions are propagated through the code calculations in order to develop uncertainty distributions over the model output. The steps that the uncertainty analyst takes when transforming the uncertainty distributions provided by panels of experts into the distributions over code input variables are termed "processing" or "post-processing." In this study, processing of the elicited data breaks down into two main steps:

- combining expert uncertainty assessments (aggregation),
- developing distributions over code input variables.

Alternative aggregation schemes, the first step, are discussed in Appendix D of this document. The second step, obtaining distributions over code input variables, is necessary when variables for which distributions are elicited from experts are not code input variables.

A fundamental ground-rule adopted in this study was that distributions would be elicited from experts only on parameters that are directly measurable in the environment.* In this study, the dry deposition code input parameters are dry deposition velocities, which are directly measurable parameters; subsequently distributions were elicited on these variables. In the case of wet deposition and dispersion, the code input parameters are not directly measurable in the environment, and the elicitation variables for these phenomena were therefore not the code input variables. The elicitation variables for dispersion and wet deposition were, however, variables from which values for the code input variables could be derived. Mathematical processing techniques were therefore developed for this study, which enabled the development of distributions over code input parameters from the aggregated elicited distributions. This appendix reviews the methods used in the NRC/CEC study to develop distributions over code variables from aggregated elicited distributions.

* The decision to elicit only on measurable parameters was imposed so that there would be no ambiguity when presenting the definition of the elicitation variables If the experts assess poorly defined variables, the potential for incompatible assessments is high. Also, assessments on physically measurable parameters are not inherently dependent on any given theoretical model and may therefore be developed from a combination of relevant information sources.

E.2 Consequence Code Dispersion and Wet Deposition Input Parameters

One of the objectives of this study was to develop uncertainty distributions that could be applied in the MACCS and COSYMA consequence codes without modification of the basic models implemented in these codes. Both the European consequence code, COSYMA, and the US code, MACCS, employ a Gaussian plume model for atmospheric dispersion. At a given downwind distance and given atmospheric conditions, the model predicts the time-integrated concentration at various horizontal and vertical displacements from the center-line of the plume. The equation for determining the concentration relative to the source strength is:

$$\frac{\chi}{Q} = \frac{1}{2\pi\sigma_y\sigma_z\bar{u}}\exp\left(-\frac{y^2}{2\sigma_y^2}\right)\left(\exp\left(-\frac{(z-h)^2}{2\sigma_z^2}\right)+\exp\left(-\frac{(z+h)^2}{2\sigma_z^2}\right)\right)$$

where:

χ = time integrated air concentration
Q = the source strength
y = the horizontal displacement relative to the plume centerline
z = the vertical displacement
h = the vertical height of the plume centerline
$\bar{u}$ = the average wind velocity
σ_y and σ_z are parameters that depend on the downwind distance x

The parameters σ_y and σ_z define the expansion of the Gaussian plume in the crosswind and vertical directions, respectively, as a function of downwind distance (x). The dependency of σ_y and σ_z on the downwind distance depends on the coefficients a_y, b_y, and a_z, b_z through the power law relations:

$$\sigma_y = a_y x^{b_y} \; ; \; \sigma_z = a_z x^{b_z}$$

The parameters a_y, b_y, a_z, b_z are the important dispersion code input parameters and the parameters for which uncertainty distributions are required. In consequence code calculations they are typically assigned nominal values per stability class.

The consequence code input parameters for wet deposition are also power law coefficients. The washout coefficient, Λ, is defined as a function of rain intensity I through the power law:

$$\Lambda = a_\lambda I^{b_\lambda}$$

The important code input parameters for wet deposition are the a_λ and b_λ coefficients.

In the past, MACCS and COSYMA calculations assumed constant values for the code input parameters, a_y, b_y, a_z, b_z, a_λ, b_λ. In an uncertainty analysis of consequence code calculations, they are assigned distributions. The dispersion code input parameters are assigned distributions for each atmospheric stability class.

E.3 Overview of Processing Methodologies

Prior to this study, a method was developed under CEC sponsorship that was capable of deriving, from the aggregated elicited wet deposition distributions, distributions over the wet deposition code input parameters (a_λ, b_λ). The PARFUM[1] software package was developed prior to this study for the implementation of this methodology. The PARFUM methodology was selected for the development of a joint distribution over the a_λ and b_λ parameters using the power law relationship for the washout coefficient. Processing of the aggregated elicited dispersion distributions into distributions over code input parameters was more complex because it required the development of a joint distribution over four code input parameters (a_y, b_y, a_z, b_z) and the application of a number of different relationships between elicitation variables derived from the Gaussian Plume Model (GPM).

Two different methods were devised in this study for the development of distributions over dispersion code input parameters from the aggregated elicited dispersion distributions. Under the sponsorship of the present study, the capabilities of the PARFUM methodology were expanded to include the capability to process the aggregated elicited dispersion distributions. The expanded PARFUM methodology developed to process the aggregated elicited dispersion distributions is referred to in this study as the Sigma processing methodology. The Sigma processing methodology is an under-constrained optimization method, based on the GPM, which utilizes only the aggregated elicited distributions for s_y and χ_c/Q. In the Sigma method, s_y is equated to the σ_y of the GPM. The Sigma processing methodology is designed to capture the uncertainty in crosswind plume growth and χ_c/Q. The Sigma method processes 5th, 50th, and 95th percentile elicited data.

The Chi processing methodology was developed for this project as a more general approach designed to capture the uncertainty in the plume profile as well as the uncertainty in cross-wind plume growth and χ_c/Q. The Chi processing methodology is an over-constrained optimization method which utilizes the aggregated elicited distributions for χ_c/Q, χ_y/χ_c, and χ_z/χ_c. Unlike the Sigma processing methodology, the Chi processing methodology is not inherently based on the GPM. However, because of a project constraint against the modification of the code GPM, it was necessary to use the code GPM with the Chi methodology for the transformation of the elicited aggregated distributions into distributions over the code input variables. The Chi methodology is designed to process 0th, 5th, 50th, 95th, and 100th percentile elicited data.

E.4 PARFUM and Sigma Processing Methodologies

This section briefly describes the Sigma method for obtaining distributions on the code parameters a_y, b_y, a_z, b_z. Distributions over a_λ and b_λ were developed using the PARFUM methodology and are not discussed separately. Detailed information regarding both the PARFUM and Sigma processing methodologies may be found in the document "Methods for CEC/USNRC Accident Consequence Uncertainty Analysis of Dispersion and Deposition,"[2] published by the Delft University of Technology of the Netherlands.

As stated above, the parameters a_y, b_y, a_z, b_z are not measured directly. In fact, the vertical dispersion σ_z is measurable only close to the source of release. Beyond a

few hundred meters, σ_z is not measured directly. Instead, its values are derived from measurements of σ_y and the centerline concentration ratio, that is, the ratio of the time-integrated concentration on the plume centerline at downwind distance x to the release rate. On the GPM, when the release height is small relative to s_z, the centerline concentration ratio is given by

$$\frac{\chi}{Q} = \frac{1}{\pi \sigma_y \sigma_z \bar{u}}$$

where ū is the average wind speed (always in the x direction). When σ_y and σ_z obey the power laws, then

$$\frac{Q}{\chi} = \pi \bar{u} a_c x^{b_c}$$

where:

$$\pi \bar{u} a_c = a_y a_z$$

and

$$b_c = b_y + b_z$$

To determine a joint distribution on a_y, b_y, a_z, b_z, it is sufficient to determine a joint distribution on a_y, b_y, a_c, b_c. To sample a value from a_y, b_y, a_z, b_z, one simply samples a value from a_y, b_y, a_c, b_c and sets $a_z = \pi^* u^* a_c / a_y$ and $b_z = b_c - b_y$.

The Sigma method for determining a joint distribution on a_y, b_y, a_c, b_c breaks down into two steps: (1) determine joint bivariate distributions on a_y, b_y, and on a_c, b_c, and (2) join these two bivariate distributions to yield a joint distribution on a_y, b_y, a_c, b_c.

E.4.1 Bivariate Joint Distribution: the PARFUM Method

The method for determining joint bivariate distributions applies equally to the crosswind dispersion $\sigma_y(x)$, the concentration ratio χ/Q, and to the washout coefficient Λ. It is therefore discussed only for s_y. The method uses the computer code PARFUM.[1] Inputs for this method are percentile assessments for σ_y at various downwind distances $x_1, \ldots x_n$ (n is typically 3 to 5). PARFUM outputs a joint distribution over $\ln(a_y)$, b_y, which of course determines a distribution on a_y, b_y. The method involves the following steps:

- determine a uniform search grid G of possible values of $\ln(a_y)$ and b_y,
- for each downwind distance, x_i, determine a distribution P_i on G that is minimally informative relative to the uniform measure on G under the following constraint: the 5%, 50% and 95% percentiles of $a_y^* x_i^{b_y}$ must agree with the input percentiles for $s_y(x_i)$,
- determine a distribution P on G that is minimally informative with respect to $P_1, \ldots P_n$. In other words, P solves

$$P = argmin \sum_{i=1}^{n} I(P_i, P)$$

where $I(P_i, P)$ denotes the relative information of P_i with respect to P. It can be shown that P is just the average of the P_i:

$$P = (1/n) \sum_{i=1}^{n} P_i .$$

The most important step is the first, in which the initial search grid G is chosen. If G is large enough, then the final distribution P is insensitive to the choice of G. The determination of "large enough" depends on the number of percentiles elicited and the number of downwind distances elicited. For numbers that are realistic from a practical point of view, P becomes insensitive to the choice of G only when G is so large as to include "unreasonable" pairs of values in (a_y), b_y. This point is best illustrated with an example. For this purpose we take logs of the power law and neglect the constant $\pi^* u$; then the power law becomes:

$$\ln(\sigma_y(x_i)) = \ln(a_y) + b_y^* \ln(x_i); \quad i = 1, \ldots n.$$

Figure E.1 shows the 5th, 50th and 95th percentiles for $\sigma_y(x)$ at three downwind distances x_1, x_2, x_3. At each distance, the 50th percentiles are represented by ‖s, and the 5% and 95% percentiles are represented by |s. A pair of values $\ln(a_y)$, b_y corresponds to a line via the equation $\ln\sigma_y(x) = \ln(a_y) + b_y^* \ln(x)$. Two lines are shown corresponding to two pairs of values. Both lines intersect the central mass of the uncertainty distributions for σ_y at the three downwind distances. Hence both pairs would look "reasonable" to the PARFUM optimization routine for this small set of input data. However, the dashed line predicts that σ_y actually gets smaller as downwind distance increases. If assessments at greater downwind distances had been elicited, this line would surely look less reasonable. With sparse input data, the dashed line must be

excluded by an intelligent steering of the optimization routine, which is accomplished by the choice of G.

The problem of finding a distribution on a_y, b_y, a_c, b_c is split into the two smaller problems of finding a distribution on a_y, b_y and a distribution on a_c, b_c, exactly, in order to facilitate a heuristic steering of the optimization routine. The choice of G in each bivariate problem is supported by graphs like that of Figure E.1. When we find an optimal distribution P, we may then compute distributions on the $\sigma(x_i)$ using power law coefficients drawn from P. The resulting distributions are somewhat wider than the distributions from which we started. This reflects a contribution to uncertainty that arises because the power law does not perfectly describe the downwind propagation of the experts' uncertainty.

E.4.2 Joining Bivariate Distributions

PARFUM yields a bivariate distribution on a_y, b_y and a bivariate distribution on a_c, b_c. These two bivariate distributions must now be joined; that is, we must specify a 4-dimensional joint on a_y, b_y, a_c, b_c whose 2-dimensional marginals on a_y, b_y and a_c, b_c agree with those from PARFUM. The most tractable way to do this is to specify a correlation between *one* of the pairs (a_y, a_c), (a_y, b_c), (b_y, a_c) or (b_y, b_c) and to choose a minimally informative distribution under bivariate and correlational constraints (if correlations are specified on more than one pair, this might lead to inconsistent constraints). It turns out that the correlation between $\sigma_y(x)$ and $\sigma_z(x)$ (or between $\sigma_y(x)$ and χ/Q) becomes independent of the downwind distance, x, as x gets larger, and approaches the correlation between b_y and b_z (or between b_y and b_c). It was therefore decided to specify a correlation between b_y and b_c.

One possibility would be to configure the elicitation in such a way that a correlation between b_y and b_c could be extracted from the expert data. Since b_y and b_c are not directly measurable, a direct query is not possible. Exploratory simulation exercises indicated that the residual influence of the correlation is small once the two dimensional marginal on a_y, b_y and on a_c, b_c are fixed. Table E.1 shows the 5th, 50th and 95th percentiles for σ_z at 500 meters downwind for stability classes A, C, and F under three values for the correlation $\rho(b_y, b_c)$ between b_y and b_c. The data are from the equal weight decision maker; the 2-dimensional marginal distributions on a_y, b_y and on a_c, b_c are derived from PARFUM, and the residual correlation $\rho(b_y, b_c)$ is varied. The differences in Table E.1 are scarcely visible in the time-integrated concentrations.

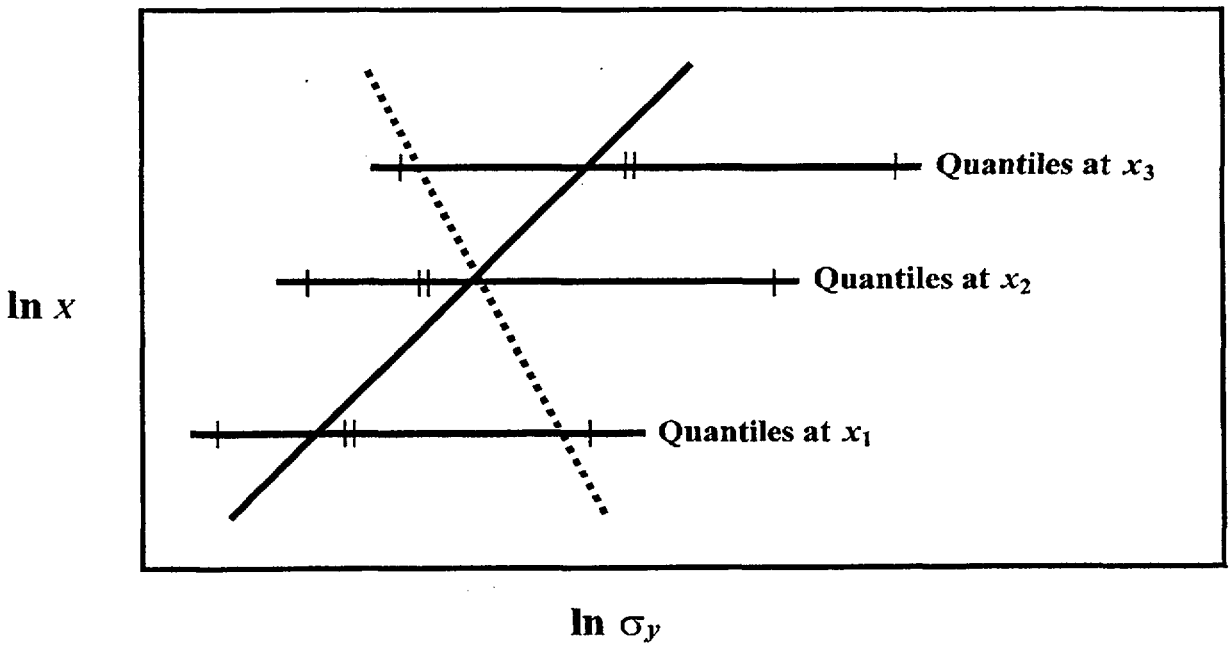

Figure E.1 50% percentiles (‖) and 5th and 95th percentiles (|) at three downwind distances with two possible combinations for $\ln(a_y)$, b_y

Table E.1 5th, 50th and 95th percentiles for σ_z at 500 meters downwind, data from equal weight decision maker; the 2 dimensional marginal distributions on a_y, b_y and on a_c, b_c are derived from PARFUM, and the residual correlation $\rho(b_y, b_c)$ is varied

	$\rho(b_y, b_c) = 0$			$\rho(b_y, b_c) = 0.5$			$\rho(b_y, b_c) = 1.0$		
Percentiles σ_z	5%	50%	95%	5%	50%	95%	5%	50%	95%
Stability Class F	1.73	27.0	336	1.93	27.3	326	1.98	25.7	277
Stability Class C	6.56	58.4	469	7.27	58.5	439	7.97	59.9	404
Stability Class A	6.97	1280	1700	8.20	1273	1640	8.65	1177	1380

In light of the relative unimportance of the residual correlation between b_y and b_c, it was decided not to burden the elicitation further, but instead to assess this correlation by other means. Two methods were available: previous expert assessments and an equilibrium method based on the so-called Cournot duopoly. In previous European uncertainty analyses, the correlation between the uncertainties in σ_y and σ_z was assessed to be small.[3,4] The reason for this assessment was that the turbulence scales responsible for wind meander, the principle contributor to uncertainty in σ_y, are independent of scales causing fluctuations in σ_z. The equilibrium method is described in Cooke et al.[2] and can be rendered very intuitively as follows: Imagine two "players" contesting the correlation between b_y and b_c. The first player wants the correlation ρ_{yc} between $\sigma_y(x)$ and χ/Q to depend as little as possible on downwind distance x, for the elicited values $x_1, \ldots x_n$. The second player wants the correlation ρ_{zc} between $\sigma_z(x)$ and χ/Q to depend as little as possible on downwind distance for the elicited values $x_1, \ldots x_n$. The goals of these two players are antagonistic, but they will eventually agree on a pair of "equilibrium" values ρ^*_{yc}, ρ^*_{zc}. Setting the correlation between b_y and b_c equal to ρ_{yc}* leads to values for the correlation between σ_y and σ_z that are very close to zero (the actual values depend on the input data).

Simulation exercises indicate that the major influence on the time-integrated concentrations is captured by a distribution which preserves the *one*-dimensional marginals on a_y, b_y, a_c, b_c and the correlations $\rho(a_y,b_y)$, $\rho(a_c,b_c)$ and which is minimally informative under these constraints. The software package UNICORN[5] was used in this study to construct such distributions. The information lost by replacing the two-dimensional joint distributions by one-dimensional marginals plus correlations is not great. Tables E.2 and E.3 compare the quantiles of the equal weight decision maker with the results using the PARFUM method and using the minimal information distributions from UNICORN for downwind distances 1 km, 3 km, and 10 km, for stability classes A and F.

Three final remarks on the PARFUM method are appropriate. First, the rather large spread in σ_z shown in Table E.1 above reflects modeling uncertainty with respect to the GPM. Indeed, the quantities s_y and χ_c/Q are empirically defined in a model-independent way. When developing their distributions, experts took account of factors that are not taken into account in the GPM. When we project distributions onto the parameters of the GPM and then extract a distribution for σ_z, additional uncertainty is being factored in as well. This, of course, is exactly what we want to happen, as the distributions over model parameters should, if possible, also take account of uncertainty in the model itself. The additional modeling uncertainty captured in this way concerns only the uncertainty with regard to the power law models for plume growth. Non-Gaussianality may also express itself in non-Gaussian crosswind and vertical profiles, the type of uncertainty not captured in the PARFUM approach. The Chi method discussed in the following section attempts to do this. Second, a problem arose in processing stability class A. At 30 km downwind in this stability class, σ_z is significantly affected by the mixing layer, which reflects vertical diffusion. This effect was

Table E.2 Stability Class A: Comparison of equal weight DM, PARFUM and UNICORN 5th, 50th, and 95th percentile values for χ_c/Q and σ_y at three downwind distances

Stability Class A							
	χ_c/Q				σ_y		
	Eq. wgt DM	PARFUM	UNICORN	Quantiles	Eq. wgt DM	PARFUM	UNICORN
1 km	9.06E-8	1.02E-7	1.03E-7	5%	103.4	92	80.7
	1.83E-6	2.08E-6	2.31E-6	50%	329.7	303	329
	1.90E-5	2.24E-5	2.62E-5	95%	1274	1372	1430
3 km	2.24E-8	1.63E-8	1.61E-8	5%	279	274	216
	3.04E-7	3.30E-7	3.66E-7	50%	739	827	897
	2.48E-6	3.51E-6	4.26E-6	95%	3638	3764	3960
10 km	2.30E-9	2.16E-9	2.11E-9	5%	677	728	626
	5.57E-8	4.42E-8	4.86E-8	50%	2303	2475	2740
	4.52E-7	4.77E-7	5.64E-7	95%	11560	11589	12000

Table E.3 Stability Class F: Comparison of equal weight DM, PARFUM and UNICORN 5th, 50th, and 95th percentile values for χ_c/Q and σ_y at three downwind distances

Stability Class F							
	χ_c/Q				σ_y		
	Eq. wgt DM	PARFUM	UNICORN	Quantiles	Eq. wgt DM	PARFUM	UNICORN
1 km	1.69E-6	3.22E-6	4.12E-6	5%	25.8	23	22.4
	4.92E-5	4.82E-5	5.39E-5	50%	87.8	88	85.8
	2.97E-4	3.88E-4	5.97E-4	95%	243.2	270	286
3 km	1.03E-6	5.06E-7	6.66E-7	5%	64.6	57	56.4
	1.07E-5	1.06E-5	1.24E-5	50%	231.3	230	216
	8.47E-5	1.07E-4	1.66E-4	95%	639.8	726	774
10 km	1.22E-7	6.05E-8	8.64E-8	5%	158	152	151
	1.94E-6	1.97E-6	2.16E-5	50%	632.8	642	613
	2.11E-5	2.70E-5	2.39E-5	95%	2106	2140	2330

visible in the experts' assessments of χ_c/Q. It was therefore decided to exclude assessments at 30 km in this case in the PARFUM algorithm, as the power law for χ_c/Q ceases to hold when σ_z is reflected from the mixing layer. Finally, at 500 m from the source, the 5th percentile of σ_z is quite small. The approximation:

$$\frac{\chi}{Q} = \frac{1}{\pi \sigma_y \sigma_z \bar{u}}$$

holds only when σ_z is large relative to the release height, and this condition does not hold for the lower percentiles of σ_z at 500 m. The error in the above approximation may exceed 10 percent. A correction term was derived, but its implementation would require change of the COSYMA and MACCS codes.

E.5 Chi Methodology

This section reviews the development of a joint (4-variate) probability distribution for the vector of parameters (a_y, b_y, a_z, b_z) using the Chi methodology. The objective is to find the minimally informational joint distribution that is consistent with the elicited probability distributions. Minimally informational means that the joint distribution has the largest entropy among distributions that are consistent with the experts' judgments, which consist of the percentile assessments of the elicited variables. This

discussion will employ the following three elicited variables: χ_c/Q, χ_y/χ_c, and χ_z/χ_c.

The following relationships for the elicited variables χ_c/Q, χ_y/χ_c, and χ_z/χ_c can be derived from the GPM:

$$\frac{\chi_z}{\chi_c} = \left(\exp\left(-\frac{(z-h)^2}{2\sigma_z^2}\right)+\exp\left(-\frac{(z+h)^2}{2\sigma_z^2}\right)\right)\times \left(1+\exp\left(-\frac{2h^2}{\sigma_z^2}\right)\right)^{-1} \text{ assuming: } y=0$$

$$\frac{\chi_y}{\chi_c} = \exp\left(\frac{-y^2}{2\sigma_y^2}\right) \text{ assuming: } z=h$$

$$\frac{\chi}{Q} = \frac{1}{2\pi\sigma_y\sigma_z\bar{u}}\left(1+\exp\left(-\frac{2h^2}{\sigma_z^2}\right)\right)$$

assuming: $y = 0$ and $z = h$.

The goal of processing the judgments is to obtain a probability distribution for (a_y, b_y, a_z, b_z) that is consistent with the set of assessed probability distributions for χ_c/Q, χ_y/χ_c, and χ_z/χ_c. For example, when the GPM is exercised by sampling from the distribution of (a_y, b_y, a_z, b_z), the computed values of χ_c/Q, χ_y/χ_c, and χ_z/χ_c should fall into the various assessed intervals with the correct probabilities.

The three assessed percentiles for each elicitation variable generate four intervals: lower 5%, lower 45%, upper 45%, and upper 5% intervals. Each vector (a_y, b_y, a_z, b_z) yields values of σ_y and σ_z, which, in turn, give values of χ_c/Q, χ_y/χ_c, and χ_z/χ_c. These values can be classified with respect to which intervals they fall into, and the vector that generated these values can also be associated with the intervals. For example, a particular vector (a_y, b_y, a_z, b_z) might generate a value of χ_c/Q in the lowest interval, a value of χ_y/χ_c in the second highest interval, and a value of χ_z/χ_c in the second-lowest interval. By keeping track of which vectors map into which intervals, it becomes possible to assign probabilities to the vectors so that the assessed probabilities of the elicitation variables are closely reproduced when the model is exercised.

Let the symbol m_{ijk} be the number of vectors mapping into the i^{th}, j^{th} and k^{th} intervals for χ_c/Q, χ_y/χ_c, and χ_z/χ_c, respectively. Let the symbol P_{ijk} denote the collective probabilities to be assigned to these vectors. It is a necessary condition for maximizing entropy that each of these vectors be assigned an equal probability so that $P(a_y, b_y, a_z, b_z) = P_{ijk}/m_{ijk}$ for each (a_y, b_y, a_z, b_z) mapping into the i^{th}, j^{th}, and k^{th} intervals. Let α_1, α_2, α_3, α_4, and α_5 represent the percentiles for which assessments are available (where the lower, α_1, and upper, α_5, bounds may be elicited or analytical values).

Now consider determination of the probabilities for P_{ijk}. In order for the probabilities to be consistent with the assessments, they must satisfy the following three constraints:

(1) $\Sigma_j\Sigma_k P_{ijk} = \alpha_{i+1} - \alpha_i$ for $i=1,\ldots,4$,
(2) $\Sigma_i\Sigma_k P_{ijk} = \alpha_{j+1} - \alpha_j$ for $j=1,\ldots,4$,
(3) $\Sigma_i\Sigma_j P_{ijk} = \alpha_{k+1} - \alpha_k$ for $k=1,\ldots,4$.

As a first order approximation to maximizing entropy of the probability distribution over the (a_y, b_y, a_z, b_z) vectors, the expected or average probability of the vectors is minimized. This is accomplished by minimizing

(4) $\Sigma_i\Sigma_j\Sigma_k m_{ijk}(P_{ijk}/m_{ijk})^2$.

Minimization of (4), subject to the constraints (1) through (3), can be accomplished via an optimization procedure known as quadratic programming. If solutions exist that satisfy (1) through (3), then the quadratic program will have as its solution the set of probabilities P_{ijk}, which minimizes the expected probabilities while generating the quantities of χ_c/Q, χ_y/χ_c, and χ_z/χ_c in a manner consistent with the elicited distributions.

E.5.1 Quadratic programming

Let P_{ijk} be the probability of the ijk^{th} cell in the elicitation variable space, and let m_{ijk} be the number of vectors mapping into that cell. The probability assigned to any one vector in that cell is simply P_{ijk}/m_{ijk}. In order to spread the probability of the vectors as evenly as possible, the expected probability across all vectors is minimized. This is a first-order approximation to minimizing entropy because it is equivalent to minimizing the first term in the Taylor series expansion of entropy.

The expected probability of a randomly chosen vector is simply the probability of the vector squared, summed across all possible vectors. Thus $E(P_{ijk}/m_{ijk}) = \Sigma_{ijk} m_{ijk} (P_{ijk}/m_{ijk})^2 = \Sigma_{ijk} P_{ijk}^2/m_{ijk}$, which is a quadratic function of the cell probabilities. Of course, in assigning the probabilities to cells, the constraints imposed by the elicitation intervals must be satisfied. Joining the objective

of spreading the probability as evenly as possible with the information from the aggregated distributions given by the experts leads to the problem:

Minimize $\Sigma_{ijk}P_{ijk}^2/m_{ijk}$

subject to:

$\Sigma_{jk}P_{ijk} = \alpha_{i+1} - \alpha_i$ for i = 1, ..., 4,
$\Sigma_{ik}P_{ijk} = \alpha_{j+1} - \alpha_j$ for j = 1, ..., 4,
$\Sigma_{ij}P_{ijk} = \alpha_{k+1} - \alpha_k$ for k = 1, ..., 4,

and

$P_{ijk} \geq 0$ for all i, j, k.

Note that satisfaction of the constraints is sufficient for $\Sigma_{ijk}P_{ijk} = 1.0$ so that an additional constraint is not necessary in order to guarantee that the probability sums to one.

This mathematical problem has a quadratic objective function and linear constraints. Conceptually, the problem can be solved using classical techniques through a large number of LaGrangian multipliers that augment the objective function. Practically, however, the problem is most easily solved using an approach known as quadratic programming. A quadratic program will converge to the solution to this problem in a finite number of steps, provided the constraints can be simultaneously satisfied.

A solution may not exist when some of the cells in the elicitation space are impossible. This can occur when the elicited values are highly inconsistent with the GPM. For example, it may be impossible to find any (a_y, b_y, a_z, b_z) vectors that, vis-à-vis the GPM, map into certain cells in elicitation space. If a cell is empty, the coefficient in the objective function corresponding to the cell is undefined (division by zero). The variable must then be removed from the formulation and that cell assigned zero probability. If enough of these cells are empty and the corresponding variables removed, their pattern can be such that no solution is possible.

Quadratic programming employs the simplex algorithm of linear programming to solve a quadratic program. It does so by first converting the quadratic objective function into a set of linear equations by first attaching each constraint to the objective function in the form of a LaGrangian multiplier and then differentiating with respect to the solution variables (the P_{ijk}) and the LaGrangian multipliers. Each differentiation generates a linear expression that is set equal to zero. However, it is also necessary to deal with the non-negativity constraints on the P_{ijk}. The theory of constrained optimization proposed by Kuhn and Tucker[7] leads to the following set of equations, which, when satisfied, give the solution to the problem of determining cell probabilities. These equations are:

$\Sigma_j\Sigma_k P_{ijk} = \alpha_{i+1} - \alpha_i$ for i = 1, ..., 4,
$\Sigma_i\Sigma_k P_{ijk} = \alpha_{j+1} - \alpha_j$ for j = 1, ..., 4,
$\Sigma_i\Sigma_j P_{ijk} = \alpha_{k+1} - \alpha_k$ for k = 1, ..., 4;
$2(P_{ijk}/m_{ijk}) + \lambda_{1i} + \lambda_{2j} + \lambda_{3k} + v_{ijk} = 0$ for all i, j, k;
$P_{ijk}v_{ijk} = 0$ for all i, j, k;

and

$P_{ijk}, v_{ijk} \geq 0$ for all i, j, k.

In this formulation λ represents the usual LaGrangian multipliers while v_{ijk} represent the complementary slack variables introduced so the linear programming algorithm can be used. The implementation used in this study is through a commercial mathematical programming package called LINDO.[8]

E.5.2 Implementation of the Proposed Solution

The goal of the processing methodology is to find probabilities for the coefficient (a_y, b_y, a_z, b_z) vectors so that when these vectors are sampled, the probability distributions of the variables in the elicited variable space (χ_c/Q, χ_y/χ_c, and χ_z/χ_c) match those given by the experts. To understand how the methodology works, recognize that each point in the coefficient vector space maps to a unique point in the elicited variable space. This is true because χ_c/Q, χ_y/χ_c, and χ_z/χ_c are functions of σ_y and σ_z, which, in turn, can be calculated from the following relations:

$$\sigma_y = a_y x^{b_y} \; ; \; \sigma_z = a_z x^{b_z}$$

A distribution of the (a_y, b_y, a_z, b_z) vectors is developed independently for each stability class via the following steps:

1. The development of an initial set of (a_y, b_y, a_z, b_z) vectors.
2. The development, at each downwind distance, of subsets of the (a_y, b_y, a_z, b_z) vector space defined by the intersection of intervals of the elicited χ_c/Q, χ_y/χ_c, and χ_z/χ_c values.
3. The elimination from the initial set of (a_y, b_y, a_z, b_z) vectors those vectors whose values, when mapped into the elicitation variable space, are outside the range of any elicitation variable at any downwind distance.

4. The determination of the number of (a_y, b_y, a_z, b_z) vectors that are contained in each subset. These numbers provide coefficients needed to accomplish step 5 below.
5. The solving of a quadratic program to determine the allocation of probability to the subsets of vectors so as to: (a) satisfy the elicited percentiles, and (b) spread the probability across the vectors as evenly as possible subject to (a).
6. The calculation of a probability for each (a_y, b_y, a_z, b_z) vector at each downwind distance. This calculation is simply the quotient of the probability allocated to a subset and the number of vectors in that subset.
7. The averaging of the (a_y, b_y, a_z, b_z) vector probabilities across the various downwind distances to obtain the final vector probabilities.

Step 1: Development of the initial set of (a_y, b_y, a_z, b_z) vectors.

The first step is the development of an initial set of four-dimensional (a_y, b_y, a_z, b_z) vectors. The requirement for the initial set of vectors is that it contain a range of values sufficient to adequately cover the range of elicited χ_c/Q, χ_y/χ_c, and χ_z/χ_c values at every downwind distance with only vectors that are within the range of elicited χ_c/Q, χ_y/χ_c, and χ_z/χ_c values for each downwind distance.

In the construction of this set of vectors, the principle of minimum relative information with respect to $\log(\sigma_y)$ and $\log(\sigma_z)$ is evoked in order to establish the spacing of the grid of values to be sampled. This translates into an initial grid of points that are uniformly spaced in the log of the coefficients and uniformly spaced in the exponents.

A typical set of (a_y, b_y, a_z, b_z) vectors can be constructed from the values presented in Table E.4 by taking the product of the four sets of values. The values of the coefficients in Table E.4 consist of 6 values for a_y and a_z and 21 values for b_y and b_z, yielding a total of $6\times6\times21\times21=15{,}876$ unique vectors. A large set of vectors is required to ensure a reasonable level of fineness (e.g., a doubling of the value of b_y might result in a step size so large that no vector would map into one of the sets in elicited variable space).

Step 2: The development, for each downwind distance, of sets of the elicited χ_c/Q, χ_y/χ_c, and χ_z/χ_c values.

Figure E.2 provides three-dimensional representations of the sets formed with the elicited percentile values for χ_c/Q, χ_y/χ_c, and χ_z/χ_c for each downwind distance. In the following discussion the subsets in the (χ_c/Q, χ_y/χ_c, and χ_z/χ_c) space will be called cells. Note that each (a_y, b_y, a_z, b_z) vector maps into one or none of these cells at each downwind distance.

Table E.4 Typical initial (a_y, b_y, a_z, b_z) values

a_y	b_y	a_z	b_z
0.23	0.50	0.23	0.50
0.38	0.55	0.38	0.55
1.06	0.60	1.06	0.60
1.77	0.65	1.77	0.65
2.96	0.70	2.96	0.70
4.93	0.75	4.93	0.75
	0.80		0.80
	0.85		0.85
	0.90		0.90
	0.95		0.95
	1.00		1.00
	1.05		1.05
	1.10		1.10
	1.15		1.15
	1.20		1.20
	1.25		1.25
	1.30		1.30
	1.35		1.35
	1.40		1.40
	1.45		1.45
	1.50		1.50

Step 3: The elimination of (a_y, b_y, a_z, b_z) vectors outside of the χ_c/Q, χ_y/χ_c, and χ_z/χ_c cells at any downwind distance.

A vector is eliminated from the initial set of vectors if it produces values for χ_c/Q, χ_y/χ_c, or χ_z/χ_c that fail at any downwind distance to map into one of the cells created in Step 2. For example, a vector which produces a value for χ_c/Q, χ_y/χ_c, or χ_z/χ_c less than the elicited 0th percentiles or greater than the 100th percentile at any distance would

be eliminated from the set of vectors during this step. Therefore, a vector that produces values of the elicitation variables that are outside the 100% probability intervals are not allowed. This step is consistent with the tenet that values deemed impossible should not be permitted in the analysis. The product of this step is a reduced set of vectors for the particular stability class under analysis.

Step 4: The determination of the number of (a_y, b_y, a_z, b_z) vectors that are contained in each cell of χ_c/Q, χ_y/χ_c, χ_z/χ_c space at each downwind distance.

In order to calculate a probability for each vector, it is first necessary to calculate the probability of each cell within the three-dimensional χ_c/Q, χ_y/χ_c, χ_z/χ_c matrix formed for each downwind distance. This probability is then evenly distributed across all (a_y, b_y, a_z, b_z) vectors within that cell.

The cell probabilities are calculated using the quadratic program discussed in this appendix. In order to satisfy Step 5b (spread the probability as evenly as possible), it is necessary to have a measure of the size of each cell. This measure is the number of (a_y, b_y, a_z, b_z) vectors mapping into each cell. The reciprocal of this number becomes the coefficient for the cell probability in the objective function of the quadratic program. The rationale is explained above in the section on quadratic programming.

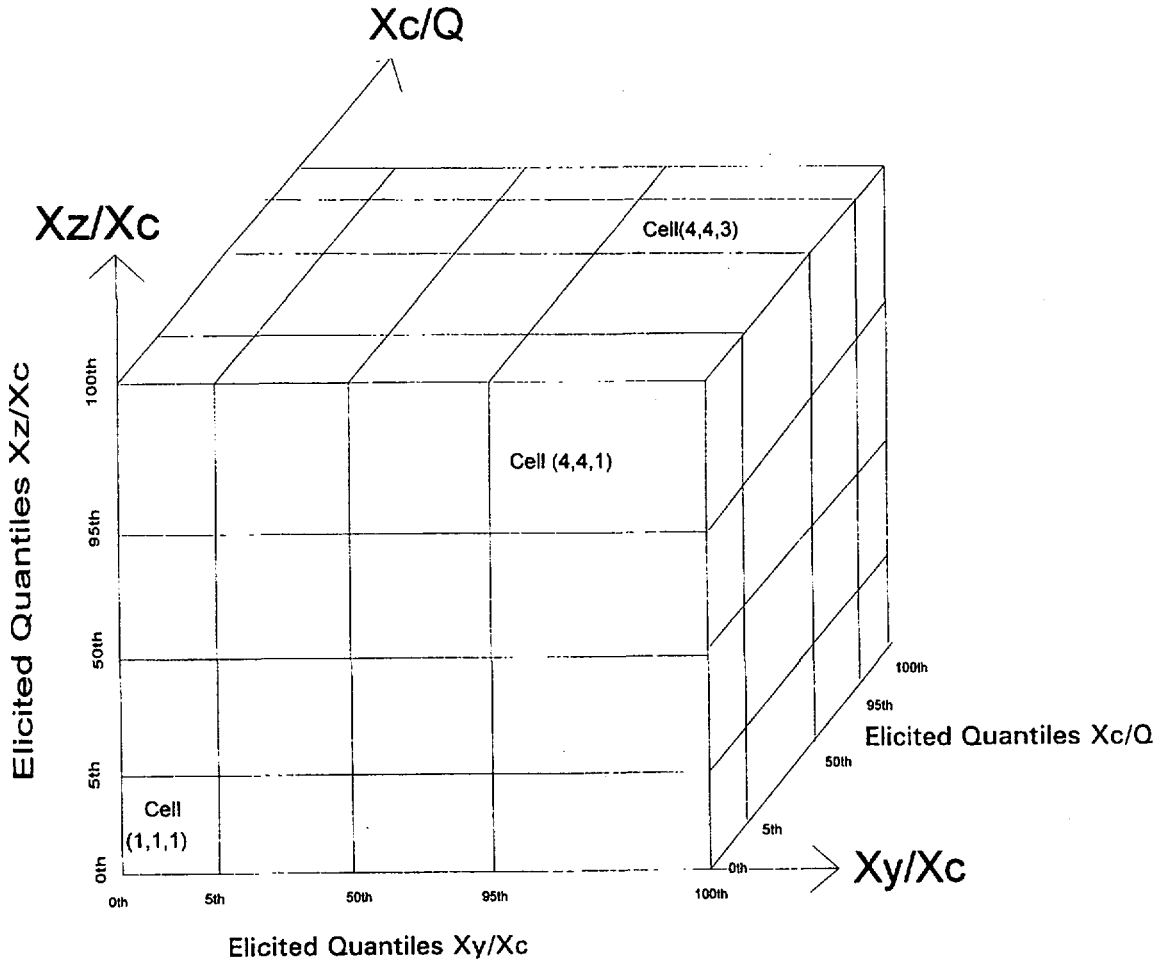

Figure E.2 Three dimensional space defined by the elicited χ_c/Q, χ_y/χ_c, and χ_z/χ_c values

Step 5: The numerical solution for probabilities of cells in the elicitation variable space.

A quadratic program is solved to find the assignment of probabilities to cells that (1) satisfies the probability intervals in the elicitation variable space when the (a_y, b_y, a_z, b_z) vectors are "pushed" through to that space, and (2) spreads the probability across the (a_y, b_y, a_z, b_z) vectors as evenly as possible, subject to satisfying (a). The objective function is given as proposed solution (4) above; the accompanying constraints (1) through (3) ensure that the probability intervals are satisfied.

Step 6: The calculation of the probability of each (a_y, b_y, a_z, b_z) vector for each downwind distance.

A probability for each vector in each cell is then calculated by dividing the cell probability by the number of vectors determined to fall within that cell. All vectors within a specific cell are thereafter assigned the same probability.

Step 7: Averaging of the (a_y, b_y, a_z, b_z) vector probabilities calculated for each distance to obtain the final vector probability values.

The probability values calculated at the various distances for each of the possible (a_y, b_y, a_z, b_z) vectors are then averaged over the downwind distances in order to establish the final vector probabilities, which are to be used at all downwind distances under consideration.

E.5.3 Application of Methodology to Elicited Data

Because the Chi method is by design an over-constrained methodology and the method was required to process the elicited data through the GPM in the consequence codes, the successful application of this methodology was dependent on the level of consistency between the data elicited from the experts and the GPM. In the Chi processing method there were two potential sources of inconsistency between the elicited dispersion data and the GPM.

In the first case, the GPM does not permit χ_y/χ_c and χ_z/χ_c values greater than one. Two of the eight dispersion experts provided 95th percentile values for χ_y/χ_c and χ_z/χ_c greater than one. In the aggregated distributions, this resulted in 95th percentile values greater than one for χ_y/χ_c and χ_z/χ_c for all stability classes. For processing, the 100th percentiles of χ_y/χ_c and χ_z/χ_c for all downwind distances and all stability classes were therefore assigned a value of 1.0 and the 95th χ_y/χ_c and χ_z/χ_c percentiles were not used. This required that the cells illustrated in Figure E.2 be modified to the form illustrated in Figure E.3.

A second area of potential inconsistency between the elicited data and the GPM is the relationship between the elicited χ_c/Q and the χ_y/χ_c and χ_z/χ_c values. The *individual* experts sometimes provided a range of values for χ_c/Q between the 0th and 5th percentiles, which, using the GPM, were inconsistent with the elicited range of values for χ_y/χ_c and χ_z/χ_c from the same expert; that is, the set of (a_y, b_y, a_z, b_z) vectors consistent with the range (between the 0th and 100th percentiles) of elicited χ_y/χ_c and χ_z/χ_c values did not provide values for χ_c/Q that fell within the elicited 0th to 5th percentile range for the χ_c/Q parameter. Because of the unwillingness of some of the experts to provide 0th and 100th percentiles, aggregated elicited values for the 0th and 100th percentiles were not available for the χ_c/Q, χ_y/χ_c, and χ_z/χ_c parameters. It was therefore not possible to determine if this consistency would have been present for the aggregated data. For the processing of the aggregated elicited data, it was assumed that zero was the logical lower bound (0th percentile) for the χ_y/χ_c and χ_z/χ_c parameters. The 0th and 100th values for χ_c/Q, provided by one of the experts, were used for the processing of the aggregated elicited data.

E.5.4 Implications of χ_y/χ_c and χ_z/χ_c Greater Than 1

Table E.5 presents the range of values and the average values for aggregated χ_y/χ_c and χ_z/χ_c elicited data (equal weighting method of aggregation) at the 95th percentile. It is apparent that the GPM implemented in the consequence codes cannot be used for the representation of plume profile uncertainty without limiting the range of the χ_y/χ_c and χ_z/χ_c to values equal to or less than one.

In order to process values of χ_y/χ_c and χ_z/χ_c greater than one with the GPM, it would be necessary to add an error term to the Gaussian equations which would enable the GPM to accommodate χ_y/χ_c and χ_z/χ_c values greater than one. Although the concentration fluctuations represented by the concentration ratios greater than one are generally not thought to be an important source of uncertainty for most of the endpoints of accident consequence assessments, the next section presents an example method for adding an error term to the GPM that would enable the determination of the significance of concentration ratios greater than one to consequence code output.

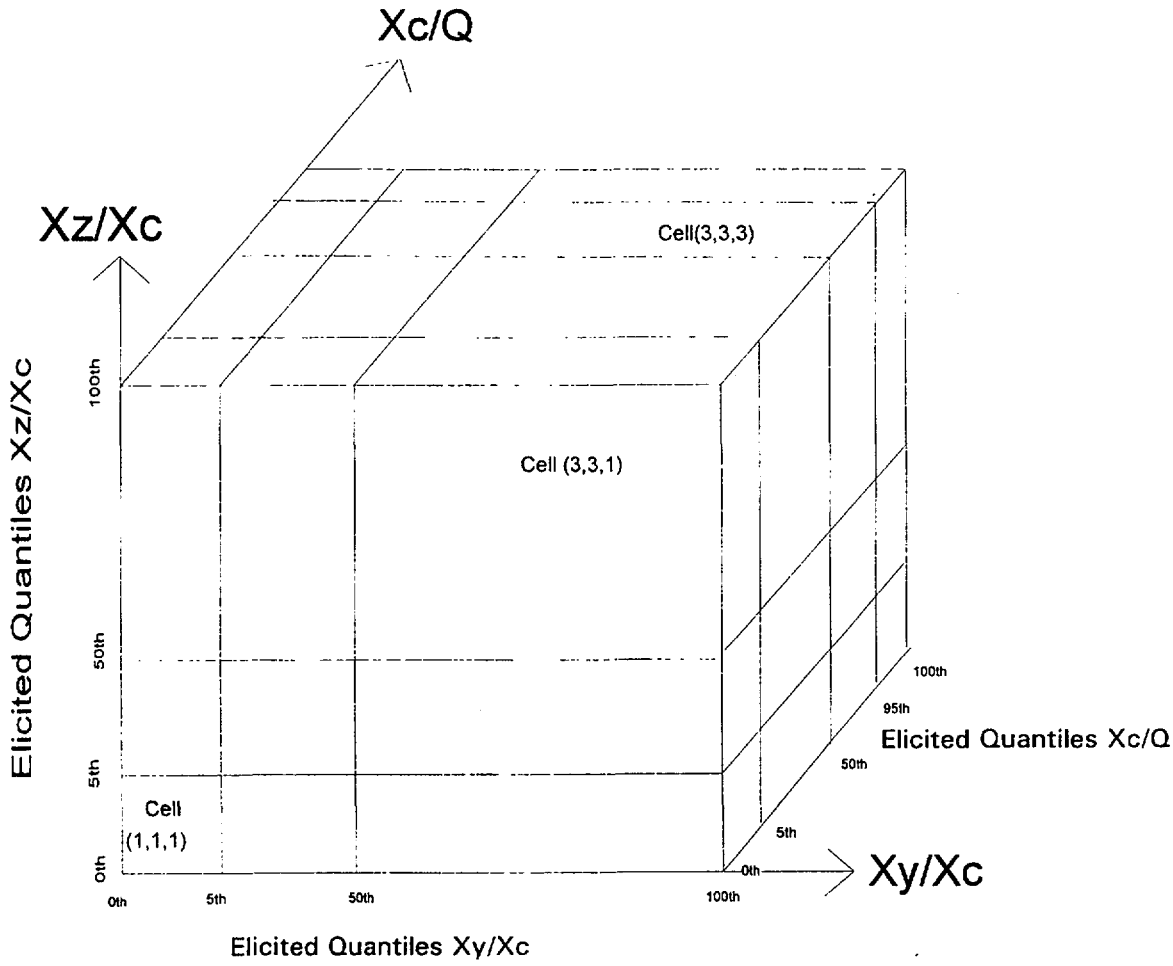

Figure E.3 Three-dimensional matrix modified to process actual elicited data

Table E.5 Range of Aggregated Elicited χ_y/χ_c and χ_z/χ_c values for different stability classes

95th Percentile[1]		95th Percentile[2]		Percentile ($\chi_y/\chi_c = \chi_z/\chi_c = 1$)[3]	
χ_y/χ_c Range	χ_z/χ_c Range	$(\chi_y/\chi_c)_m$	$(\chi_z/\chi_c)_m$	χ_y/χ_c	χ_z/χ_c
1.45 to 3.91	1.44 to 3.63	2.49	2.27	0.63	0.65

[1] Range of aggregated elicited χ_y/χ_c and χ_z/χ_c values for different stability classes.
[2] Average values for the aggregated 95th percentile χ_y/χ_c and χ_z/χ_c values (averaged over stability classes)
[3] Linear interpolated percentile at which the χ_y/χ_c and χ_z/χ_c values would equal 1, assuming the average values for the aggregated 95th percentile.

E.5.5 The GPM with an Error Term

Three types of variables are assessed in the CEC/NRC study of dispersion. These are concentrations (χ_c/Q), ratios of concentrations (χ_y/χ_c, χ_z/χ_c), and standard deviations (σ_y). The GPM provides that, for a downwind distance x that is not too large for the subject stability class,

$$\chi_c/Q \propto 1/(\sigma_y\sigma_z),$$

$$\chi_y/\chi_c = \exp[-.5(y/\sigma_y)^2], \text{ and}$$

$$\chi_z/\chi_c = \exp[-.5(z/\sigma_z)^2].$$

It is also assumed that $s_y \approx \sigma_y$ because s_y is a statistic that estimates σ_y. In reality, measurements of concentrations will not exactly follow the equations above. Measurements will deviate from the values that would be assigned by the model because plumes are somewhat irregular, having pockets of high and low concentrations. It is these deviations from the GPM that give rise to greater variability in concentrations than would arise from uncertainty about σ_y and σ_z alone. Because concentrations such as χ_c, χ_y, and χ_z are affected by these sources of variation, the ratios of concentrations will also be affected. The effect on σ_y, however, will be minimal because this statistic is computed from an average in which deviations are apt to cancel.

Modeling these additional sources of uncertainty can be accomplished by adding an error term to the concentrations predicted by the GPM. For example, the center-line concentration would be modeled as

$$\chi_c/Q \propto [1/(\sigma_y\sigma_z)]\varepsilon_c,$$

where ε is a multiplicative deviation or noise such that $\varepsilon > 0$. The ratio measures are subject to two deviations because two concentrations are involved in their calculation. For example:

$$\chi_y/\chi_c = \exp[-.5(y/\sigma_y)^2](\varepsilon_y/\varepsilon_c).$$

To obtain a workable analysis of the GPM with an error term, three assumptions are made. First, it is assumed that the distribution of ε is stationary throughout the plume, meaning that a concentration measured at one position in the plume will have the same distribution of relative deviation as a concentration measured at some other point.

The second assumption is concerned with the dependence of the two deviation terms that appear in the ratio measurements. Although these deviations will be dependent when the measurements are taken close to one another, the dependency will lessen and, for offset distances used in the CEC/NRC study, it will be assumed that the dependence is negligible. Third, it is assumed that the deviations are stochastically independent of the values of σ_y and σ_z.

Perhaps surprisingly, the three assumptions given above are sufficient to derive the distributions of the deviations, their ratios, and that of σ_z directly from the elicited data. It will now be demonstrated how this can be accomplished. For a given stability class and downwind distance, denote the distribution function of $-.5(y/s_y)^2$ by $G(x)$, the distribution function of $\log(\chi_y/\chi_c)$ by $H(x)$, and the unknown density of $\log(\varepsilon_y/\varepsilon_c)$—the log of the ratio of deviations—by $f(x)$. These three functions are related by the convolution integral:

$$H(x) = \int_{-\infty}^{\infty} G(x-w)f(w)dw$$

From a practical point of view, it is easiest to approach convolution problems using Fourier, or LaPlace transforms. Let $g(t)$ and $h(t)$ be the Fourier transforms of the densities corresponding to the densities of $G(x)$ and $H(x)$, and let $r(t)$ be the Fourier transform of $f(x)$. Then $r(t) = h(t)/g(t)$. The probability elicitation provides the distribution of $H(x)$ directly and that of $G(x)$ through the assessed distribution s_y. Finally, let $P(x)$ be the assessed distribution of $\log(\chi_z/\chi_c)$ and let $s(t)$ be the Fourier transform of the corresponding density. Then the Fourier transform of $-.5(z/\sigma_z)^2$ is just $s(t)/r(t)$ so that the density of σ_z can be found be inverting the Fourier transform and making a monotone transformation of the variable.

Modeling an error term in the GPM accomplishes three objectives. First, the model more nearly corresponds to the thinking of the experts, and thus there is less forcing of judgments into the model. Second, the noise can be decoded (removed) from the assessed distributions and the distribution of σ_z found. Having the distributions for the center line concentration, σ_y, and σ_z allows an inference on the joint distribution without making assumptions about the correlation among parameters. Third, the distribution of the plume noise can be found directly from its characteristic function, which is $[r(t)]^{1/2}$. Knowing this distribution permits the exercising of the GPM with noise so that additional sources of uncertainty can be included.

E.6 Comparison of χ_c/Q and σ_y Values Resulting From Sigma and Chi Methodologies

The tables contained in this section compare the χ_c/Q and σ_y values for stability classes A/B and E/F, calculated using the Chi and Sigma processing methodologies. Case A-1 represents stability class A/B, which is regarded as very unstable atmospheric conditions. Case A-4 represents stability class E/F, which is regarded as very stable atmospheric conditions. Values developed from both equal- and item-weighted aggregated distributions are presented for the EXCALIBR, PARFUM, and UNICORN data. Equal-weighted aggregated assessments processed by the Chi method are also presented in these tables. Additional results from the two methodologies are contained in Chapter 3 of Volume I of this document. Typically both methods accurately reproduce the χ_c/Q and σ_y aggregated elicited values, although the Sigma method in general predicts these values more accurately than the Chi methodology.

Case A-1: x = 500 m

χ (x, 0, H)/Q_0 VALUES AT DOWNWIND DISTANCE: 500 m							
Quantile	EXCALIBR (item)	PARFUM (item)	UNICORN (item)	EXCALIBR (equal)	PARFUM (equal)	UNICORN (equal)	CHI (equal)
5%	7.33E-07	6.95E-07	6.84E-07	4.64E-07	3.22E-07	3.33E-07	7.19E-07
50%	9.80E-06	1.07E-05	1.13E-05	7.31E-06	6.68E-06	7.44E-06	7.17E-06
95%	9.01E-05	9.59E-05	1.43E-04	7.42E-05	7.38E-05	8.26E-05	5.03E-05

σ_y VALUES AT DOWNWIND DISTANCE: 500 m							
Quantile	EXCALIBR (item)	PARFUM (item)	UNICORN (item)	EXCALIBR (equal)	PARFUM (equal)	UNICORN (equal)	CHI (equal)
5%	4.89E+01	4.57E+01	4.78E+01	5.34E+01	4.84E+01	4.39E+01	5.50E+01
50%	1.54E+02	1.37E+02	1.32E+02	1.76E+02	1.62E+02	1.74E+02	1.72E+02
95%	3.09E+02	3.28E+02	3.49E+02	6.54E+02	7.38E+02	7.49E+02	7.24E+02

Case A-1: x = 1 km

χ (x, 0, H)/Q_0 VALUES AT DOWNWIND DISTANCE: 1 km							
Quantile	EXCALIBR (item)	PARFUM (item)	UNICORN (item)	EXCALIBR (equal)	PARFUM (equal)	UNICORN (equal)	CHI (equal)
5%	1.94E-07	1.76E-07	1.75E-07	9.06E-08	1.02E-07	1.03E-07	7.85E-07
50%	2.80E-06	2.94E-06	3.08E-06	1.83E-06	2.08E-06	2.31E-06	6.37E-06
95%	2.34E-05	2.82E-05	4.46E-05	1.90E-05	2.24E-05	2.62E-05	3.75E-05

σ_y VALUES AT DOWNWIND DISTANCE: 1 km							
Quantile	EXCALIBR (item)	PARFUM (item)	UNICORN (item)	EXCALIBR (equal)	PARFUM (equal)	UNICORN (equal)	CHI (equal)
5%	9.55E+01	8.26E+01	8.61E+01	1.03E+02	9.20E+01	8.07E+01	8.90E+01
50%	2.94E+02	2.69E+02	2.58E+02	3.30E+02	3.03E+02	3.29E+02	3.08E+02
95%	5.98E+02	6.69E+02	7.17E+02	1.27E+03	1.37E+03	1.43E+03	1.51E+03

Case A-1: x = 3 km

χ (x, 0, H)/Q_0 VALUES AT DOWNWIND DISTANCE: 3 km							
Quantile	EXCALIBR (item)	PARFUM (item)	UNICORN (item)	EXCALIBR (equal)	PARFUM (equal)	UNICORN (equal)	CHI (equal)
5%	2.26E-08	1.98E-08	1.93E-08	2.24E-08	1.63E-08	1.61E-08	5.27E-08
50%	4.08E-07	3.76E-07	3.88E-07	3.04E-07	3.30E-07	3.66E-07	5.01E-07
95%	2.85E-06	4.09E-06	6.93E-06	2.48E-06	3.51E-06	4.26E-06	3.71E-06

σ_y VALUES AT DOWNWIND DISTANCE: 3 km							
Quantile	EXCALIBR (item)	PARFUM (item)	UNICORN (item)	EXCALIBR (equal)	PARFUM (equal)	UNICORN (equal)	CHI (equal)
5%	2.63E+02	2.09E+02	2.19E+02	2.79E+02	2.74E+02	2.16E+02	1.98E+02
50%	7.78E+02	7.69E+02	7.35E+02	7.39E+02	8.27E+02	8.97E+02	7.68E+02
95%	1.65E+03	2.41E+03	2.32E+03	3.64E+03	3.76E+03	3.96E+03	4.84E+03

Case A-1: x = 10 km

χ (x, 0, H)/Q_0 VALUES AT DOWNWIND DISTANCE: 10 km							
Quantile	EXCALIBR (item)	PARFUM (item)	UNICORN (item)	EXCALIBR (equal)	PARFUM (equal)	UNICORN (equal)	CHI (equal)
5%	1.69E-09	1.71E-09	1.72E-09	2.30E-09	2.16E-09	2.11E-09	5.31E-09
50%	4.73E-08	3.89E-08	4.33E-08	5.57E-08	4.42E-08	4.86E-08	6.72E-08
95%	6.06E-07	5.08E-07	8.77E-07	4.52E-07	4.77E-07	5.64E-07	4.95E-07

σ_y VALUES AT DOWNWIND DISTANCE: 10 km							
Quantile	EXCALIBR (item)	PARFUM (item)	UNICORN (item)	EXCALIBR (equal)	PARFUM (equal)	UNICORN (equal)	CHI (equal)
5%	4.86E+02	5.71E+02	5.97E+02	6.77E+02	7.28E+02	6.26E+02	5.68E+02
50%	1.95E+03	2.43E+03	2.25E+03	2.30E+03	2.48E+03	2.74E+03	2.09E+03
95%	8.82E+03	7.74E+03	8.16E+03	1.16E+04	1.16E+04	1.20E+04	1.73E+04

Case A-1: x = 30 km

χ (x, 0, H)/Q_0 VALUES AT DOWNWIND DISTANCE: 30 km							
Quantile	EXCALIBR (item)	PARFUM (item)	UNICORN (item)	EXCALIBR (equal)	PARFUM (equal)	UNICORN (equal)	CHI (equal)
5%	1.43E-09	1.73E-10	1.83E-10	1.08E-09	3.40E-10	3.31E-10	6.11E-10
50%	2.28E-08	4.58E-09	5.73E-09	1.88E-08	6.95E-09	7.77E-09	8.45E-09
95%	4.59E-07	7.84E-08	1.32E-07	1.95E-07	7.71E-08	9.76E-08	7.87E-08

The χ (x, 0, H)/Q_0 values at 30 km for case A-1 cannot actually be compared because data from the PARFUM input file were removed for case A-1 because of the presence of the mixing layer.

σ_y VALUES AT DOWNWIND DISTANCE: 30 km							
Quantile	EXCALIBR (item)	PARFUM (item)	UNICORN (item)	EXCALIBR (equal)	PARFUM (equal)	UNICORN (equal)	CHI (equal)
5%	1.67E+03	1.41E+03	1.49E+03	2.05E+03	1.88E+03	1.65E+03	1.23E+03
50%	6.52E+03	6.97E+03	6.37E+03	5.93E+03	6.77E+03	7.35E+03	5.11E+03
95%	1.89E+04	2.52E+04	2.59E+04	3.31E+04	3.33E+04	3.33E+04	5.56E+04

Case A-4: x = 500 m

χ (x, 0, H)/Q_0 VALUES AT DOWNWIND DISTANCE: 500 m							
Quantile	EXCALIBR (item)	PARFUM (item)	UNICORN (item)	EXCALIBR (equal)	PARFUM (equal)	UNICORN (equal)	CHI (equal)
5%	1.73E-05	7.45E-06	7.32E-06	1.76E-05	1.00E-05	1.26E-05	1.70E-05
50%	1.30E-04	8.63E-05	9.59E-05	1.22E-04	1.25E-04	1.44E-04	1.37E-04
95%	8.68E-04	8.71E-04	1.04E-03	8.27E-04	8.90E-04	1.34E-03	9.14E-04

σ_y VALUES AT DOWNWIND DISTANCE: 500 m							
Quantile	EXCALIBR (item)	PARFUM (item)	UNICORN (item)	EXCALIBR (equal)	PARFUM (equal)	UNICORN (equal)	CHI (equal)
5%	1.81E+01	1.67E+01	1.61E+01	1.42E+01	1.30E+01	1.26E+01	9.27
50%	3.83E+01	4.54E+01	4.42E+01	4.70E+01	4.80E+01	4.73E+01	3.83E+01
95%	9.90E+01	1.13E+02	1.19E+02	1.33E+02	1.47E+02	1.55E+02	2.31E+02

Case A-4: x = 1 km

χ (x, 0, H)/Q_0 VALUES AT DOWNWIND DISTANCE: 1 km							
Quantile	EXCALIBR (item)	PARFUM (item)	UNICORN (item)	EXCALIBR (equal)	PARFUM (equal)	UNICORN (equal)	CHI (equal)
5%	1.24E-06	3.12E-06	3.04E-06	1.69E-06	3.22E-06	4.12E-06	6.98E-06
50%	4.07E-05	3.75E-05	4.23E-05	4.92E-05	4.82E-05	5.39E-05	5.72E-05
95%	2.99E-04	3.95E-04	4.84E-04	2.97E-04	3.88E-04	5.97E-04	4.40E-04

σ_y VALUES AT DOWNWIND DISTANCE: 1 km							
Quantile	EXCALIBR (item)	PARFUM (item)	UNICORN (item)	EXCALIBR (equal)	PARFUM (equal)	UNICORN (equal)	CHI (equal)
5%	3.43E+01	2.87E+01	2.79E+01	2.58E+01	2.30E+01	2.24E+01	1.55E+01
50%	7.72E+01	8.43E+01	8.18E+01	8.78E+01	8.80E+01	8.58E+01	6.77E+01
95%	1.86E+02	2.12E+02	2.28E+02	2.43E+02	2.70E+02	2.86E+02	4.67E+02

Case A-4: x = 3 km

χ (x, 0, H)/Q_0 VALUES AT DOWNWIND DISTANCE: 3 km							
Quantile	EXCALIBR (item)	PARFUM (item)	UNICORN (item)	EXCALIBR (equal)	PARFUM (equal)	UNICORN (equal)	CHI (equal)
5%	1.01E-06	7.46E-07	7.47E-07	1.03E-06	5.06E-06	3.33E-07	1.00E-06
50%	7.87E-05	9.90E-06	1.15E-05	1.07E-05	1.06E-05	6.18E-05	8.58E-05
95%	1.07E-04	1.15E-04	1.46E-04	8.47E-05	1.07E-04	8.32E-04	9.94E-04

σ_y VALUES AT DOWNWIND DISTANCE: 3 km							
Quantile	EXCALIBR (item)	PARFUM (item)	UNICORN (item)	EXCALIBR (equal)	PARFUM (equal)	UNICORN (equal)	CHI (equal)
5%	7.90E+01	6.77E+01	6.50E+01	6.46E+01	5.70E+01	5.64E+01	3.18E+01
50%	2.48E+02	2.23E+02	2.21E+02	2.31E+02	2.30E+01	2.16E+01	1.43E+02
95%	5.65E+02	6.05E+02	6.67E+02	6.94E+02	7.26E+02	7.74E+02	1.46E+03

Case A-4: x = 10 km

χ (x, 0, H)/Q_0 VALUES AT DOWNWIND DISTANCE: 10 km							
Quantile	EXCALIBR (item)	PARFUM (item)	UNICORN (item)	EXCALIBR (equal)	PARFUM (equal)	UNICORN (equal)	CHI (equal)
5%	2.04E-07	1.53E-07	1.56E-07	1.22E-07	6.05E-08	8.64E-08	1.32E-07
50%	1.88E-06	2.32E-06	2.62E-06	1.94E-06	1.97E-06	2.16E-06	1.35E-06
95%	2.68E-05	3.08E-05	4.08E-05	2.11E-05	2.70E-05	2.39E-05	2.10E-05

σ_y VALUES AT DOWNWIND DISTANCE: 10 km							
Quantile	EXCALIBR (item)	PARFUM (item)	UNICORN (item)	EXCALIBR (equal)	PARFUM (equal)	UNICORN (equal)	CHI (equal)
5%	1.81E+02	1.68E+02	1.58E+02	1.58E+02	1.52E+02	1.51E+02	7.37E+01
50%	7.90E+02	6.47E+02	6.31E+02	6.33E+02	6.42E+02	6.13E+02	3.66E+02
95%	2.02E+03	1.96E+03	2.17E+03	2.11E+03	2.14E+03	2.33E+03	5.12E+03

Case A-4: x =30 km

χ (x, 0, H)/Q_0 VALUES AT DOWNWIND DISTANCE: 30 km							
Quantile	EXCALIBR (item)	PARFUM (item)	UNICORN (item)	EXCALIBR (equal)	PARFUM (equal)	UNICORN (equal)	CHI (equal)
5%	7.18E-08	3.70E-08	3.66E-08	1.45E-08	9.90E-09	1.32E-08	1.75E-08
50%	7.13E-07	6.10E-07	7.12E-07	5.40E-07	4.23E-07	5.47E-07	2.16E-07
95%	1.07E-05	9.07E-06	1.26E-05	7.66E-06	7.84E-06	1.33E-05	4.67E-06

σ_y VALUES AT DOWNWIND DISTANCE: 30 km							
Quantile	EXCALIBR (item)	PARFUM (item)	UNICORN (item)	EXCALIBR (equal)	PARFUM (equal)	UNICORN (equal)	CHI (equal)
5%	3.77E+02	3.70E+02	3.57E+02	3.42E+02	3.66E+02	3.60E+02	1.58E+02
50%	1.83E+03	1.72E+03	1.64E+03	1.86E+03	1.64E+03	1.59E+03	7.47E+02
95%	4.98E+03	6.07E+03	6.35E+03	5.83E+03	5.92E+03	6.40E+03	1.47E+03

E.7 Development of Final Distributions Over Dispersion Code Input Parameters

The Sigma method was chosen for the development of the final distributions over the dispersion code input parameters. The choice of the Sigma method was based on the following two factors:

1. The Sigma method successfully processed and accurately reproduced the aggregated elicited χ_c/Q and s_y data on which it was based.

2. The assumption of the Sigma method, based on the Gaussian plume model, is consistent with the fixed code model constraint of this joint study. (Use of the Chi method would require modifications of MACCS and COSYMA in order to handle χ_z/χ_c and χ_y/χ_c values greater than 1.0.)

E.8 References

1. Cooke, R.M., and F. Vogt, Delft University of Technology, "PARFUM - Parameter Fitting for Uncertain Models, Concepts and Code for Accident Consequence Modeling," Delft, The Netherlands, February 1993.

2. Cooke, R.M., L.H.J. Goossens, and B.C.P. Kraan, Delft University of Technology, "Methods for CEC/USNRC Accident Consequence Uncertainty Analysis of Dispersion and Deposition - Performance Based Aggregating of Expert Judgments and PARFUM Method for Capturing Modeling Uncertainty," EUR-15856-EN, Luxembourg, June 1994.

3. Fischer, F., J. Päsler-Sauer, and J. Raicevic, Kernforschungszentrum Karlsruhe GmbH, "Uncertainty Analyses for the Atmospheric Dispersion Submodule of UFMOD with Emphasis on Parameter Correlations," KfK-4447, Karlsruhe, Germany, August 1989.

4. Jones, J.A., National Radiological Protection Board, "Uncertainty in Dispersion Detimates Obtained from the Working Group Models," NRPB-R-199, Chilton UK, August, 1986.

5. van Dorp, J.R., and A. Vinovarov, Delft University of Technology, "UNICORN - User's Manual for the UNICORN Computerized Uncertainty Analysis System," Delft, The Netherlands, February, 1992.

6. Kuhn, H.W., and A.W. Tucker, "Nonlinear Programming" (J. Neyman, ed.) *Proceedings of the Second Berkeley Symposium on Mathematical Statistics and Probability*, University of California Press, Berkeley, CA, 481-492, 1950.

7. Schrage, L., University of Chicago, "LINDO - An Optimization & Modeling System," 4th edition, Cincinnati, OH: Boyd & Fraser, 1991.

APPENDIX F

Case Structures

F. Case Structures

F.1 Case Structure for Atmospheric Dispersion

For the dispersion case structures, the experts were asked to provide 5th, 50th, and 95th percentile data for each elicitation variable. Values for the 0th and 100th percentiles were also requested but not required.

The atmospheric dispersion elicitation questions refer to five cases:

A. Dispersion within 30 km of the release under four different meteorological conditions (specified by wind speeds, standard deviations of wind directions, and lapse rate).

B. Dispersion in the near field under five different meteorological conditions (specified by wind speeds, standard deviations of wind directions, and lapse rate or Monin-Obukhov length). These assessments are relevant to understand the behavior of the plume near and close to the ground for short ranges and flat terrain.

C. Dispersion in the near field only under stable meteorological conditions (specified by wind speeds and standard deviations of wind directions). These assessments are relevant to understand the downwind behavior of the plume near the ground for low wind speeds at varying time-integrated concentrations in cases of a one-hour release.

D. Dispersion very close to the release source with no wake effects and under stable meteorological conditions with a very short sampling time. These assessments are relevant to understand the "snap-shot" plume start.

E. Dispersion into the far field at three distances: 80 km, 200 km, and 1000 km from the source.

		Case A-1	Case A-2
Meteorological Conditions	Temperature Lapse Rate	-2.0 K/100m	-1.6 K/100m
	Average Wind Speed	2.0 m/s	4.0 m/s
	Standard Deviation of Wind Direction at 10 m over 10 min	25 degrees	15 degrees
	Monin-Obukhov Length (1/L)	unknown	unknown
	Surface Roughness	Urban & Rural	Urban & Rural
	Release Height	10 meters	10 meters
	Sampling Time	60 min	60 min
	Downwind distance (km)		
Elicitation Variables	**0.5**	χ_c/Q	χ_c/Q
		χ_y/χ_c at 170 meters crosswind	χ_y/χ_c at 100 meters crosswind
		χ_z/χ_c at 50 meters above centerline	χ_z/χ_c at 50 meters above centerline
		s_y	s_y
	1.0	χ_c/Q	χ_c/Q
		χ_y/χ_c at 300 meters	χ_y/χ_c at 200 meters
		χ_z/χ_c at 150 meters above centerline	χ_z/χ_c at 100 meters above centerline
		s_y	s_y
	3.0	χ_c/Q	χ_c/Q
		χ_y/χ_c at 850 meters crosswind	χ_y/χ_c at 500 meters crosswind
		χ_z/χ_c at 500 meters above centerline	χ_z/χ_c at 250 meters above centerline
		s_y	s_y
	10.0	χ_c/Q	χ_c/Q
		χ_y/χ_c at 2.5 km crosswind	χ_y/χ_c at 1.5 km crosswind
		s_y	s_y
	30.0	χ_c/Q	χ_c/Q
		χ_y/χ_c at 6.7 km crosswind	χ_y/χ_c at 4 km crosswind
		s_y	s_y

		Case A-3	Case A-4
Meteorological Conditions	Temperature Lapse Rate	-1.0 K/100m	2.5 K/100m
	Average Wind Speed	6.0 m/s	3.0 m/s
	Standard Deviation of Wind Direction at 10 m over 10 min	10 degrees	2.5 degrees
	Monin-Obukhov Length	unknown	unknown
	Surface Roughness	Urban & Rural	Urban & Rural
	Release Height	10 meters	10 meters
	Sampling Time	60 min	60 min
Elicitation Variables	**Downwind distance (km)**		
	0.5	χ_c/Q	χ_c/Q
		χ_y/χ_c at 100 meters crosswind	χ_y/χ_c at 30 meters crosswind
		χ_z/χ_c at 50 meters above centerline	χ_z/χ_c at 10 meters above centerline
		s_y	s_y
	1.0	χ_c/Q	χ_c/Q
		χ_y/χ_c at 150 meters crosswind	χ_y/χ_c at 60 meters crosswind
		χ_z/χ_c at 100 meters above centerline	χ_z/χ_c at 30 meters above centerline
		s_y	s_y
	3.0	χ_c/Q	χ_c/Q
		χ_y/χ_c at 350 meters crosswind	χ_y/χ_c at 150 meters crosswind
		χ_z/χ_c at 250 meters above centerline	χ_z/χ_c at 100 meters above centerline
		s_y	s_y
	10.0	χ_c/Q	χ_c/Q
		χ_y/χ_c at 1.0 km crosswind	χ_y/χ_c at 500 meters crosswind
			χ_z/χ_c at 250 meters above centerline
		s_y	s_y
	30.0	χ_c/Q	χ_c/Q
		χ_y/χ_c at 6.7 km crosswind	χ_y/χ_c at 4 km crosswind
			χ_z/χ_c at 500 meters above centerline
		s_y	s_y

Meteorological Conditions	Case B-1	Case B-2
Temperature Lapse Rate	unknown	unknown
Average Wind Speed	6.0 m/s	5.0 m/s
Standard Deviation of Wind Direction at 10 m over 10 min	5 degrees	10 degrees
Monin-Obukhov Length (1/L)	-0.005	-0.01/m
Surface Roughness	Flat	Flat
Release Height	22 meters	22 meters
Sampling Time	60 min	60 min
	Elicitation Variable	
	χ_c/Q at 220 meters downwind	χ_c/Q at 220 meters downwind
	χ_c/Q at 315 meters downwind	χ_c/Q at 315 meters downwind

Meteorological Conditions	Case B-3	Case B-4
Temperature Lapse Rate	unknown	-1.0 K/100m
Average Wind Speed	8.0 m/s	3.0 m/s
Standard Deviation of Wind Direction at 10 m over 10 min	15 degrees	10 degrees
Monin-Obukhov Length (1/L)	-0.02/m	unknown
Surface Roughness	Flat	Flat
Release Height	22 meters	22 meters
Sampling Time	60 min	60 min
	Elicitation Variable	
	χ_c/Q at 300 meters downwind	χ_c/Q at 300 meters downwind
	χ_c/Q at 600 meters downwind	χ_c/Q at 600 meters downwind

Meteorological Conditions	Case B-5
Temperature Lapse Rate	-3.0 K/100m
Average Wind Speed	3.0 m/s
Standard Deviation of Wind Direction at 10 m over 10 min	2.5 degrees
Monin-Obukhov Length (1/L)	unknown
Surface Roughness	Flat
Release Height	22 meters
Sampling Time	60 min
Downwind Distance (m)	**Elicitation Variable**
600	χ_y/χ_c at 50 meters crosswind
	χ_z/χ_c at 10 meters below centerline
	s_y at release height
	s_y of overhead locations height

Dry Deposition Velocity (v_d) of Elemental Iodine		
Surface Type	**Wind Speed at 10 m height**	**Elicitation Variable**
urban	2 m/s	v_d
	5 m/s	v_d
meadow	2 m/s	v_d
	5 m/s	v_d
forest	2 m/s	v_d
	5 m/s	v_d
human skin	2 m/s	v_d
	5 m/s	v_d

Dry Deposition Velocity (v_d) of Methyl Iodide		
Surface Type	**Wind Speed at 10 m height**	**Elicitation Variable**
urban	2 m/s	v_d
	5 m/s	v_d
meadow	2 m/s	v_d
	5 m/s	v_d
forest	2 m/s	v_d
	5 m/s	v_d
human skin	2 m/s	v_d
	5 m/s	v_d

Dry Deposition velocity (v_d) of aerosols on Specific Surfaces				
Surface Type	**Wind Speed**	**Surface Roughness length**	**Particle Size**	**Elicitation Variable**
Moorland/peatland with vegetation of 40 cm high tussocks and dry grass underlain by wet peat	5 m/s at 5 meter height	5 $\pm$1 cm	0.55μ	v_d
			0.7μ	v_d
			0.9μ	v_d
			1.2μ	v_d
			1.6μ	v_d
Heather and green grass, soil partly covered	5 m/s at 5 meter height	4.5 $\pm$1.5 cm	0.55μ	v_d
			0.7μ	v_d
			0.9μ	v_d
			1.2μ	v_d
			1.6μ	v_d
			2.3μ	v_d
			3.2μ	v_d
			4.2μ	v_d
Grassland	unknown	unknown	1.0μ mass average, with a range of 0.5 to 2.0μ	v_d

Meteorological Conditions	Case C	Case D
Temperature Lapse Rate	stable conditions	stable conditions
Average Wind Speed	1.9 m/s	3.0 m/s
Standard Deviation of Wind Direction at 10 m over 10 min	6 degrees	unknown
Monin-Obukhov Length (1/L)	unknown	unknown
Surface Roughness	Urban & Rural	Flat
Release Height	45 meters	12 meters
Sampling Time	60, 120, & 240 min	1 min
Downwind Distance (km)	**Elicitation Variable**	
60		χ_c/Q
		s_z of vertical concentration
		s_y
360	χ_g/Q	
970	χ_g/Q	
1970	χ_g/Q	

Meteorological Conditions	Case E *
Temperature Lapse Rate	-3.0 K/100m
Average Wind Speed	3.0 m/s
Standard Deviation of Wind Direction at 10 m over 10 min	2.5 degrees
Monin-Obukhov Length (1/L)	unknown
Surface Roughness	Flat
Release Height	22 meters
Sampling Time	60 min
Downwind Distance (km)	**Elicitation Variable**
80	χ_y/χ_c at 50 meters crosswind
200	χ_z/χ_c at 10 meters below centerline
1000	s_y at release height
	s_y of overhead locations height

* For Case E the experts were asked to provide the shortest arc or sum of lengths of arcs at a distance from the release point crossed by 90% of the material, assuming that the material does not deposit during transport. Variable is in terms of the length of arc or sum of arcs crossed by 90% of the material

F.2 Case Structure for Dry Deposition

Only 5th, 50th, and 95th percentile data were requested for the dry deposition elicitation variables. Values for the 0th and 100th percentiles were also requested but not required. The experts were asked to provide the dry deposition velocity of aerosols, elemental iodine, and methyl iodide for four surface types: urban, meadow, forest, and human skin.

The dry deposition velocity of aerosols was also solicited for three specific surfaces: (1) moorland/ peatland with vegetation consisting of 40 cm high tussocks, old dry grass partly filling the spaces between the tussocks, all underlain by a wet peat layer; (2) a surface of heather and green grass with vegetation only partly covering the soil; and (3) grassland.

Dry Deposition velocity (v_d) of aerosols			
Surface Type	**Particle Size**	**Elicitation Variable**	
		Wind Speed at 10 m height	
		2 m/s	5 m/s
urban	0.1μ	v_d	v_d
	0.3μ	v_d	v_d
	1.0μ	v_d	v_d
	3.0μ	v_d	v_d
	10.0μ	v_d	v_d
meadow	0.1μ	v_d	v_d
	0.3μ	v_d	v_d
	1.0μ	v_d	v_d
	3.0μ	v_d	v_d
	10.0μ	v_d	v_d
forest	0.1μ	v_d	v_d
	0.3μ	v_d	v_d
	1.0μ	v_d	v_d
	3.0μ	v_d	v_d
	10.0μ	v_d	v_d
human skin	0.1μ	v_d	v_d
	0.3μ	v_d	v_d
	1.0μ	v_d	v_d
	3.0μ	v_d	v_d
	10.0μ	v_d	v_d

F.3 Case Structure for Wet Deposition

Only 5th, 50th, and 95th percentile data were requested for the wet deposition elicitation variables. Values for the 0th and 100th percentiles were also requested but not required. The experts were asked to supply values for the fraction of elemental iodine, methyl iodide, and aerosols removed by rain ($1\text{-}f_w$). For the elemental iodine variables, the rainfall, time period and windspeeds were specified. For the methyl iodide, the rainfall and time period were specified. For the fraction of aerosols removed by rain, the particle sizes were specified to have a unit density of 1 g/cm^3; the rainfall and time period were specified.

Elemental Iodine: fraction removed by rain ($1\text{-}f_w$)			
Rainfall Amount	**Time Period**	**Wind Speed**	**Elicitation Variable**
0.3 mm	1 hour	unknown	$1\text{-}f_w$
2.0 mm	1 hour	unknown	$1\text{-}f_w$
0.075 mm	10 minutes	10 m/s	$1\text{-}f_w$
0.05 mm	10 minutes	unknown	$1\text{-}f_w$
0.17 mm	10 minutes	5 m/s	$1\text{-}f_w$
0.17 mm	10 minutes	14 m/s	$1\text{-}f_w$
0.23 mm	10 minutes	12 m/s	$1\text{-}f_w$
0.5 mm	10 minutes	unknown	$1\text{-}f_w$
0.33 mm	10 minutes	unknown	$1\text{-}f_w$
1.0 mm	10 minutes	14 m/s	$1\text{-}f_w$
1.67 mm	10 minutes	unknown	$1\text{-}f_w$

Methyl Iodide: fraction removed by rain ($1\text{-}f_w$)			
Rainfall Amount	**Time Period**	**Wind Speed**	**Elicitation Variable**
0.3 mm	1 hour	unknown	$1\text{-}f_w$
2.0 mm	1 hour	unknown	$1\text{-}f_w$
0.05 mm	10 minutes	unknown	$1\text{-}f_w$
0.33 mm	10 minutes	unknown	$1\text{-}f_w$
1.67 mm	10 minutes	unknown	$1\text{-}f_w$

Aerosols: fraction removed by rain ($1-f_w$)				
Rainfall Amount	**Time Period**	**Particle Size**	**Wind Speed**	**Elicitation Variable**
0.3 mm	1 hour	0.1μ	unknown	$1-f_w$
		0.3μ		$1-f_w$
		1.0μ		$1-f_w$
		10.0μ		$1-f_w$
2.0 mm	1 hour	0.1μ	unknown	$1-f_w$
		0.3μ		$1-f_w$
		1.0μ		$1-f_w$
		10.0μ		$1-f_w$
0.05 mm	10 minutes	0.1μ	unknown	$1-f_w$
		0.3μ		$1-f_w$
		1.0μ		$1-f_w$
		10.0μ		$1-f_w$
0.33 mm	10 minutes	0.1μ	unknown	$1-f_w$
		0.3μ		$1-f_w$
		1.0μ		$1-f_w$
		10.0μ		$1-f_w$
1.67 mm	10 minutes	0.1μ	unknown	$1-f_w$
		0.3μ		$1-f_w$
		1.0μ		$1-f_w$
		10.0μ		$1-f_w$

APPENDIX G

Summary of MACCS and COSYMA Consequence Codes

G. Summary of MACCS and COSYMA Consequence Codes

G.1 Introduction

This appendix provides a brief overview of the MACCS and COSYMA consequence codes. A more complete discussion of MACCS and COSYMA can be found in the reports by Jow et al.[1] and Kelly,[2] listed among the references.

G.2 Brief Description of MACCS and COSYMA Dispersion and Deposition Models

The information developed in this study will be used to perform uncertainty studies using the CEC consequence code COSYMA and the USNRC code MACCS. COSYMA and MACCS model the offsite consequences of postulated severe reactor accidents that release a plume of radioactive material to the atmosphere. These codes model the transport and deposition of radioactive gases and aerosols into the environment and the potential resulting human health and economic consequences.

COSYMA and MACCS both employ a Gaussian plume model (GPM) for atmospheric dispersion. At a given downwind distance and given atmospheric conditions, the Gaussian model predicts the time-integrated concentration at various horizontal and vertical displacements from the center-line of the plume. When the plume is not constrained by the ground or the inversion layer, the basic Gaussian plume equation for determining the concentration relative to the release rate is:

$$\frac{\chi}{Q} = \frac{1}{2\pi\sigma_y\sigma_z\bar{u}}\exp\left(-\frac{y^2}{2\sigma_y^2}\right)\exp\left(-\frac{(z-h)^2}{2\sigma_z^2}\right)$$

where:

χ = time integrated air concentration
Q = the source strength
y = the horizontal displacement relative to the plume centerline
z = the vertical displacement
h = the vertical height of the plume centerline
$\bar{u}$ = the average wind velocity
σ_y and σ_z are plume expansion parameters

In MACCS and COSYMA, the plume expansion parameters, σ_y and σ_z, are modeled by the following power law:

$$\sigma_y = a_y x^{b_y} \; ; \; \sigma_z = a_z x^{b_z}$$

where x = the downwind distance from the plume release point.

Currently, constant values for a_y, b_y, and a_z, b_z are provided in the codes. The values for the a_y, b_y, and a_z, b_z parameters are determined by the atmospheric stability class and the roughness length of the terrain.

Two types of deposition are modeled in the MACCS and COSYMA codes: wet and dry deposition. Dry deposition incorporates removal from the plume by diffusion, impaction, and settling; it is modeled through a dry deposition velocity, which is a user input. The dry deposition velocity depends on particle size; therefore, if the aerosol size distribution is divided into ranges, a dry deposition velocity must be specified for each range. The washout of radioactive material from the plume, wet deposition, is modeled as dependent on the rain intensity. The fraction of material, f_w, that remains in the plume is given by:

$$f_w = \exp\left\{-a I^b \Delta t\right\}$$

where I is the rain intensity and Δt is the amount of time the plume is exposed to the rain. The parameters a and b are the user-specified parameters that determine the amount of material washed from the plume as a result of rain intensity. Rainout, in which droplets nucleate on the aerosol particles, is not modeled.

G.3 Summary of the MACCS Radiological Consequence Code

The MACCS code was originally developed under NRC sponsorship to estimate the offsite consequences of potential severe accidents at nuclear power plants by using meteorological data that varies on an hourly basis. The code models the transport and dispersion of plumes of radioactive material released from the facility to the atmosphere. As the plumes travel through the atmosphere, material may be deposited on the ground via wet and dry

deposition processes. There are seven pathways through which the general population can be exposed: cloudshine, groundshine, direct and resuspension inhalation, ingestion of contaminated food and water, and deposition on skin. Emergency response and protective action guides for both the short and long term are also considered as means for mitigating the extent of the exposures. As a final step, the economic costs that would result from the mitigative actions are estimated. Variability in consequences as a result of weather may be obtained in the form of a complementary cumulative distribution function.

MACCS is organized into three modules. The ATMOS module performs the atmospheric transport and deposition portion of the calculation. The EARLY module estimates the consequences of the accident immediately following the incident (usually within the first week), and the CHRONC module estimates the long-term consequences of the accident. A schematic representation of these modules and the input files that provide information to them is shown in Figure G.1. The phenomena modeled in MACCS are described in more detail below.

G.3.1 Atmospheric Dispersion and Transport

The release of radioactive materials to the atmosphere can be divided into successive plume segments, which can have different compositions, release times, durations, release heights, and amounts of sensible heats. The plume segment lengths are determined by the product of the segment's release duration and the average windspeed during release. The initial vertical and horizontal dimensions of each plume segment are user-specified.

A lift-off criterion based on a critical windspeed determines whether or not a plume is subject to buoyant plume rise. Momentum plume rise is not modeled. If the windspeed at release is greater than the critical windspeed, plume rise is prevented.

After release from the facility, windspeed determines the rates at which plume segments transport in the downwind direction, and the wind direction at the time of release determines the direction of travel. MACCS neglects wind trajectories, as do most other consequence codes. Sixteen compass-sector population distributions are assumed to constitute a representative set of downwind exposed populations. The exposure probability of each of the 16 compass-sector population distributions is assumed to be given by the frequency with which the wind blows from the site into the sector. During transport, dispersion of the plume in the vertical and horizontal directions is estimated using an empirical model, the GPM. In this model, dispersion depends on atmospheric stability and windspeed. Horizontal dispersion of the plume segments is unconstrained. However, vertical dispersion is bounded by the ground and by the mixing layer, which are both modeled as totally reflecting layers. A single value for the mixing layer is specified by the user for each season of the year and is constant during a calculation. Eventually the vertical distribution of each plume segment becomes uniform and is so modeled. Figure G.2 contains an illustration showing the dispersion and deposition phenomena modeled in MACCS.

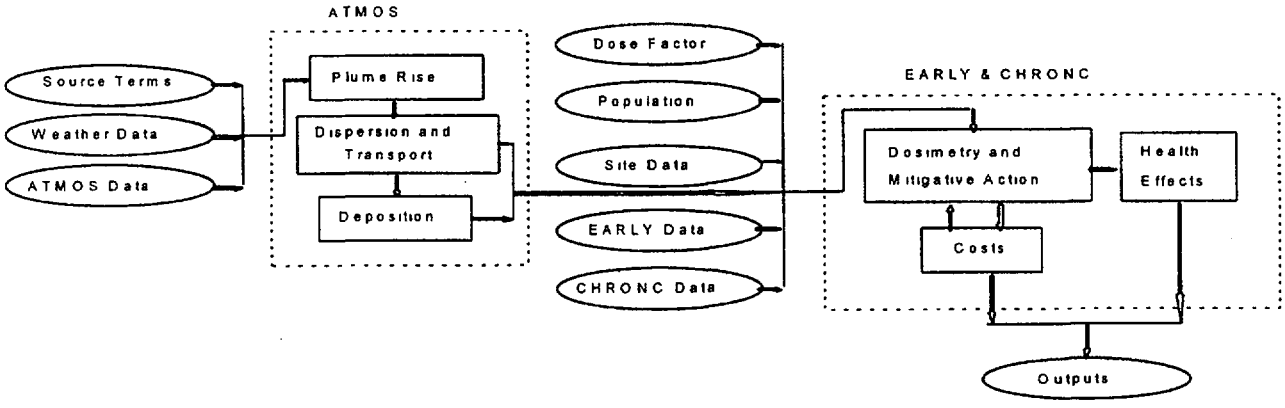

Figure G.1 Progression of a MACCS consequence calculation

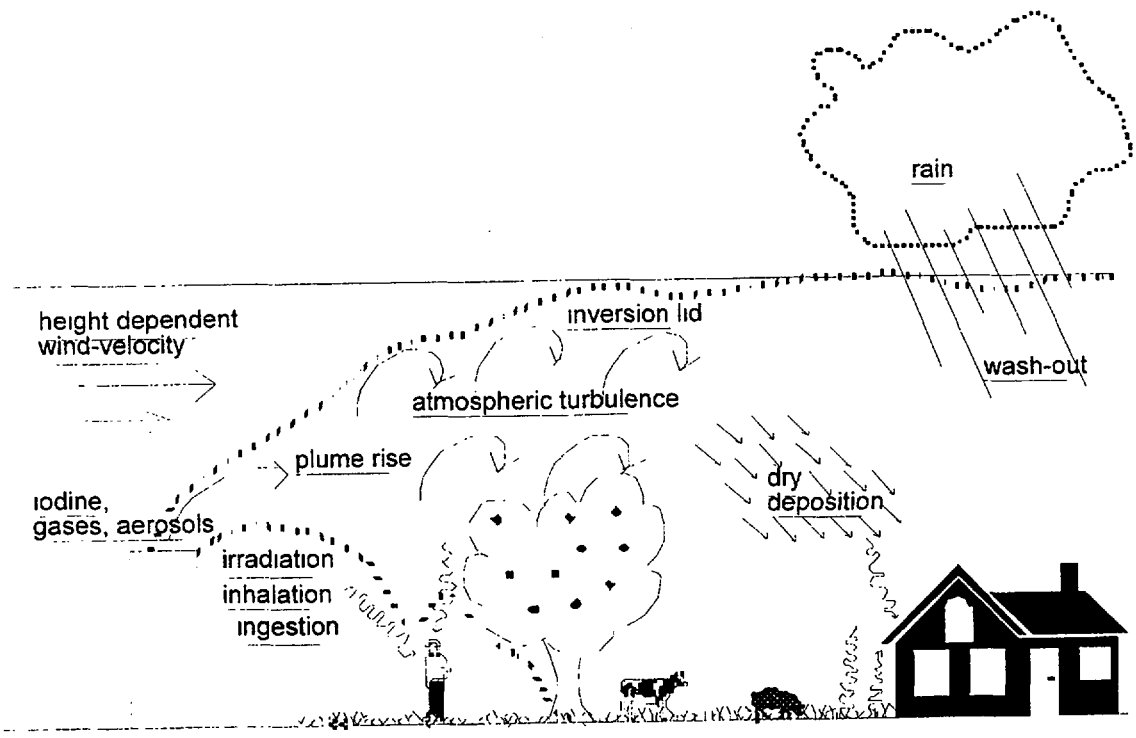

Figure G.2 Dispersion and deposition phenomena considered in a MACCS calculation

G.3.2 Deposition, Weathering, Resuspension, and Decay

As noted earlier, two types of deposition are modeled in MACCS: wet deposition and dry deposition. Weathering, resuspension, washoff, and radioactive decay decrease the deposited concentrations of radioactive materials. Radioactive decay treats only first generation daughter products.

G.3.3 Weather

Plume rise, dispersion, downwind transport, and deposition depend on the prevailing meteorological conditions. These conditions can be modeled as time-invariant or as varying hour-by-hour. If they are modeled as variable, the user may specify them directly or through an input file.

G.3.4 Dosimetry

The MACCS dosimetry model consists of three interacting processes: (1) the projection of individual exposures to radioactive contamination for each of the seven exposure pathways modeled over a user-specified time, (2) mitigation of these exposures by protective-measure actions, and (3) calculation of the actual exposures incurred after mitigation by protective-measure actions. For each exposure pathway, MACCS models the radiological burden for the pathway as reduced by the actions taken to mitigate that pathway dose. The total dose to an organ is obtained by summing the doses delivered by each of the individual pathways.

G.3.5 Dose Mitigation

The time after accident initiation is divided into three phases: (1) an emergency phase, (2) an optional intermediate phase, and (3) a long-term phase. During the emergency phase, which can last up to seven days, doses are reduced by evacuation, sheltering, and temporary relocation of people. During the intermediate phase, doses may be avoided by temporary relocation of people. During the long-term phase, doses are reduced by decontamination of property that is not habitable, by temporary interdiction of property that cannot be restored to habitability by decontamination alone, by condemnation of property that cannot be restored to habitability at a cost below or equal

to the worth of the property, by disposal of contaminated crops, and by banning farming on contaminated farmland.

G.3.6 Exposure Pathways

MACCS models seven exposure pathways: (1) exposure to the passing plume (cloudshine), (2) exposure to materials deposited on the ground (groundshine), (3) exposure to materials deposited on skin, (4) inhalation of materials directly from the passing plume (inhalation), (5) inhalation of materials resuspended from the ground by natural and mechanical process (resuspension inhalation), (6) ingestion of contaminated foodstuffs (food ingestion), and (7) ingestion of contaminated water (water ingestion). Ingestion doses do not contribute to the doses calculated for the emergency phase of the accident. Only groundshine and inhalation of resuspended materials produce doses during the optional intermediate phase of the accident. Long-term doses are caused by groundshine, resuspension inhalation, water ingestion, and food ingestion. Ingestion of contaminated food or water generates doses to people who reside at unknown locations both on and off of the computational grid.

G.3.7 Population Cohorts

People on the computational grid are assigned to three groups: (1) evacuees, (2) people actively taking shelter, and (3) people who continue normal activities. Shielding factors for each of the groups are specified by the user.

G.3.8 Health Effects

Health effects are calculated from doses to specific organs using dose conversion factors. Early injuries and fatalities (those occurring within one year of the accident) are estimated using nonlinear dose-response models. Latent cancers are estimated using a piecewise linear dose-response model that is discontinuous. Two equations are implemented in the code, one for high exposures and one for low exposures.

G.3.9 Economic Effects

Economic consequences result from the implementation of mitigative actions. The following costs are considered in this estimate: (1) evacuation costs, (2) temporary relocation costs, (3) costs of decontaminating land and buildings, (4) lost return-on-investments from temporarily interdicted properties, (5) value of crops destroyed or not grown, and (6) value of condemned property. Costs associated with damage to the reactor, the purchase of replacement power, medical care, life-shortening, and litigation are not considered.

G.4 Summary of COSYMA Radiological Consequence Code

COSYMA (COde SYtem from MAria) is a computer program package used for calculating off-site consequences of accidental releases to the atmosphere. The code was developed by the National Radiological Protection Board (NRPB) of the UK and Kernforschungszentrum Karlsruhe GmbH (KfK) of Germany as part of the MARIA project.[2,3] It represents a fusion of ideas and modules from the NRPB program MARC, the KfK program system UFOMOD, and input from other MARIA contractors. The program package was made available in the autumn of 1990. Several updates have since been released. A PC version was released in 1993.

COSYMA is intended for probabilistic calculations of the health effects, economic costs, and effects of countermeasures following postulated accidents at nuclear sites. The results can be presented in a variety of ways, depending on what is required. COSYMA can be applied to accidental releases ranging from small perturbations in operations to large hypothetical accidents at both fission and fusion installations.

Figure G.3 provides an outline of the COSYMA program. COSYMA is a package of programs and data bases rather than a single program. It contains three main accident consequence assessment programs together with a number of preprocessing and evaluation programs. The three main programs of COSYMA are known as the NE (near, early), NL (near, late), and FL (far, late) subsystems. These three programs are designed for application in different time periods and distance ranges. The terms "near" and "far" indicate the range of the calculation; the terms "early" and "late" characterize the kind of health effects and countermeasures considered.

The main endpoints of COSYMA are the numbers representing health effects, economic costs, and the effect of countermeasures resulting from the accidental releases.

A large number of intermediate results are obtained in the process of calculating the endpoints; these results include activity concentrations, individual and collective doses, and the areas and numbers of people affected by countermeasures. The package contains a series of evaluation programs that allow these results to be presented in a variety of ways.

G.4.1 Atmospheric Dispersion and Transport

A complete description of the modeling of atmospheric dispersion and deposition, including plume rise, is given in the report describing UFOMOD.[4] In the atmospheric dispersion module ATMOS of the COSYMA code, two ranges are distinguished:

- near range modeling up to about 50 km,
- far range modeling from about 50 km up to about 3000 km.

COSYMA's standard atmospheric dispersion model of the near range is the Gaussian segmented plume model MUSEMET.[5] Alternative models can be used for special calculations:

- the Gaussian puff model RIMPUFF,[6] if 2-dimensional wind fields will be considered,
- the straight-line Gaussian plume model COSGAP, extracted from the NRPB code MARC,[7]
- the statistical Gaussian plume model ISOLA,[8] for use with quasi-stationary releases of weeks to months.

The far-range model of COSYMA is the trajectory puff dispersion model MESOS.[9]

G.4.2 Standard Near-Range Modeling of Atmospheric Dispersion and Deposition in COSYMA

Time steps, release phases, and plume segmentation:

The dispersion model implemented in COSYMA is a segmented GPM, which allows for the modeling of time-dependent meteorological conditions and release rates. The time-step length of the release and the dispersion calculations is one hour, (i.e., variations of the release rates and meteorological conditions can be considered only hourly).

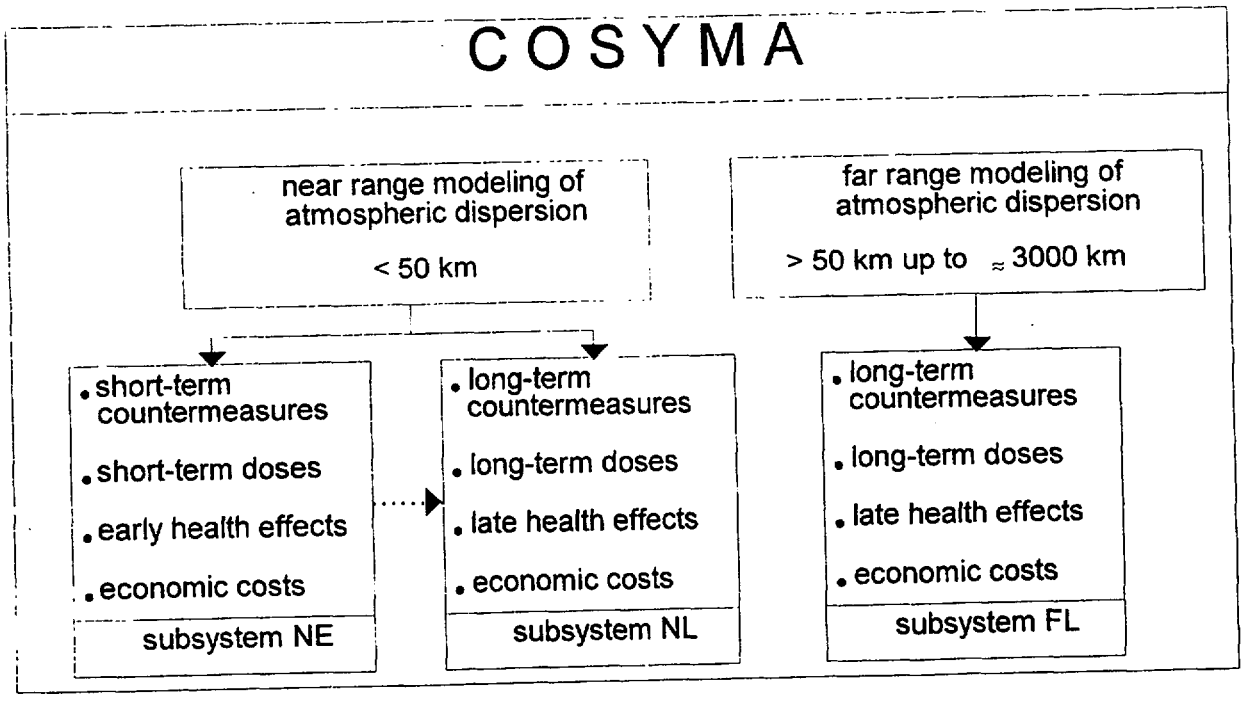

Figure G.3 General structure of the program system

During the time intervals, constant average conditions are assumed. The lengths of the straight-line plume segments correspond to these time intervals. The source term can be represented as a series of up to nine independent release phases with one hour durations for each, but with arbitrary gaps of one-hour multiples.

Meteorological data input:

The meteorological data are a series of hourly averages of windspeed and direction, diffusion category (Pasquill), precipitation intensity, and mixing layer height measured at or representative of the nuclear power production (NPP) site. Probabilistic risk assessment (PRA) runs use a set of weather sequences from a one-year or larger pool with hourly meteorological data. Different sampling methods (stratified, random, cyclic) for deriving this set can be chosen by the user.

Gaussian formulas used:

The normal Gaussian plume formulas are used for calculating the concentration $\chi(x,y)$ in the air 1 m above ground with consideration of reflection at the ground surface and at the mixing height level. The Gaussian equation in COSYMA includes an error function, which describes the drop of the concentration curve in the downwind direction for both ends of the i^{th} plume segment.

Deposition:

Dry deposition of aerosols and iodine is calculated in COSYMA by using deposition velocities that relate the surface contamination to the time-integrated concentration in the air above the surface. Particulate materials are assumed to have particle diameters of 1 m. Gravitational settling is not considered. Average deposition velocities used in COSYMA are: 0.001 m/s (aerosols), 0.01 m/s (elemental iodine), and 0.0005 m/s (organic iodine). The loss of activity in the plume caused by dry deposition is accounted for by reducing the source strength with downwind distance. This source depletion model assumes that the depletion occurs over the whole depth of the plume rather than in a layer close to the surface. As discussed in section G.4, wet deposition is modeled by washout. The loss of activity in the plume caused by wet deposition is modeled by source depletion.

Modeling of plume rise, lift-off, and the influence of buildings:

In COSYMA, the plume rise model of Briggs[10] is used to calculate the rising phase and the final rise of the plume in case of a release of thermal energy. This model considers different atmospheric stratifications (like unstable, neutral, and stable stratification), wind profiles, temperature profiles, and turbulent heat flows together with the conservation equations of mass, momentum, and enthalpy for modeling the interaction of a hot plume with a turbulent atmosphere. Initial momentum and radioactive self-heating of the plume are not treated in the COSYMA version of the Briggs model.

If there is sufficient advection, a hot release from an NPP building may get drawn into the cavity zone of the lee flow of the building. The heat energy density in this zone then determines whether there is enough buoyancy that the air still can rise. This component is decided by a lift-off criterion.

The influence of buildings is considered as far as it can reduce the height of the plume axis by lee flow effects; they cause an initial broadening of the plume by enhanced mixing in the turbulent wake zone. Initial plume broadening depends on the building size and is modeled by using a virtual source concept.

G.4.3 Dose Mitigation

Besides the assessment of the radiological situation after a release of radioactive material, COSYMA allows the user to specify a wide range of emergency actions and countermeasures to reduce the exposure of the population. The program allows the user considerable freedom in specifying the criteria at which these actions will be imposed and withdrawn so that most of the criteria presently adopted in different EC countries (and some of those that may be suggested in the future) can be modeled. Sheltering and evacuation can be implemented automatically or on the basis of doses received in definable time periods. Relocation can be implemented on a dose criterion. The criteria for returning from evacuation and/or relocation can also be specified by the user. Food bans can be imposed on the basis of doses received within specified periods or on the basis of the instantaneous radionuclide concentrations in food.

G.4.4 Health Effects

COSYMA calculates the doses from external radiation of the cloud and contaminated surfaces, including skin, and from internal radiation caused by inhalation and ingestion

activity. The data bases for external radiation and inhalation comprise 145 nuclides. The number of nuclides for ingestion is about 35. The default number of foodstuffs is 10, but larger numbers of foodstuffs can also be considered.

The risk of early health effects is calculated using "hazard functions." Ten different fatal and nonfatal early effects are quantified. Late health effects are calculated using linear dose-response relationships. COSYMA considers both fatal and nonfatal cancer in each of a series of internal human organs. COSYMA can provide information on the time at which the late health effects occur, the number of effects occurring in those people alive at the time of the accident, and the number of effects occurring in their descendants. Results can also be given in terms of life shortening.

G.4.5 Economic Effects

COSYMA can calculate the economic cost of the accident, considering the costs arising from countermeasures and the costs of health effects. The countermeasures for which costs are considered are movement of the population, food restrictions, and decontamination. The costs arising from lost production in the area from which people are moved can be assessed in terms of the per capita contribution of the relocated population to gross domestic product (GDP) or in terms of the value of the land area affected. The costs of food bans include contribution to GDP as well as the lost capital value of the affected land and the costs of affected food disposal. The costs arising from health effects in the exposed population may be calculated in terms of treatment costs and lost economic productivity. Alternatively, an estimate of the health effects using a more general approach to the valuation of life may be applied.

G.5 References

1. Jow, H.-N., et al., Sandia National Laboratories, "MELCOR Accident Consequence Code System (MACCS): Model Description," NUREG/CR-4691, Vol. 2, SAND86-1562, Vol. 2, Albuquerque, NM, February 1990.

2. Kelly, G.N., Commission of the European Communities (CEC), "COSYMA: A New Programme Package for Accident Consequence Assessment," EUR-13028, Luxembourg, 1991.

3. Ehrhardt, J., and J.A. Jones, "An Outline of COSYMA, A New Program Package for Accident Consequence Assessments," *Nuclear Technology*, 94:196-203, 1991.

4. Panitz, H.J., C. Matzerath, and J. Päsler-Sauer, Kernforschungszentrum Karlsruhe, "UFOMOD - Atmospheric Dispersion and Deposition," KfK-4332, Karlsruhe, 1989.

5 Straka, J., H. Geiss, and K.J. Vogt, "Diffusion of Waste Air Puffs and Plumes Under Changing Weather Conditions," *Contrib. Atoms. Phys. (Germany)*, 54:207-221, 1981.

6. Mikkelsen, T., S.E. Larsen, and S. Thykier-Nielsen, "Description of the RISo Puff Diffusion Model," *Nuclear Technology*, 67:56-65, 1984.

7. Clark, R.G., and G.N. Kelly, "MARC - The NRPB Methodology for Assessing Radiological Consequences of Accidental Releases of Activity," National Radiological Protection Board, NRPB-R127, Chilton, UK, Didcot, 1981.

8. Huebschmann, W., and W. Raskob, Kernforschungszentrum Karlsruhe GmbH, "ISOLA V - A Fortran 77 Code for the Calculation of the Long-Term Concentration Distribution in the Environment of Nuclear Installations," KfK 4604, Karlsruhe, 1990.

9. ApSimon, H.M., A.J. Goddard, and J. Wrigley, "Long-Range Atmospheric Dispersion of Radio-isotopes - I. The MESOS Model," *Atmospheric Environment*, 19:99-111, 1985.

10. Briggs, G.A., "Plume Rise Predictions," (D.A. Haugen, ed.), *Lectures on Air Pollution and Environmental Impact Analyses*, 59-111, American Meteorological Society, Boston, MA, pp.59-135, 1975.

APPENDIX H

Non-Gaussian Information Survey

H. Non-Gaussian Information Survey

Two of the eight dispersion experts provided values greater than one for the 95th percentile ratios of the off-centerline-plume concentration and the centerline-plume concentration (χ_y/χ_c, χ_z/χ_c). The following is a very general summary of the rationales provided by two experts for their specification of concentration ratios greater than one.

Expert P

The values for χ_y/χ_c and χ_z/χ_c greater than one result from complicated cross-wind concentration distributions as frequently observed in reality. For instance, a bifurcated chimney plume may have two off-centerline concentration maxims so that the ratios as quoted above may well exceed the value of one.

Expert J

The values for χ_y/χ_c and χ_z/χ_c greater than one result from the fact that the concentration distributions in plumes are not always Gaussian. Complex meteorology—such as convective conditions, vertical wind shear, or changing wind directions—can result in non-Gaussian shaped plumes. The center of a plume in a certain cross section has been defined as the center of mass in this cross section. In the case of non-Gaussian-shaped plumes, the concentration in the center of a cross section (as defined earlier) usually does not coincide with the highest concentration in the cross section. Therefore the ratio of the off-centerline concentration to the centerline concentration may be greater than one.

DISTRIBUTION

Pietro Cagnetti
Indirrizzo Postalc
Post Address
C.P.2400
00100 ROMA
(ITALIA)

Frank Gifford
109 Gorgas Lane
Oak Ridge, TN 37830

Paul Gudiksen
L.L. National Laboratory
P.O. Box 808 L-262
Livermore, CA 94550

Steve Hanna
Sigma Research Corporation
196 Baker Avenue
Concord, MA 01742

Jan Kretzschmar
Vareselaan 13
B-2400 Mol
Belgium

Klaus Nester
Institut fur Meteorologie
& Klimaforschung
Kernforschungszentrum
GmbH Postfach 3640
D-76021 Karlsruhe
GERMANY

Shankar Rao
NOAA/ERL/Air Resources
Laboratory
456 South Illinois Avenue
P.O. Box 2456
Oak Ridge, TN 37831

Han van Dop
Princetonplein 5 3584 CC
P.O. Box 80.005 3508 TA Utrecht
The NETHERLANDS

John Brockmann
Sandia National Laboratories
Department 6422
P.O. Box 5800
Albuquerque, NM 87185

Sheldon Friedlander
5531 Boelter Hall
University of California
Los Angeles, CA 90024

John Garland
AEA Technology
Culham
Abingdon
Oxfordshire OX14 3DB
United Kingdom

Jozef Pacyna
Norwegian Institute for
Air Research
Lillestrom
Norway

Joern Roed
RISO National Laboratory
P.O. Box 49
DK-4000 Roskilda
Denmark

Richard Scorer
2 Stanton Road
London SW20 8RL
United Kingdom

George Sehmel
Battelle
Battelle Blvd.
LSL2 Building
Richland, WA 99352

Sean Twomey
11280 E. Escalante Rd.
Tuscon, AZ 85730

Roger Cooke
Delft University of Technology
Julianalaan 132
P.O. Box 356
2600 AJ Delft
The Netherlands

Louis Goossens (50)
Delft University of Technology
Kanaalweg 2
2628 EB Delft
The Netherlands

Steve Hora
University of Hawaii
Dept. Business & Economics
P.O. Box 5622
Hilo, HI 96720

Bernd Krann
Kloosterkade 171
2628 JA Delf
the Netherlands

Juergen Paesler-Saur
Nuclear Research Center
INR, Bldg. 433
Postfach 3640
D-7500 Karlsruhe
West Germany

Oak Ridge National Laboratory(2)
Attn: Steve Fisher
Sherrel Greene
MS-8057
P.O. Box 2009
Oak Ridge, TN 37831

Westinghouse Savannah River Co. (2)
Attn: Kevin O'Kula
Jackie East
Safety Technology Section
1991 S. Centennial Ave. Bldg. 1
Aiken, SC 29803

Vern Peterson
Bldg. T886B
EG&G Rocky Flats
P.O. Box 464
Golden, CO 80402

Brookhaven National Laboratory (3)
Attn: Lev Neymotin
Arthur Tingle
Trevor Pratt
Bldg. 130
Uptown, NY 11973

EG&G Idaho, Inc. (2)
Attn: Doug Brownson
Darrel Knudson
MS-2508
P.O. Box 1625
Idaho Falls, ID 83415

EG&G Idaho, Inc.(2)
Attn: Art Rood
Mike Abbott
MS-2110
P.O. Box 1625
Idaho Falls, ID 83415

Judy Rollstin
GRAM Inc.
8500 Menaul Blvd. NE
Albuquerque, NM 87112

Los Alamos National Labs (2)
Attn: Desmond Stack
Kent Sasser
N-6, K-557
Los Alamos, NM 87545

Technadyne Engineering Consultants(3)
Attn: David Chanin
Jeffery Foster
Walt Murfin
Suite A225
8500 Menaul Blvd. NE
Albuquerque, NM 87112

David M. Brown
Paul C. Rizzo Associates, Inc.
300 Oxford Drive
Monroeville, PA 15146-2347

Westinghouse Electric Company(3)
Attn: John Iacovino
Burt Morris
Griff Holmes
Energy Center East, Bldg. 371
P.O. Box 355
Pittsburgh, PA 15230

Marc Rothschild
Halliburton NUS
1303 S. Central Ave.
Suite 202
Kent, WA 98032

Knolls Atomic Power Laboratory(2)
Attn: Ken McDonough
Dominic Sciaudone
Box 1072
Schenectady, NY 12301

Mr. Dennis Strenge
Pacific Northwest Laboratory
RTO/125 P.O. Box 999
Richland, WA 99352

Mr. Fred Mann
Westinghouse Hanford Co.
W/A-53
P.O. Box 1970
Richland, WA 99352

Chuck Dobbe
EG&G Idaho
Technical Support Annex
1580 Sawtelle
Idaho Falls, ID 83402

Kamiar Jamili
DP-62/FTN
Department of Energy
Washington, DC 20585

Sarbes Acharya
Department of Energy
NS-1/FORS
Washington, DC 20585

Lawrence Livermore National Lab(4)
Attn: George Greenly
Marvin Dickerson
Rolf Lange
Sandra Brereton
Livermore, CA 94550

Mr. Terry Foppe
Safety Analysis Engineering
Rocky Flats Plant
Energy Systems Group
Rockwell International Corp.
P.O. Box 464
Golden, CO 80401

U.S. Environmental Protection Agency(2)
Attn: Allen Richardson
Joe Logsdon
Office of Radiation Programs
Environmental Analysis Division
Washington, DC 20460

U.S. Department of Energy(2)
Attn: Ken Murphy (EH351)
Ed Branagan (EH332)
Washington, DC 20545

Michael McKay
Los Alamos National Labs
A-1, MS F600
P.O. Box 1663
Los Alamos, NM 87544

Mr. Robert Ostmeyer
U.S. Department of Energy
Rocky Flats Area Office
P.O. Box 928
Golden, CO 80402

Mr. Bruce Burnett
CDRH (HFZ-60)
U.S. Department of Health
& Human Services
Food & Drug Administration
5600 Fishers Lane
Rockville, MD 20857

Mr. Scott Bigelow
S-CUBED
2501 Yale, SE, Suite 300
Albuquerque, NM 87106

David Black
American Electric Power
1 Riverside Plaza
Columbus, OH 43215

Gerald Davidson
Fauske & Associates, Inc.
16 W 070 West 83rd Street
Burr Ridge, IL 60521

Keith Woodard
Pickard, Lower, and Garrick
Suite 730
1615 M. Street
Washington, DC 20056

Jim Mayberry
Ebasco Services
160 Chubb Ave.
Lyndhurst, NJ 07071

Mr. Mike Cheok
NUS
910 Clopper Road
Gaithersburg, MD 20878

Ken O'Brien
University of Wisconsin
Nuclear Engineering Dept.
153 Engineering Research Blvd.
Madison, WI 53706

Mr. Harold Careway
General Electric Co., M/C 754
175 Curtner Ave.
San Jose, CA 95129

Zen Mendoza
SAIC
5150 El Camino Real
Suite C31
Los Altos, CA 94022

Roger Blond
SAIC
20030 Century Blvd.
Suite 201
Germantown, MD 20874

Leonel Canelas
New University of Lisbon
Quinta de Torre
2825 Monte de Caparica
PORTUGAL

Stephen Boult
Electrowatt Engineering Services (UK) Ltd.
Grandford House
16 Carfax, Horsham
West. Sussex RH12 1UP
ENGLAND

Nadia Soido Falcao Martins
Comissao Nacional de Energia Nuclear
R General Severianao 90 S/408-1
Rio de Janeiro
BRAZIL

Eli Stern
Isreal AEC Licensing Div.
P.O. Box 7061
Tel-Aviv 61070
ISRAEL

Der-Yu Hsia
Atomic Energy Council
67, Lane 144
Keelung Road, Section 4
Taipei, Taiwan 10772
TAIWAN

J. Western
Nuclear Electric plc
Barnett Way, Barnwood
GB-Gloucester GL4 7RS
UK

Dr. E. Lazo
OECD Nuclear Energy Agency
Le Seine Saint-Germain Bldg.
12, boulevard des Iles
F-92130 Issy-les-Moulineaux

Mr. Toshimitsu HOMMA
Environmental Assessment Lab.
JAERI - Tokai Research Establishment
Tokai-mura, Naka-gun
Ibaraki ken, 319-11 JAPAN

G.N. Kelly (150)
Commission of the European Communities
(DG XII/F/6 -ARTS 3/53
200, rue de la Loi
B-1049 Brussels
BELGIUM

S. Cole
Commission of the European Communities
(DG XII/D1 - SDME 3/49)
200, rue de la Loi
B-1049 Brussels
BELGIUM

G. Fraser
Commission of the European Communities
(DG XI/A/1 - WAG C3-353)
Bat Jean Monnet, Rue Alcide De Gasperi
L-2920 LUXEMBOURG

E. Lopez-Menchero
Commission of the Eureopean Communities
(DG XI - Safety in Nuclear Installations)
(DG XI - BU-5 6/140)
200, rue de la Loi
B-1049 Brussels
BELGIUM

F. Girardi, Head of Unit
Institute for the Environment
EC Joint Research Centre
I-21020 Ispra (Varese)

A. Besi
Institute for Systems Engineering
& Information Technology
EC Joint Research Centre
I-21020 Ispra (Varese)

Dr. Torben Mikkelsen
Dept. of Meteorology & Wind Energy
RISO National Laboratory
DK-4000 Roskilde
DENMARK

Dr. J. Ehrhardt
Kernforschungszentrum
Karlsruhe (KfK)
Institut fur Neutonenphysik
u. Reaktortechnik
Postfach 3640
D-76021 Karlsruhe 1,
GERMANY

Dr. E. Hofer
Gesellschaft fur Reaktorsicherheit
(GRS) mbH
Forschungsgelande
D-85764 OberschleiBheim

Dr. Peter Jacob
GSF - ISAR
Forschungszentrum fur
Umwelt und Gesundheit GmbH
Institut fur Strahlenschutz
Ingolstradter Landstr.1
D-85764 OberschleiBheim
GERMANY

Ir P.M. Roelsfsen
Netherlands Energy Research
Foundation, ECN
Westerduinweg 3
P.O. Box 1
NL-1755 LE Petten
The NETHERLANDS

Prof. Eduardo Gallego
Departamento de Ingenieria Nuclear
E.T.S. Ingenieros Industriales
Universidad Poltecnica de Madrid
C/Jose Gutierrez Abascal 2
F-28006 Madrid, SPAIN

Dr. U. Baverstam
Swedish National Institute of Radiation
Protection
Box 60204
S-10401 Stockholm, SWEDEN

Dr. Jacqueline Boardman
Safety & Reliability Directorate (SRD)
Environmental Risk Assessment Dept.
AEA Technology
Wigshaw Lane, Culchet
GB-Cheshire WA3 4NE
UNITED KINGDOM

Mrs. S. Haywood
National Radiological Protection Board
(NRPB)
Chilton, Didcot
GB-Oxon OX11 ORQ
UNITED KINGDOM

Mr. M. Herzeele
CEC Commission of the European
Communities
DG for the Environment
Nuclear Safety & Civil Protection
Centre Wagner C354
L-2920 Luxembourg
Luxembourg

Dr. R. Serro
Commission of the European Communities
DG XI - Environment & Nuclear Safety
Building Wagner
L-2920 Luxembourg
Luxembourg

M. J-L. Lamy
CEC Commission of the European
Communities
DG XI, BU-5 6/148
Rue de la Loi 200
Brussels 1049
Belgium

John Luke
Florida Power & Light
P.O. Box 14000
Juno Beach, FL 33408

Duke Power Co. (2)
Attn: Duncan Brewer
Steve Deskevich
422 South Church Street
Charlotte, NC 28242

Mr. Griff Holmes
Westinghouse Electric Co.
Energy Center East
Bldg. 371
P.O. Box 355
Pittsburgh, PA 15230

Mr. Edward Warman
Stone & Webster Engineering Corp.
P.O. Box 2325
Boston, MA 02107

Mr. William Hopkins
Bechtel Power Corporation
15740 Shady Grove Road
Gaithersburg, MD 20877

R. Toossi
Physical Research, Inc.
25500 Hawthorn Blvd.
Torrance, CA 90505

Bill Eakin
Northeast Utilities
Box 270
Hartford, CT 06141

Ian Wall
Electric Power Research Institute
3412 Hillview Avenue
Palo Alto, CA 94304

Jim Meyer
Scientech
11821 Parklawn Dr.
Suite 100
Rockville, MD 20852

Ray Ng
NUMARC
1776 Eye St. NW
Suite 300
Washington, DC 20006-2496

Robert Gobel
Clark University
Center for Technology, Environment
and Development
950 Main St.
Worcester, MA 01610-1477

Ken Keith
TVA
W 20 D 201
400 West Summit Hill
Knoxville, TN 37092

Shengdar Lee
Yankee Atomic Electric Co.
580 Main St.
Bolton, MA 01740

Paul Govaerts
Studiecentrum voor Kernenergie
(SCK/CEN)
Boeretang, 200
B-2400 Mol
BELGIUM

S. Daggupaty
Environment Canada
4905 Dufferin Street
Downsview
Ontario, M3H 5T4
CANADA

Soren Thykier-Nielsen
Riso National Laboratory
Postbox 49
DK-4000 Roskile
DENMARK

Seppo Vuori
Technical Research Centre
of Finland
Nuclear Engineering Lab
Lonnrotinkatu 37
P.O. Box 169
SF-00181 Helsinki 18
FINLAND

Daniel Manesse
IPSN
Voite Postale 6
F-92265 Fontenay-auz-Roses CEDEX
FRANCE

Dr. J. Papazoglou
National Center for Scientific
Research
"DEMOKRITOS" Institute of
Nuclear Technology
P.O. Box 60228
GR-153 10 Aghia Paraskevi
Attikis
GREECE

ENEA/DISP (2)
Attn: Alvaro Valeri
Alfredo Bottino
Via Vitaliano Brancati, 48
00144 Roma EUR
ITALY

Mr. Hideo Matsuzuru
Tokai Research Establishment
Tokai-mur
Maka-gun
Ibaraki-ken, 319-11
JAPAN

Mr. Jan Van de Steen
KEMA Laboratories
Utrechtseweg, 310
Postbus 9035
NL-6800 ET Arnhem
THE NETHERLANDS

D. Eugenio Gil Lopez
Consejo de Seguridad Nuclear
Calle Justo Dorado, 11
e-28040 Madrid
SPAIN

Lennart Devell
Studsvik Nuclear
Studsvik Energiteknik AB
S-611 82 Nykoping
SWEDEN

Hanspeter Isaak
Abteilung Strahlenschutz
Hauptabeilung fur die Dicherheit
der Kernanlagen (HSK)
CH-5303 Wurenlingen
SWITZERLAND

M. Crick
Division of Nuclear Safety
IAEA
P.O. Box 100
A-1400 Vienna
AUSTRIA

Ulf Tveten
Environmental Physics Section
Institutt for Energiteknikk
Postboks 40
N-2007 Kjeller
NORWAY

M. K. Yeung
University of Hong Kong
Mechanical Engineering Dept.
Polfulam, HONG KONG

Mr. S.P. Arsenis
Industry Enviroment Unit,
Joint Research Centre
Institute for Systems,
Engineering & Informatics
I 21020 ISPRA (Va)
Italy

Mr. E. Lyck
C/O Dr. Torbin Mikkelsen
RISO National Laboratory
DK-4000 Roskilde
Denmark

Mr. P. Lofstrom
C/O Dr. Torbin Mikkelsen
RISO National Laboratory
DK-4000 Roskilde
Denmark

Mr. H.E. Jorgensen
C/O Dr. Torbin Mikkelsen
RISO National Laboratory
DK-4000 Roskilde
Denmark

dr. M. G. Delfini
VROM/DGMilieubeheer
Directie Stoffen, Veiligheid,
Straling/655
Afdeling Straling en Nucleaire
Veiligheid
Postbus 30945
2500 GX Den Haag
the NETHERLANDS

Dr. R. Brown
British Gas plc
Research & Technology Division
Group Leader Combustion Science Division
Midlands Reseach Station
Wharf Lane, Solihull
West Midlands B91 2JW
U.K.

Dr. J.A. Jones
NRPB National Radiological
Protection Board
Assessments Department
Chilton, Didcot
Oxon OX11 0RQ
U.K.

Dr. B. Joliffe
National Physical Laboratory
DQM
Queens Road
Teddington, Middlesex
U.K. TW11 0LW

Dr. Y. Belot
Commissariat a l'Energie Atomique
Institut de Protection et
Surete Nucleaire
DPEI/SERGD
BP 6
F-92265 Fontenay aux Roses Cedex
Frankrijk

Dr. K. Shrader-Frenchette
Environmental Sciences and Policy Program
Department of Philosophy
University of South Florida
4202 East Fowler Avenue, CPR 259
TAMPA, Florida 33620

dr. J. Slanina
Group Environmental Research Fossil Fuels
ECN
Postbus 1
1755 ZG Petten NH
the NETHERLANDS

dr. J. H. Duijzer
TNO/IMW
P.O. Box 6011
2600 JA DELFT
the NETHERLANDS

dr. G. Deville-Carelin
IPSN/CE
bat 159
13108 Saint Paul les Durance Cedex
la France

Mr. Ph. Berne
IPSN
DPEI/SERAC/LESI
38041 GRENOBLE Cedex
la France

Dr. W. Biesiot
IVEM/Energie en Milieukunde
RUGroningen
Nijenborgh 4
9747 AG GRONINGEN
the Netherlands

USNRC

Denwood Ross, AEOD
MS-MNBB 3701

Themis Speis, RES
MS-NL/S 007

Brian Sheron, RES/DSR
MS-NL/S 008

Joseph Murphy, RES/DSIR
MS-NL/S 007

Mark Cunningham, RES/PRAB
MS-NL/S 372

Mat Taylor, EDO
MS-17G21

Bill Morris, RES/DRA
MS-NL/S 007

Zoltan Rosztoczy, RES/ARB
MS-NL/S 169

Donald Cool, RES/RPHEB
MS-NL/S 139

Warren Minners, RES/DSIR
MS-NL/S 007

Thomas King, RES/DSR
MS-NL/S 007

William Beckner, NRR/PRAB
MS-10E4

Frank Congel, NRR/DREP
MS-10E2

Charles Willis, NRR/DREP
MS-10E2

Richard Barrett, NRR/PD3-2
MS-13D1

Lemoine Cunningham, NRR/PRPB
MS-10DR

Ashok Thadani, NRR/DST
MS-8E2

William Russell, NRR/ADT
MS-12G18

Stewart Ebneter
Regional Administrator, RGN II
U.S.N.R.C.
101 Marietta St., Suite 2900
Atlanta, GA 30323

John Martin
Regional Administrator, RGN III
U.S.N.R.C.
801 Warrenville Rd.
Lisle, IL 60532-4351

James Glynn, RES/PRAB
MS-NL/S372

Thomas Martin
Regional Administrator RGN I
U.S.N.R.C.
475 Allendale Rd.
King Prussia, PA 19406-1415

Harold VanderMolen, RES/PRAB
MS T9F31

Christiana Lui (10), RES/PRAB
MS T9F31

Les Lancaster, RES/PRAB
MS T9F31

Chris Ryder, RES/PRAB
MS T9F31

Michael Jamgochia, RES/SAIB
MS-NL/S 324

Leonard Soffer, RES/SAIB
MS-NL/S 324

John Ridgely, RES/SAIB
MS-NL/S 324

Shlomo Yaniv, RES/RPHEB
MS-NL/S 139

Robert Kornasiewicz, RES/DE
MS-NL/S 007

Joe Levine, NRR/PRPB
MS-10D4

Robert Palla, NRR/PRAB
MS-10E4

Tom McKenna, AEOD/IRB
MS-MNBB 3206

Internal

MS0491 Norm Grandjean, 12333
MS0736 N. R. Ortiz, 6400
MS0747 A. L. Camp, 6412
MS0748 L. A. Miller, 6413
MS0748 M. L. Young, 6413
MS0748 F. T. Harper, 6413
MS0748 T. D. Brown, 6413
MS1141 L. F. Restrepo, 6453
MS1093 Hong-Nian Jow, 7714
MS9018 Central Technical Files, 8523-2
MS0899 Technical Library, 13414 (7)
MS0619 Technical Publications, 13416 (1)

NRC FORM 335 (2-89) NRCM 1102, 3201, 3202

U.S. NUCLEAR REGULATORY COMMISSION

BIBLIOGRAPHIC DATA SHEET

(See instructions on the reverse)

1. REPORT NUMBER (Assigned by NRC, Add Vol., Supp., Rev., and Addendum Numbers, If any.)

NUREG/CR-6244
EUR 15855EN
SAND94-1453
Vol. 3

2. TITLE AND SUBTITLE

Probabilistic Accident Consequence Uncertainty Analysis

Dispersion and Deposition Uncertainty Assessment

Appendices C, D, E, F, G, H

3. DATE REPORT PUBLISHED

MONTH	YEAR
January	1995

4. FIN OR GRANT NUMBER

L2294

5. AUTHOR(S)

F. T. Harper (SNL), L. H. J. Goossens (TUD), R. M. Cooke (TUD), S. C. Hora (UHH), M. L. Young (SNL), J. Pasler-Sauer (KfK), L. A. Miller (SNL), B. Kraan (TUD), C. H. Lui (USNRC), M. D. McKay (LANL), J. C. Helton (ASU), J. A. Jones (NRPB)

6. TYPE OF REPORT

Technical

7. PERIOD COVERED (Inclusive Dates)

8. PERFORMING ORGANIZATION - NAME AND ADDRESS (If NRC, provide Division, Office or Region, U.S. Nuclear Regulatory Commission, and mailing address; if contractor, provide name and mailing address.)

Sandia National Laboratories
Albuquerque, NM 87185-0748

9. SPONSORING ORGANIZATION - NAME AND ADDRESS (If NRC, type "Same as above"; if contractor, provide NRC Division, Office or Region, U.S. Nuclear Regulatory Commission, and mailing address.)

Division of Systems Technology
Office of Nuclear Regulatory Research
U.S. Nuclear Regulatory Commission
Washington, DC 20555-0001

Commission of the European Communities
DG XII and XI
200, rue de la Loi
B-1049 Brussels

10. SUPPLEMENTARY NOTES

11. ABSTRACT (200 words or less)

The development of two new probabilistic accident consequence codes, MACCS and COSYMA, was completed in 1990. These codes estimate the consequences from the accidental releases of radiological material from hypothesized accidents at nuclear installations. In 1991, the U.S. Nuclear Regulatory Commission and the Commission of the European Communities began co-sponsoring a joint uncertainty analysis of the two codes. The ultimate objective of this joint effort was to systematically develop credible and traceable uncertainty distributions for the respective code input variables. Because of the magnitude and expense required to complete a full-scale consequence uncertainty analysis, a trial study was performed to evaluate the feasibility of such a joint study by initially limiting efforts to the dispersion and deposition code input variables. A formal expert judgment elicitation and evaluation process was identified as the best technology available for developing a library of uncertainty distributions for these consequence parameters. This report focuses on the methods used in and results of this trial study.

12. KEY WORDS/DESCRIPTORS (List words or phrases that will assist researchers in locating the report.)

uncertainty analysis, atmospheric dispersion, atmospheric deposition, accident consequence analysis, nuclear accident analysis, probabilistic analysis, expert elicitation, MACCS, COSYMA, consequence uncertainty analysis

13. AVAILABILITY STATEMENT

Unlimited

14. SECURITY CLASSIFICATION

(This Page) Unclassified

(This Report) Unclassified

15. NUMBER OF PAGES

16. PRICE

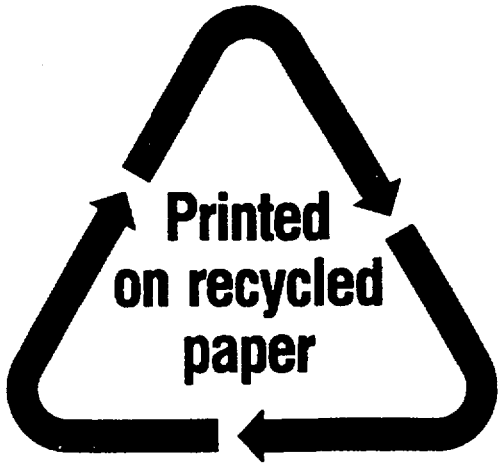

Federal Recycling Program